Post-transcriptional regulation of mPGES-1 by the balance between CUGBP1 and miR-574-5p

Vom Fachbereich Biologie der Technischen Universität Darmstadt

zur

Erlangung des akademischen Grades

eines Doctor rerum naturalium

genehmigte Dissertation von

Master of Science

Isabell Baumann

aus Offenbach

1. Referentin: Prof. Dr. B. Süß

2. Referent: Prof. Dr. D. Steinhilber

Tag der Einreichung: 24.11.2016

Tag der mündlichen Prüfung: 19.12.2016

Darmstadt 2017

D 17

Content

Content

Content

Abbreviations

I Abbreviations

5´ UTR	5´untranslated region
3´ UTR	3´untranslated region
µl	Microliter
µg	Microgramm
Amp	Ampicillin
AA	Arachidonic acid
Ago	Argonaute protein
AP1	Activator protein 1
AS	Alternative splicing
ATCC	*American Type Culture Collection*
ATP	Adenosintriphosphate
ARE	AU-rich element
AUF1	AU-binding factor 1
Bp	Branch point
bp	base pairs
C/EBP	CCAAT enhancer binding protein
cAMP	cyclic adenosine monophosphate
CMV	human cytomegalovirus
COX	Cyclooxygenases
CUGBP1	CUG-binding protein 1
Da	Dalton
DAPI	4´,6-Diamidine-2´-phenylindole dihydrchloride
DGCR8	DiGeorge syndrome chromosal region 8
DMSO	Dimethylsufoxide
DNA	Desoxyribonucleic acid
dsDNA	double stranded DNA
DSMZ	Deutsche Sammlung von Mikroorganismen und Zellkulturen
dTTP	Desoxythymidintriphosphat
EP	Prostaglandin E_2 receptor
eIF4F	Eukaryotic initiation factor 4F
et al.	and others
EDTA	Ethylenediaminetetraacetic acid
EJC	Exon-junction complex
ESE	Exonic splicing enhancer
ESS	Exonic splicing silencer
EZH2	Enhancer of Zeste homolog 2
FCS	Fetal calf serum
FLAP	5-Lipoxygenase activating protein
GRE	GU-rich elements
GSH	Glutathione
hnRNP	heterogenous RNA-binding protein
HuR	Human-antigen R
IL-1β	Interleukin-1β
ISS	Intronic splicing silencer
KH	K homology domain
LB	Luria broth
LT	Leukotriene

Abbreviations

LTC_4S	Leukotriene C_4 synthase
MAPEG	Membrane-associated proteins involved in eicosanoid and glutathione metabolism
mg	Milligramm
MGST	microsomal glutathione S transferase
min	Minute(s)
miRNA	microRNA
mPGES-1	microsomal Prostaglandin E-synthase-1
ml	Milliliter
mRNA	messenger ribonucleic acid
MTT	(3-(4,5-dimethythiazol-2-yl))-2,5-diphenyltetrazolium bromide
NSCLC	non-small cell lung cancer
ng	Nanogramm
NCN	Nucleolin
NMD	Nonsense-mediated mRNA decay
NSAIDS	Non-steroidal anti-inflammatory drugs
PABP	poly-(A)-binding protein
PAGE	Polyacrylamide gelelectrophoresis
PB	Processing-bodies
PI	Prostacyclin
PCR	Polymerase chain reaction
PG	Prostaglandin
PGE	Prostaglandin synthases
PLA_2	Phospholipase A_2
PTC	Premature termination codon
rpm	rounds per minute
RBD	RNA-binding domain
RBP	RNA-binding protein
REMSA	RNA electrophoretic mobility shift assay
RISC	RNA-inducing silencing complex
RNA	Ribonucleic acid
RNP	Ribonucleoprotein
RRM	RNA recognition motif
RUST	regulated unproductive splicing and translation
SBS	STAU1-binding site
SDS	Sodium dodecylsulfate
sec	Seconds
SF	Splicing factor
SMA	Spinal muscular atrophy
snRNPs	small ribonucleoproteins
SR	Serine/arginine-rich splicing factor
SRE	Serum response element
SS	Splice site
ssDNA	single stranded DNA
T	Time
TM	Transmembrane
TNFα	Tumour necrosis factor α
TTP	Tristetraprolin
TX	Thromboxane
UPF1	Up-frameshift protein 1

Abbreviations

V	Voltage
Tris	Tris-(hydroxymethyl)-aminomethan

List of Figures

II List of Figures

List of Figures

List of Tables

III List of Tables

1 Introduction

1.1 Prostaglandins – important lipid mediators in inflammation and cancer

Inflammation is a biological response of tissues to harmful stimuli, like pathogens, damaged cells, or irritants and responsible for recruiting immune cells, blood vessels, and molecular mediators [1,2,3,4,5]. The function of inflammation is to eliminate the initial cause of cell injury, clear out necrotic cells and damaged tissues from the original insult, initiation of tissue repair and activation of inflammatory processes. Classical signs of inflammation are heat, pain, redness, swelling and loss of function [6,7,8,9,10]. During inflammation the prostaglandin (PG) cascade is activated by calcium signaling and cytokine-dependent enzyme inductions [11,12]. The group of eicosanoids is formed by PGs, leukotrienes (LTs), prostacyclins (PGIs) and thromboxanes (TXs) (Fig. 1). PGs represent a group of potent lipid mediators, formed by most cells in mammals acting as local hormones [13]. They exert complex functions as lipid signaling molecules mainly in cell growth, inflammation or immunity as well as messengers in the central nervous system. They derive from the precursor arachidonic acid (AA), a polyunsaturated fatty acid that is metabolized by various enzymes to a wide range of biologically and clinically important eicosanoids and its metabolites (Fig. 1). Phospholipase A2 (PLA_2) is the main enzyme, which is responsible for AA cleavage, but it can also be generated from diacylglycerol by diacylglycerol lipase [14]. In the PG biosynthetic pathway, cyclooxygenases (COX)-1 and COX-2 catalyze the conversion of AA into the unstable intermediate PGH_2 [15,16], which is subsequently converted by terminal synthases into physiologically important prostanoids PGE_2, PGI_2, PGD_2, $PGF_{2\alpha}$, and TXA_2. COX-1 is constitutively expressed in all human tissues and considered to play a role mainly in physiological PG production, while COX-2 is induced by pro-inflammatory agents and primarily detected at sites of inflammation [17]. Inhibition of PGE_2 biosynthesis with non-steroidal anti-inflammatory drugs (NSAIDs) [18] or specific inhibitors of COX-1 and COX-2 activity (Coxibs), has been an important anti-inflammatory strategy for many years (Fig. 1). However, these drugs also cause serious side effects, such as gastrointestinal toxicity and kidney damage [19,20]. Several, but not all, clinical studies have revealed an increased rate of cardiovascular complications after long-term use of COX-2 inhibitors such as rofecoxib, celecoxib, and valdecoxib [21]. Despite significant variability of findings in these studies, the increased rates of myocardial infarction and stroke emerging from rofecoxib studies and cardiovascular complications found in celecoxib, some cancer prevention studies raise concerns about the cardiovascular safety of long-term treatment with selective Coxibs and

NSAIDS [22,23]. The severe cardiovascular side effects of COX-2 inhibitors are particularly high risk for cardiovascular disease [24].

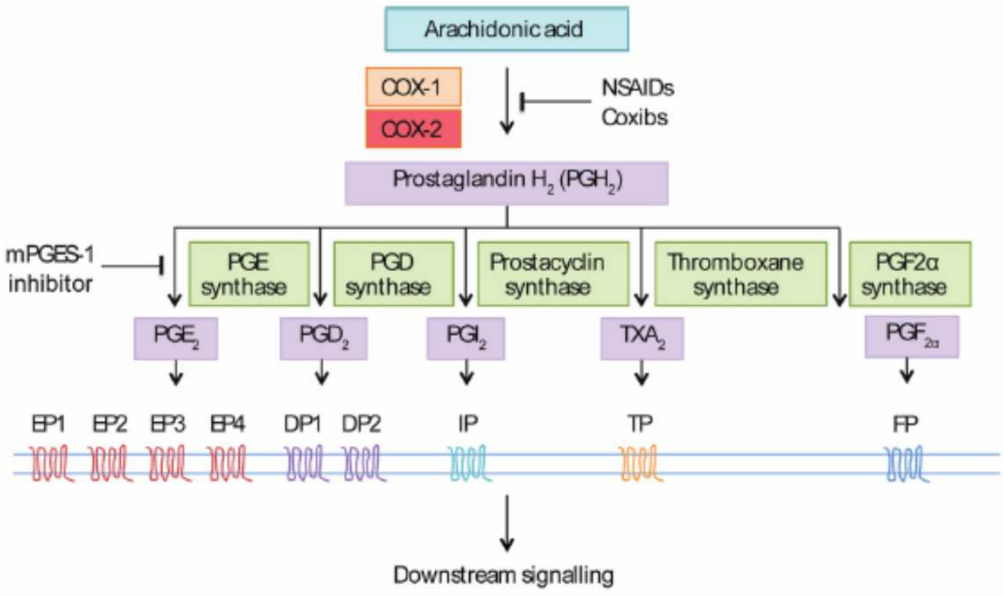

Fig. 1: Schematic overview of the COX pathway and points of inhibition. AA is converted by COX 1/2 into PGH_2. Terminal synthases convert PGH_2 into PGs and TXs. The bioactive lipids bind to their respective receptor(s): EP1–EP4 = PGE_2 receptors; DP1, DP2 = PGD_2 receptors; IP = PGI_2 receptor; TP = TXA_2 receptor and FP = $PGF_{2\alpha}$ receptor. For inhibition of PGE_2 biosynthesis either COX or microsomal PG synthase-1 (mPGES-1) can be targeted, modified [25].

It is known that selective inhibition of COX-2 has less gastrointestinal side effects, but leads to increased risk of thrombosis and cardiovascular complications due to a disrupted TXs/PGI_2s balance [26]. PGI_2 is a potent inhibitor of platelet aggregation, mainly synthesized by endothelial cells, which is blocked by COX inhibitors [27,28]. Recently, three terminal PGE_2 synthases were identified as key enzymes in the biosynthesis of PGE_2.

1.1.1 mPGES-1 – a member of the MAPEG superfamily

The three PGE synthases, including cytosolic PGE synthase (cPGES), microsomal prostaglandin E synthase-1 (mPGES-1), and mPGES-2, have been intensively studied [11,29,30]. cPGES is localized in the cytosolic region in various cells and tissues under basal conditions and is functionally coupled with COX-1. cPGES is most likely involved in the production of PGE_2 for the maintenance of homeostasis [29]. Finally, cPGES, also known as p23, associates with numerous proteins, including heat shock proteins Hsp70 and Hsp90 [29,31]. These complexes bind to genomic response elements in a hormone-dependent manner. Overexpression of cPGES in cells suggests that this enzyme converts PGH_2 derived from COX-1, but not from COX-2, to PGE_2, which is functionally linked to cPGES with COX-1

[29]. Also mPGES-2 is constitutively expressed in a wide variety of tissues and cell types and synthesized as a Golgi membrane-associated protein, contrary to mPGES-1 not inducible by pro-inflammatory stimuli [32]. There appears to be no differential coupling of mPGES-2 with the COX enzymes. Based on observations in mPGES-1 deficient mice, this enzyme and its product PGE_2 are critically important mediators of pain, angiogenesis, fever, bone metabolism, and tumourigenesis [33,34,35,36,37], while cPGES or mPGES-2 seems to constitutively produce PGE_2 possibly important for physiological reactions [32]. During inflammatory processes mPGES-1 can be induced in contrast to cPGES and mPGES-2 [11]. mPGES-1 acts downstream of COX enzymes and specifically catalyzes the conversion of PGH_2 to PGE_2 [11,38,39]. Based on amino acid sequence, size, hydropathy profile and membrane localization, mPGES-1 is classified as a member of the MAPEG (membrane-associated proteins involved in eicosanoid and glutathione metabolism) superfamily [40]. The six human protein members of the MAPEG superfamily are 16-18 kDA integral membrane proteins, including mPGES-1, 5-lipoxygenase activating protein (FLAP), leukotriene C_4 synthase (LTC_4S), and microsomal glutathione S transferase (MGST) 1-3. Multiple sequence alignments demonstrate six conserved amino acid sequences in the human members. The mPGES-1 has been characterized as an inducible, glutathione (GSH)-dependent membrane bound enzyme [11]. The primary structure of human, rat and mouse mPGES-1 demonstrated a high degree of amino acids sequence homology (>80%) [41]. Two amino acids are conserved in the MAPEG superfamily: Arg110, which is essential for the enzyme function and Tyr117 [42]. The mutation of Arg110 abrogates the catalytical function of mPGES-1, demonstrating the important role of this residue. Most recently, a crystal structure of mPGES-1 was obtained through electron crystallography by Jegerschold *et al*. (Fig. 2) [43]. Three units of mPGES-1 form the active enzyme, which is dependent on GSH for its catalytic activity. The lipid substrate PGH_2 binds together with GSH between transmembrane (TM) region one and four in neighboring subunits (Fig. 2) [43]. The gene of mPGES-1 (*PTGES*) maps to chromosome 9q34.11 and spans about 15 kb, divided into three exons. The putative promoter of the human mPGES-1 gene is GC-rich, lacks a TATA box and contains binding sites for CCAAT enhancer binding protein (C/EBP) α and β, two activator protein-1 (AP-1) sites, two tandem GC boxes, two progesterone receptors and three GRE elements, two cyclic adenosine monophosphate (cAMP) response elements and six serum response elements (SRE) [44]. mPGES-1 is expressed at minimal levels in most normal tissues, although abundant and constitutive expression is detected in a limited number of organs, such as the lung, kidney, and reproductive organs [45,46]. Clinical studies revealed an

increased expression of mPGES-1 protein in various types of cancer, including gastrointestinal, lung, stomach, brain, breast, pancreas, prostate and cervix carcinoma [37].

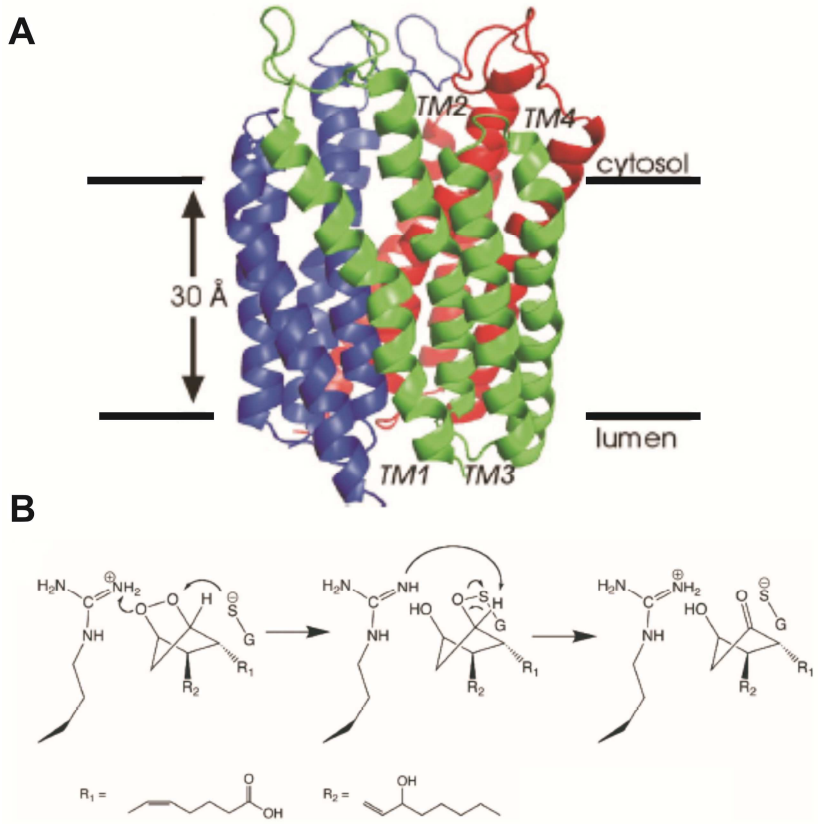

Fig. 2: Crystal structure of mPGES-1 protein and proposed model of GSH transfer. (A) mPGES-1 is composed of four TM regions connected by flexible loops. The trimer subunits have been colored in ribbon representation. Side view with the cytoplasmic side up. The TM helices of one subunit have been labeled at their C-terminal ends. (B) Suggested chemical mechanism for the mPGES-1 catalyzed PGE_2 synthesis involves an attack of the GSH thiolate on the O_9 of the endoperoxide bridge followed by proton donation to O_{11} via Arg-126. Arg-126 then abstracts a proton from C_9 where a carbonyl forms as the oxygen sulfur bond is broken. The leaving GSH thiolate is stabilized by Arg-126, modified [43].

The mPGES-1 gene is inducible by various pro-inflammatory cytokines e.g. interleukin (IL) -1β and tumor necrosis factor (TNF) α [11,47,48]. mPGES-1 is in general functionally coupled with COX-2 and its expression is often concomitantly induced with COX-2 overexpression, which contributes to the efficient generation of PGE_2 during inflammatory processes [11]. However, different studies provided evidence that COX-2 and mPGES-1 can be independently regulated [49]. This observation suggests the possibility that the pharmacological targeting of mPGES-1 may result in the suppression of PGE_2 production without causing severe cardiovascular side effects as traditional NSAIDs or selective COX-2 inhibitors may do [50,51,52]. Therefore, mPGES-1 is a potential target for the development of novel anti-inflammatory drugs that can reduce symptoms of inflammation. Several selective inhibitors of mPGES-1 activity or expression have been identified and some of them have

been already evaluated in different preclinical inflammatory models [52,53,54]. So far none of them have been developed as anti-cancer agents. The COX-2 inhibitor NS-398 [48], FLAP inhibitor MK-886 [55], and the active metabolite of another NSAID sulindac [48], were found to inhibit mPGES-1 with an IC_{50} of 20, 1.6, and 80 µM, respectively. Leukotriene C_4 was reported to inhibit mPGES-1 with micromolar IC_{50}, probably due to competing with GSH [56]. Leclerc *et al*. characterized a selective inhibitor of mPGES-1 activity (Compound III) and studied its impact on the prostanoid profile in various models of inflammation [53,57]. Compound III is a benzoimidazole, which has a submicromolar IC_{50} in both human and rat recombinant mPGES-1. In cellular assays, it reduced PGE_2 production in A549 cells, mouse macrophages and whole blood assay, causing a shunt to the prostacyclin pathway in the former two systems [53]. Not many *in vivo* studies were performed on the effect of mPGES-1 inhibition in cancer treatment, although mPGES-1 and PGE_2 have a crucial role in tumourigenesis [58]. The reasons for this are the phylogenetic differences between human and murine enzymes, which make research on the effects of mPGES-1 inhibition in cancer more difficult. Three amino acids in the active site of TM4 of mPGES-1 are not conserved between human and rodent enzyme [59] (Fig. 3).

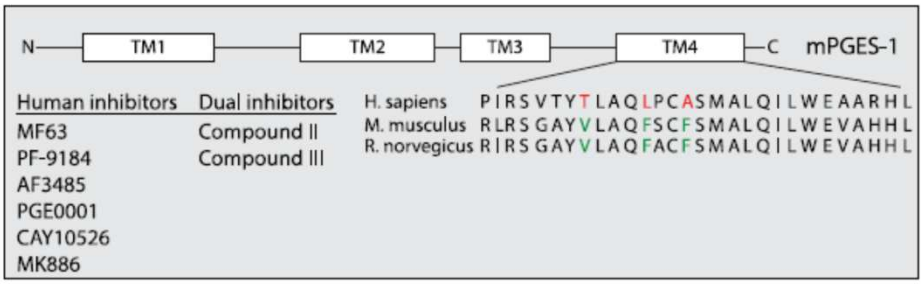

Fig. 3: Overview of mPGES-1 protein homology between species and inhibitors. mPGES-1 is contains four TM regions. Three amino acids in the active site of mPGES-1, located in TM4 are not conserved between human (red) and rat/mouse (green) enzyme. These phylogenetic differences results in a more restricted catalytic difference in the rodent enzyme, rendering most inhibitors developed for the human enzyme inefficient toward rat/mouse mPGES-1, modified [25].

Two additional amino acids are outside of the active site and have also been proposed to contribute to the human/murine inhibitor binding differences in a study [59,60]. These phylogenetic differences result in a more restricted catalytic difference in the rodent enzyme, whereby most inhibitors developed for the human mPGES-1 enzyme are inefficient towards rodent mPGES-1. Inhibitors like Compound III, active against both human and murine enzymes, are promising tools for further studies of mPGES-1 inhibition *in vivo* models.

1.1.2 PGE_2 is a key lipid mediator in inflammation and cancer

The PG cascade is activated by calcium (Ca) signaling and cytokine-dependent enzyme inductions during inflammatory processes [11]. It has been demonstrated that COX-2 and mPGES-1 are rapidly induced within hours by pro-inflammatory cytokines e.g. IL-1β or TNFα in macrophages and fibroblasts [11,61]. PGE_2 is an essential lipid mediator that regulates different physiological relevant processes [62], such as inflammation, pain, tumour development, vascular regulation, neuronal functions, female reproduction, gastric mucosal protection, and kidney function (Fig. 4).

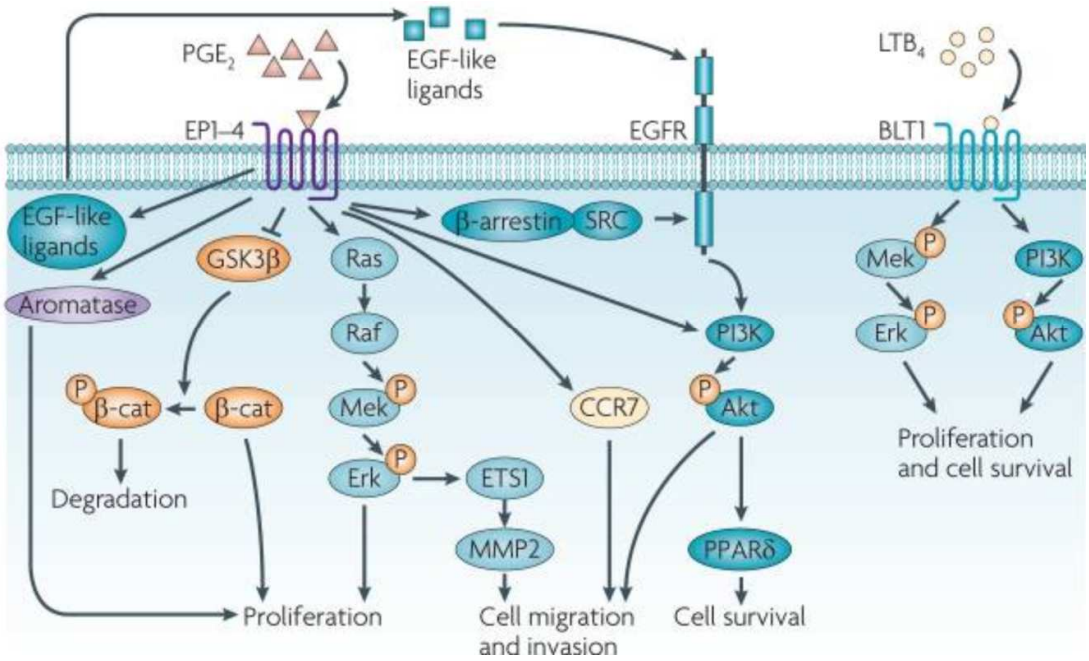

Fig. 4: PGE_2 promotes cancer progression through induction of tumor epithelial cell proliferation, survival, migration and invasion. Multiple cellular signalling pathways mediate the effects of PGE_2 and LTB_4 on the regulation of epithelial tumour cell proliferation, survival, and migration and invasion. PGE_2 stimulates cell proliferation through multiple cascades in non-small-cell lung cancer cells, modified [63].

PGE_2 production occurs in response to cell stress factors such as hypoxia, glucose deprivation or the existence of apoptotic cells [64]. PGE_2 has been described as one of the most characteristic tumour micro environmental factors, since its upregulation is also present in inflammation and inflammatory processes [65]. PGE_2 exerts its actions via four types of receptors EP1, EP2, EP3, and EP4. Activation of these receptors by PGE_2 or artificial compounds stimulates distinct signal transduction pathways and mediates various biological functions [66]. The EP1 receptor couples to G_q-proteins to increase intracellular Ca^{2+} concentration. The EP2 and EP4 receptors couple to G_s-proteins and evoke an increase in

intracellular cAMP concentration. EP3 receptor mainly couples to G_i-proteins to decrease cAMP production. Responsible for the synthesis of the pro-tumourigenic PGE_2 is mPGES-1. High levels of mPGES-1 were detected in many human cancer cell lines and tissues. Additional intermediate levels were observed in placenta, prostate, testis, and mammary gland [11]. PGE_2 is over-produced at sites of inflammation and may be involved in many types of cancer, including bladder, breast, cervical, colorectal, esophageal, head and neck, skin, lung, oral, and prostate cancers [11,65]. As lipid mediator PGE_2 can be distinguished from protein mediators e.g. cytokines. Lipid mediators are produced enzymatic from available precursors. Their levels can rapidly be increased while in contrast cytokine synthesis is slower, involving transcription and translation. Chronic inflammation can cause cancer suggesting NF-κB activation to be critically involved in tumourigenesis by initiating the expression of inflammatory genes, including those coding for the enzymes COX-2 and mPGES-1 [67,68]. The use of NSAIDs inhibiting COX isoenzymes has been shown to have cancer preventive effects in a large number of clinical trials demonstrating the tumour inducing properties of PGs [69]. The siRNA-mediated knockdown of mPGES-1 reduced the tumourigenic potential of DU145 and A549 cells in nude mice [70]. Recently, it was shown that genetic deletion of mPGES-1 reduced the synthesis of inducible PGE_2 and markedly suppressed intestinal tumour formation in $Apc^{\Delta 14}$ mice [71]. Neither cell turnover nor β-catenin expression was affected by mPGES-1 levels, suggesting the potent tumour suppressive properties were associated with impaired neovessel formation within the adenomas. PGE_2 may be dominant in many types of cancer exerting tumouric properties [63,65]. However, not all PGs attribute a major pro-tumourigenic function [72,73]. Indeed, a study showed the shunting of tumour associated PG metabolism towards PGD_2 due to deletion of mPGES-1 in colorectal cancer, which indicates that mPGES-1 deficient bone marrow derived cells (BMDCs) produce less IL-12 [74]. This appears maybe due to shunting of PG precursors down the PGD_2 synthetic pathway in the absence of mPGES-1. Kapoor *et al*. demonstrated that mPGES-1 gene deletion resulted in diversion of prostanoid production from PGE_2 to 6-keto $PGF_{1\alpha}$ in a gene dose-dependent manner in heterozygous (Het) and null mouse embryonal fibroblasts (MEF) compared with their wildtype counterparts [75]. Eicosanoid profiling reveals shifting towards PGD_2 pathway in mPGES-1 knockout mice [76]. Shunting of prostanoid synthesis towards PGD_2 could potentially be one mechanism of immunomodulation in the absence of mPGES-1. The shunting of prostaglandins towards anti-tumourigenic metabolites as the immune suppressive role of PGD_2 appears as highly desirable from the therapeutic point of view.

In contrast to this, PGE_2 may also have tumour suppressive properties, occurred despite increased in cell turnover demonstrated by elevated thymidine incorporation [77]. These findings could not be reproduced by others assuming that the effect may have been environmentally influenced or perhaps the result of genetic changes occurring within the *Apc*^{Min} mouse colony under study [78].

1.2 Post-transcriptional regulation of gene expression in eukaryotes

The way from DNA to a functional active protein is a complex and strongly regulated cellular process (Fig. 5). The regulation of gene expression depends on a variety of mechanisms that can either increase or decrease the amount of gene products, such as transcriptional or translational control. During transcription the RNA is generated from a DNA template by RNA Polymerases. After transcription the RNA transcript is further processed (Fig. 5). The accessibility of large regions of DNA can depend on the chromatin structure that can be altered as a result of histone modifications directed by DNA methylation or DNA binding proteins [79]. Transcription by RNA Polymerases can be regulated by e.g. enhancers, silencers and activators. Enhancers are sites on the DNA helix that are bound by activators in order to loop the DNA bringing a specific promoter to the initiation complex. Silencers are regions of DNA sequences that, when bound by particular transcription factors, can silence expression of the gene. Stability, distribution and translation of transcribed mRNA can be regulated e.g. by the binding of RNA-binding proteins (RBPs) or microRNAs (miRNAs) to this mRNA. Genes can be switched on and off completely by means of these post-transcriptional mechanisms such as splicing, degradation, processing, export, capping and polyadenylation. However, a fine adjustment can also be carried out, which leads to the amplification or reduction of the expression of certain genes.

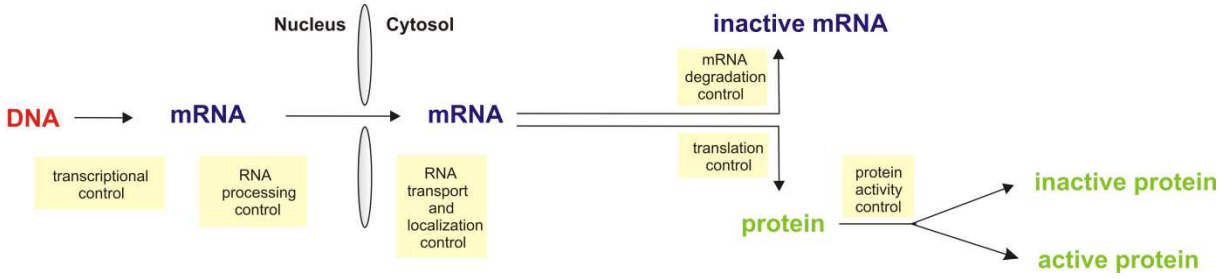

Fig. 5: Gene expression regulation in eukaryotes. Eukaryotic transcription and translation is compartmentally separated, eukaryotic mRNAs must be exported from the nucleus to the cytoplasm, a process that may be regulated by different signaling pathways.

1 Introduction

Before eukaryotic mRNA is spliced, the mRNA is modified in the nucleus at the 5´-end by addition of a methyl guanosine cap and at the 3´-end by addition of a poly-(A) tail. The poly-(A) tail is then recognized by the cytoplasmic poly-(A)-binding protein 1 (PABPc1), and the 5′ cap is bound by eukaryotic initiation factor 4F (eIF4F), a complex consisting of eIF4E (the direct cap-binding component), eIF4G and eIF4A [80,81]. Direct or indirect interactions between cap-binding and poly-(A)-binding factors effectively circularize the mRNA, which increases its stability and translation efficiency [82]. Degradation of mRNA is influenced by both 5´ cap and 3´ poly-(A) tail, and by destabilizing elements within the 5´ untranslated region (UTR), 3´UTR or coding sequence [83,84,85,86].

1.2.1 Splicing

Splicing involves the removal of intronic segments from the nascent pre-mRNA of eukaryotic genes by cleavage and rejoining the exonic fragments [87,88]. This is due to the presence of non-coding introns in many eukaryotic genes. Splicing is catalyzed by a highly dynamic ribonucleoprotein complex, termed spliceosome. It consists of of small-ribonucleoproteins (snRNPS) and more than 100 additional proteins. There are five snRNPs (U1, U2, U4, U5, U6) that recognize three sites on the pre-mRNA [89]. The 5´ and 3´ splice sites (SS) and the branch site. Most commonly, the RNA sequence that is removed begins with the dinucleotide GU at its 5′ end, and ends with AG at its 3´-end [90]. Another important sequence occurs at what is called the branch point (BP), located anywhere from 18 to 40 nucleotides upstream from the 3′ end of an intron. The BP always contains an adenine, but it is otherwise loosely conserved. A typical sequence is YNYYRAY, where Y indicates a pyrimidine, N denotes any nucleotide, R any purine, and A adenine [91]. The reaction occurs in two successive transesterifications (Fig. 6). The first step is a nucleophilic attack of the 2´OH group to the adenosine BP to the 5´SS. This leads to a ligation of the intron 5´-end with the 2´OH group of adenosine. As a second step the released 3´OH of the 5´SS attacks the phosphate of the 3´SS. The outcomes are two linked exons and the released intron in lariat structure [92,93].

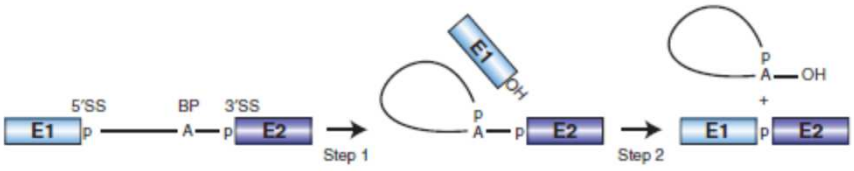

Fig. 6: Schematic model of the two transersterifications during splicing, modified [93].

1 Introduction

The spliceosome is a highly dynamic complex and consists of various factors that interact with the pre-mRNA and thereby bringing the reactive groups of the pre-mRNA into spatial proximity. Small-ribonucleoprotein U1 interacts through base pairing via the U1 snRNA with the 5´SS (Fig. 7 A). Splicing factor 1 (SF1) binds the adenosine of the BP and U2 auxiliary factor (U2AF) binds to polypyrimidine tract and the 3´SS. Next, the U2 snRNP binds to the branch point and forms the A complex. Then, the preassembled tri-snRNP (U4/U5/U6) is passed to the complex and forms the pre-catalytic B complex. By larger rearrangements of RNA-RNA and RNA-protein interactions, the binding of U1 and U4 triggers, at which the catalytically active B complex is formed, this takes the first step of catalysis. The second step takes place in the consequential complex C (Fig. 7 A). The spliceosome is resolved under adenosine 5´ triphosphate (ATP) consumption and recycled for the next round of splicing [93]. There exist alternative pathways at the early stages of spliceosome assembly. Most mammalian pre-mRNAs contain introns whose sizes varied from hundred to thousand nucleotides (nt), while their exons almost have a fixed length of only ~120 nucleotides [94,95]. If introns are longer than 200-250 nts, a first complex on the exon is formed (Fig. 7 B), this process is referred to as exon definition [96,97]. During exon definition, U1 snRNP binds to the 5´SS downstream of an exon and promotes the association of U2AF with the polypyrimidine tract at 3´SS upstream of this exon. This leads to the recruitment of the U2 snRNP to the BP. Splicing enhancer sequences within the exon (ESE) recruit proteins of the serine/arginine-rich splicing factor (SR) protein family, which establish a network of protein–protein interactions across the exon that stabilize the exon-defined complex [98,99].

Splicing can occur during transcription (co-transcriptional) or after transcription (post-transcriptional) [100,101]. This difference is functionally important as co-transcriptional splicing can regulate splicing by diverse transcription-dependent mechanisms, whereas post-transcriptional splicing might allow additional regulatory mechanisms to operate or couple splicing with other downstream events [102].

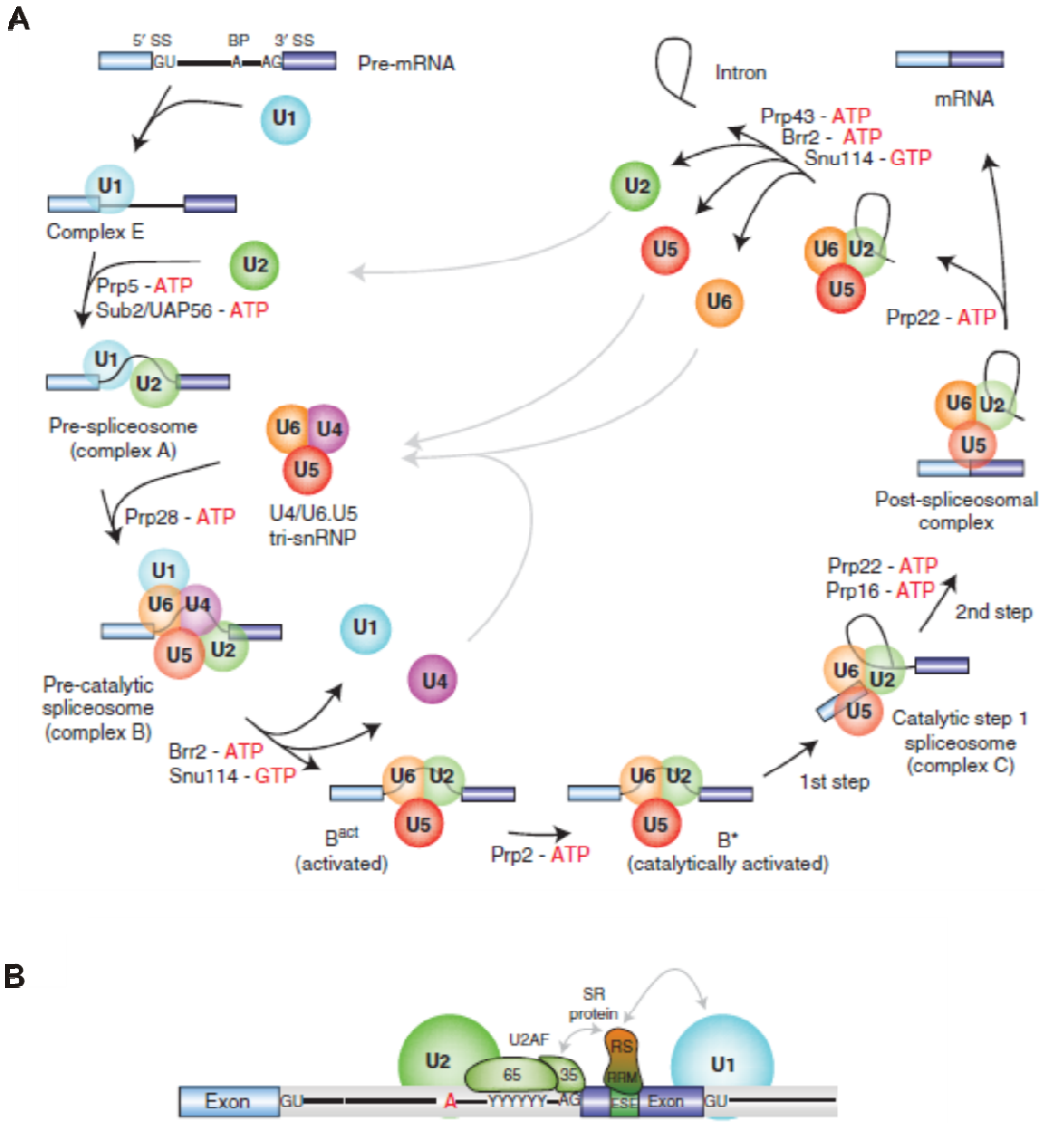

Fig. 7: Schematic representation of the structural changes of the spliceosome during splicing process. The snRNPs are shown as circles and the exons and introns as boxes, respectively lines (A). Model of interactions occurring during exon definition (B), modified [93].

1.2.2 Alternative splicing

In eukaryotes alternative splicing (AS) occurs as a common phenomenon increasing the biodiversity of proteins that are encoded by the genome [92]. About ~95% of multi-exonic genes in humans are alternatively spliced [89,103]. Studies on human tissues have shown that 50% or more of alternative spliced isoforms are differently expressed among tissues, which indicates that most AS occurs due to tissue-specific regulation [104]. Numerous modes of alternative splicing are observed, most frequently is exon skipping [105]. In this case, a particular exon may be included in mRNAs depending on specific conditions or in

particular tissues, and omitted from the mRNA in others [92]. AS can be divided into four types: cassette exons, alternative 3´SS and 5´SS and intron retention (Fig. 8). The most prominent types are cassette exons, that are either included in the mature mRNA (inclusion) or not (exclusion) [105,106,107]. In certain cases, these exons can occur as mutually exclusive exons. Always one of these exons is included, but not both. Furthermore, different 5´ or 3´SS can extend or shorten exon length. Alternative 3´SS and 5´SS selection account for 18.4% and 7.9% of all AS events in higher eukaryotes, respectively [107]. A retained intron is not spliced and included in the mature mRNA. All four types can occur in both the coding and non-coding area. Alternative exons contain the same conserved regions as constitutive exons, but differ in their strength of their splices sites. The consistency of the 5´SS sequence with the consensus sequence GURAGU is crucial, as the splice site is weaker the more the sequence differs [108]. In general alternative exons have a weaker 5´SS, moreover, they are shorter and the branch point is located further upstream. AS underlies the control of associated protein factors with specific pre-mRNA sequences, thereby regulating the course of spliceosome assembly and splice site usage.

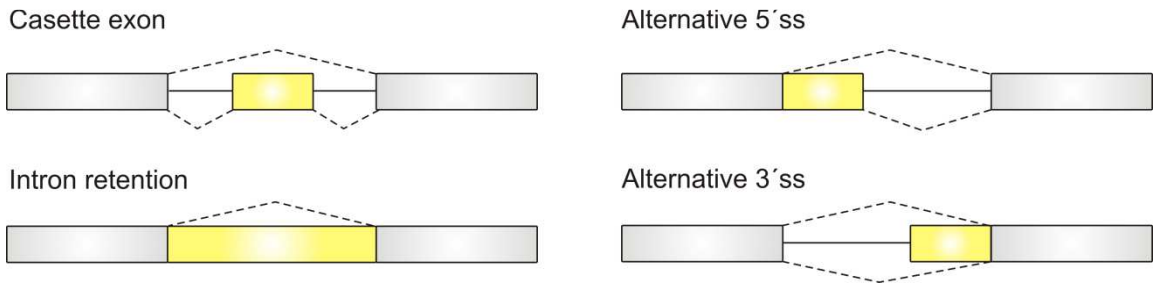

Fig. 8: Different types of alternative splicing in eukaryotes. In the figure, constitutive exons are shown in gray and alternatively spliced regions in yellow. Introns are represented by solid lines, and dashed lines indicate splicing options, modified [106].

RNA processing and AS are important either for generating protein diversity and modulating levels of protein expression or regulating post-transcriptional mechanisms [92]. Important mediators of AS are RBPs that have been shown to control AS [109,110]. Exons and introns contain short, degenerate binding sites for splicing auxiliary proteins. The classical splicing regulators are SR proteins (SR1-12), which, when bound to exonic sequences known as exonic splicing enhancers (ESEs), tend to promote exon inclusion. Exon exclusion is mediated by heterogeneous RNPs (hnRNPs) binding to exonic splicing silencers (ESSs) and/or intronic splicing silencers/enhancers (ISSs/ISEs) [110,111,112]. Many hnRNPs alternate between the nucleus and the cytoplasm to exert their various functions. Besides

their function in splicing they play a role in transcription, mRNA stability, mRNA export and translation [113,114,115].

Defects in splicing are often correlated with diseases and involved in the progression of cancer [116]. At least 15% of all human diseases are due to aberrant splicing, e.g. spinal muscular atrophy (SMA) [117,118]. Most of them are point mutations in the consensus sequences within splice sites. It is estimated that up to 50% of disease-causing mutations in exons affect splicing. Due to mutations, exon skipping or premature termination codon (PTC) insertion into the mRNA can occur, resulting in non-functional proteins. Aberrant splicing has been shown to promote tumour cell proliferation which is often associated with deregulated expression of splicing factors or aberrant splicing of tumour suppressors [119,120].

1.2.3 Nonsense mediated mRNA decay

Alternative pre-mRNA splicing is a fundamental regulatory process for most mammalian multi-exon genes to increase proteome diversity. Nonsense mediated mRNA decay (NMD) is the best characterized mRNA surveillance mechanism in eukaryotes which provides an important way of controlling mRNA quality and expression. NMD functions in at least two distinct cellular processes. First the downregulation of abnormal mRNA transcripts that are generated as a consequence of routine errors in gene expression, and second to maintain an appropriate level of gene expression by downregulating physiological mRNAs in response to changes in cellular environment. One function is to reduce errors in gene expression by eliminating mRNA transcripts that harbor PTCs. PTCs situated more than ~50-55 nucleotides upstream of an exon-junction-complex (EJC) generally trigger NMD [121]. Transcripts that contain PTCs can arise from transcription of pseudo genes, nucleotide disincorporation during transcription of *bona fide* genes, or more frequently due to processing errors during the post-transcriptional maturation of the primary transcript [122,123]. In fact, PTCs shorten the length of the coding region and any downstream EJCs that normally are localized within the coding region fail to be removed from what becomes the 3´UTR. Further, NMD is a key control step, conserved in eukaryotes. It prevents the synthesis of C-terminal truncated proteins, which probably leads to protection of the cell from resultant destructive effects [123,124,125]. The fact that 30% of inherited genetic diseases are due to PTC accentuates the biological importance of NMD [126,127]. Generally, NMD is thought to play a protective role, by destroying truncated transcripts, but it also regulates gene expression through AS coupled with NMD (AS-NMD) [128,129,130]. AS-NMD is better known as a negative

feedback control mechanism to maintain homeostatic expression of RBPs and splicing regulator [131,132]. It has been shown that several splice factors, including SR proteins, regulate splicing of their own pre-mRNA [133,134,135]. In this mode of negative feedback loop regulation, high levels of the SR cause its own pre-mRNA splicing into an unproductive isoform and followed by degradation, which results in lower protein levels [134]. Lewis *et al*. have named this process regulated unproductive splicing and translation (RUST) [136,137]. It seems that 10-15% of human transcripts can be switched off by NMD coupled to AS [136]. Since NMD isoforms are not effectively translated into proteins, switching between the translational isoform and the NMD isoform allows alternative splicing to control overall abundance of the transcript and protein [131,132,137,138]. Finally, the NMD pathway has also been reported to modulate the expression of several normal genes by mechanisms involving the presence of an upstream open reading frame or an intron in the 3´UTR, both of which are predicted to elicit NMD [129,139,140]. Whether this is used in a regulatory context is not fully understood, but it has been proposed that different tissues display different efficiencies of NMD, which in turn may lead to tissue specific differences in mRNAs containing NMD features [141].

There are further mRNA quality control mechanisms termed non-stop decay, which appear when mRNAs lack a termination codon and the no-go decay, occurring when mRNA translation elongation stops [142,143,144]. Staufen1 (STAU1)-mediated mRNA decay (SMD) is an mRNA degradation process in mammals that is mediated by the binding of STAU1 to a STAU1-binding site (SBS) within 3´UTR of target mRNAs [145]. During SMD, STAU1, a double-stranded RNA-binding protein, recognizes dsRNA structures formed either by intramolecular base-pairing of 3´UTR sequences or by intermolecular base-pairing of 3´UTR sequences with a long noncoding RNA via partially complementary [146].

1.3 RNA-binding proteins

RNA-binding proteins are proteins that bind specifically to target RNA molecules. They play a key role during gene expression and RNA processing [147]. Due to their specific binding they have also a crucial role in various cellular processes. They are generally found in the cytoplasm and nucleus and involved in post-transcriptional processes including RNA splicing, editing, stability and transport [148,149,150]. However, often more than one RBP has the capacity to bind to a specific sequence on the target RNA [151]. Cellular RNAs are always associated with RBPs to form high dynamic ribonucleoprotein (RNP) complexes [152,153].

This interaction begins during transcription as some RBPs remain bound to RNA until degradation. Others in contrast only transiently bind to RNA to regulate RNA splicing, processing, transport, and localization. The composition and recruitment of RNPs varies depending on mRNA localization and processing level [154]. Their remodeling allows adjustments in gene expression under conditions requiring adaptive changes. Dysfunction of RBPs is often linked to disease which reflects the relevance of protein-RNA interactions in cellular homeostasis [155].

RNA-binding proteins exhibit highly specific recognition of their target RNAs by recognizing their sequences and structures. Although all RBPs bind RNA, they do so with different RNA-sequence specificities and affinities. The latter is mediated by a relatively small number of RNA-binding scaffolds whose properties are further modulated by auxiliary domains. Normally, RBPs contain one or more RNA binding and auxiliary domains. The auxiliary domains can also mediate the interactions of the RBP with other proteins and, in many cases, are subject to regulation by post-translational modification. Hence, cells can generate numerous RNPs whose composition and modeling of individual components is unique for each mRNA. The RNPs are further remodeled during the maturation of the mRNA into its functional form. Further, diversity of RBPs is achieved by post-translational modifications. Three types of modifications have been described: phosphorylation, arginine methylation and small ubiquitin-like modification [156,157,158]. Most of the RBPs discovered over the last three decades match the classical view of RBP architecture with a modular combination of well-characterized RNA-binding domains (RBDs) such as the RNA recognition motif (RRM), the K homology domain (KH) and the DEAD box helicase domain (Fig. 9). Single RBD can bind short stretches of RNA, typically 2–6 nucleotides [159]. RBPs usually build their affinity and specificity for RNA on the cooperative function of multiple classical RBDs as exemplarily illustrated by the four RRMs that work together in nucleolin (NCL) or the poly(A)-binding protein. There is evidence that RBPs play a crucial role in tumour development and progression [160]. Aberrant expression and regulation of RBPs results in misregulation of splicing observed in cancer [161,162]. Many RBPs are differentially expressed in different cancer types for example KHDRBS1 (Sam68), ELAVL1 (HuR) and FXR1 [163,164,165]. For some RBPs, the change in expression levels are related with copy number variations e.g. CELF3 in breast cancer, RBM24 in liver cancer, IGF2BP2, IGF2BP3 in lung cancer or copy number losses of KHDRBS2 in lung cancer [166]. Some expression changes are caused by

mutations on these RBPs for example SF3B1, SRSF2, RBM10, U2AF1, SF3B1, PPRC1, RBMXL1, or HNRNPCL1 [167,168,169,170,171].

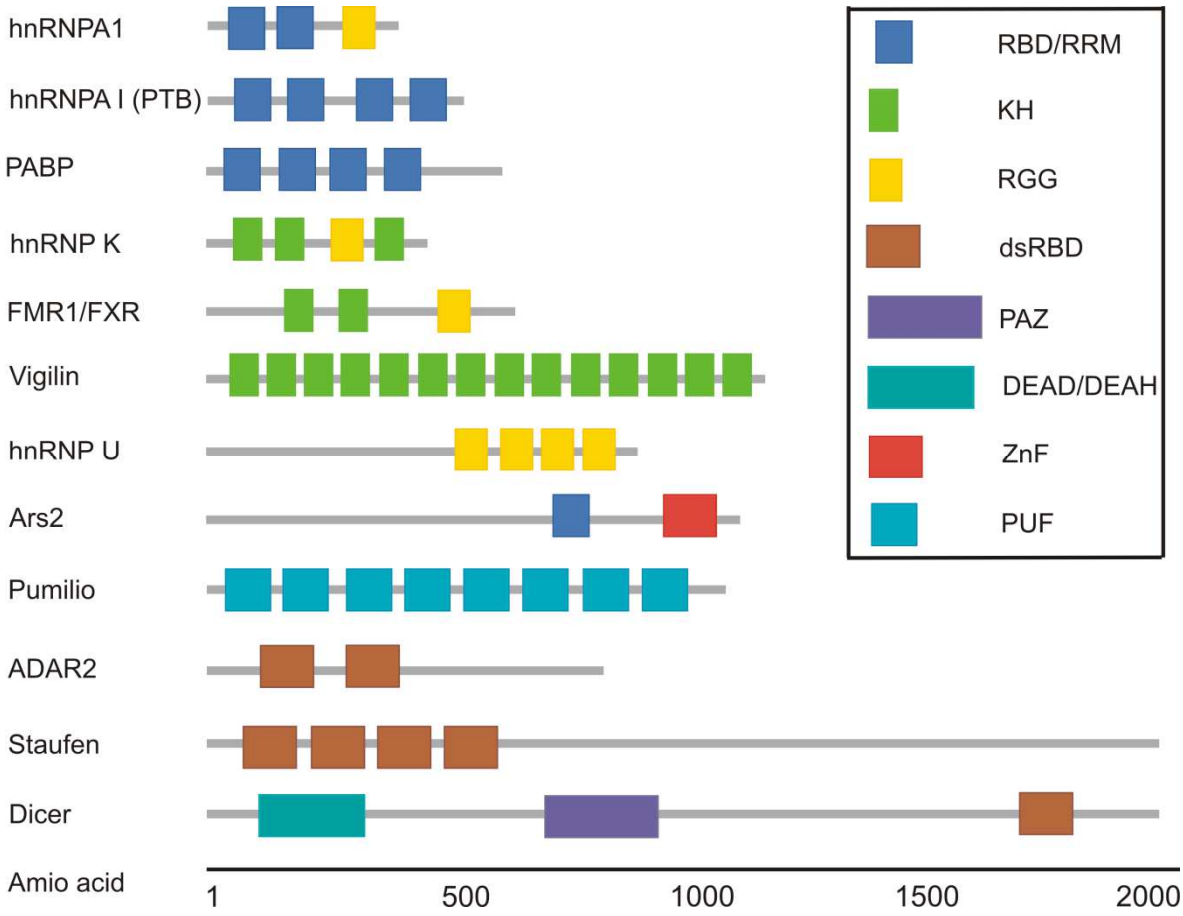

Fig. 9: RNA-binding domains of RBPs. Different RNA-binding domains include the RNA-binding domain (RBD), K-homology (KH) domain, RGG (Arg-Gly-Gly) box, double stranded RNA-binding domain (dsRBD), Piwi/Argonaute/Zwille (PAZ) domain, RNA helicase DEAD/DEAH box, RNA-binding zinc finger (ZnF) and Puf RNA-binding repeats (PUF), modified [172].

1.3.1 AU-rich and GU-rich elements

Generally the 3´UTRs are conserved through species. Transcripts harbor specific motifs that serve as binding sites for RBPs and thereby they regulate mRNA stability and translation. They contain various *cis*-acting regulatory elements that are specifically recognized by binding elements, usually RBPs or RNAs, termed *trans*-acting factors. The interplay between both is crucial for the post-transcriptional regulation of gene expression. The adenylate uridylate (AU) rich elements (AREs), often characterized by AUUUA pentamers, are the most common regulatory elements in the 3´UTR of mRNA. They influence mRNA stability, translation and alternative pre-mRNA processing. Their presence is typical for short-lived

mRNAs. AREs are recognized by ARE-binding proteins (ARE-BPs). It depends on the binding RBP how the mRNA is regulated. RBPs e.g. from the ELAV protein family or HuR enhance mRNA stabilization and translation, in contrast to e.g. tristetraprolin (TTP) or AU-binding factor 1 (AUF1) that are responsible for mRNA destabilization and translational repression [173,174,175].

A global assessment showed that 5% of the human mRNAs harbor GU-rich elements (GREs) in their 3´UTRs that are highly conserved through species [83]. Furthermore, they exist in groups of 2 to 5 overlapping GUUUG pentamers. GREs are functionally linked to rapid mRNA decay in short-lived transcripts and contribute to regulation of deadenylation, mRNA decay and pre-mRNA splicing [176,177]. Recently, proteins from the CELF family have been identified to recognize GREs [178].

1.3.2 CUGBP1 – a prominent member of the CELF family

There are six CELF proteins CELF1-6 of the CELF family that can be separated by sequence similarity into two subgroups CELF1-2 and CELF3-6 (Tab. 1). The RBPs CUG-binding protein 1 (CUGBP1), also called ELAV-like family member 1 (CELF1) and CELF2 (Embryonic lethal abnormal vision Type RNA-binding protein, ETR-3, CUGBP2) are the most relevant members of the CELF family that bind to $(CUG)_8$ RNA nucleotides [109,179].

Tab. 1: Sequence conservation of amino acids between the six CELF family members [180]

	CELF1	CELF2	CELF3	CELF4	CELF5	CELF6
CELF1	100	76	45	42	44	43
CELF2		100	43,5	43	45	46
CELF3			100	61	62	64
CELF4				100	63,5	65
CELF5					100	64,5
CELF6						100

Along with HuR, CUGBP1 is a prototypic member of a family of RBPs that are known as the CUGBP and ELAV-like family proteins. These RBPs regulate a network of transcripts that control important cellular functions such as cell growth and apoptosis by binding to target transcripts. Each member of the family of CELF proteins contains three RBDs that bind to RNA, two in the N-terminal and one in the C-terminal region (Fig. 10). The RBDs show high

sequence similarity but the sequence of the linker between RBD2 and RBD3 is less well conserved. RBD1 and RBD2 are separated by a short spacer and critical for the CUGBP1 interaction with all examined RNAs.

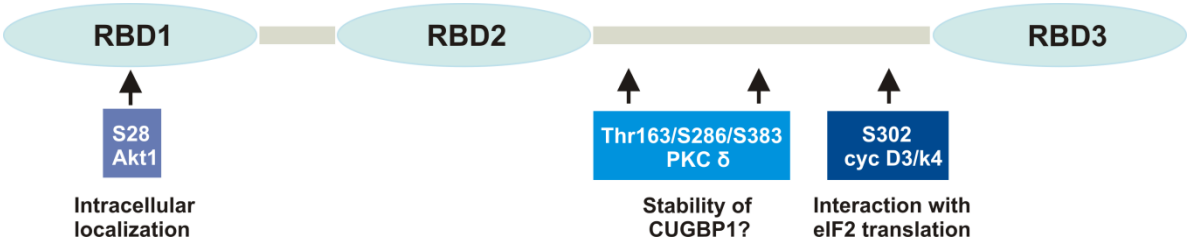

Fig. 10: Schematic representation of CUGBP1 RNA-binding domains (RBDs), modified [181]. CUGBP1 consists of three RBDs separated by spacers. The key amino acids which regulate intracellular localization of CUGBP1 (S28), translational activity of CUGBP1 (S302), and stability of CUGBP1 are shown on the bottom. The amino acids for the phosphorylation of CUGBP1 by PKCδ were found by the prediction program.

RBD3 is separated from the first two RBDs by a long linker region, which seems to be important for the regulation of RNA binding activity of CUGBP1 and for regulation between the interactions of CUGBP1 with other proteins. Although, CUGBP1 and 2 have 76% identical protein sequences and share almost identical RBPs they play different roles in post-transcriptional regulation on genes [180]. CUGBP2 stabilizes mRNA, whereas CUGBP1 acts as destabilization factor [182]. However, the effects of both proteins are cell type specific and depend on cellular conditions. CUGBP2 is mostly expressed in heart, skeletal muscle and brain, while CUGBP1 is ubiquitously expressed [183,184,185]. Both are localized in the cytoplasm as well as the nucleus [109,184,186,187]. These dual locations also suggest that these CELF proteins are multifunctional proteins implicated in molecular processes specific to each cellular compartment. Indeed a role in control of AS and translational regulation has been described [188,189,190,191].

The binding sites for CELF proteins are usually U-rich, although binding sites may contain other nucleotides like A or G. CUGBP1 and CUGBP2, almost identical in their RNA-binding domains, play different roles in post-transcriptional mRNA regulation. It has been demonstrated that CUGBP2 also binds to AREs, is sufficient to block C to U RNA editing of Mammalian apolipoprotein B (apoB) transcripts and is necessary for repression of apoB editing in cells [192]. Furthermore, CUGBP2 stabilizes and inhibits translation of COX-2 mRNAs by direct interaction with AREs in the 3´UTR [193]. In addition to the canonical GREs, CUGBP1 binds to U-rich, GU-rich sequences, or GU-repeat sequences within pre-mRNA introns or mRNA 3'UTRs. It is known that CUGBP1 regulates alternative splicing by binding to a U/G rich sequence element in the pre-mRNA [194,195]. It has been shown that

overexpression of CUGBP1 in a normal fibroblast cell line induced a strong intron retention in human specific chloride channel (CIC-1) [188]. In addition to its role as splice factor CUGBP1 has an important role in the control of mRNA translation and or stability by association with specific sequence motifs in the 3´UTR [195,196]. CUGBP1 can control translation either by acting at the 5´end of the mRNA via a G/C-rich element or mRNA deadenylation and hence degradation via a GU-rich element located in the 3´UTR. Two mRNAs were identified to bind CUGBP1 to sequence specific elements in their 5´UTR region. These are the C/EBPβ and p21 mRNAs [197,198,199]. C/EBPβ mRNA encodes a transcription factor belonging to a family of proteins that bind the enhancer CCAAT and it plays an important role in hepatocyte growth and differentiation [200]. Binding specificities, localization and functions of CUGBP1 are dependent on the different phosphorylation states of CUGBP1 [201] [202,203]. CUGBP1 has to be hyperphosphorylated for binding to the G/C rich element of p21 and C/EBPβ mRNAs [200,204]. In contrast, the deadenylation activity to GREs is activated by dephosphophorylation [202]. Additionally, CUGBP1 is functionally linked to mRNA translation in processing-bodies (PBs). Yu *et al*. described the role of CUGBP1 as translational repressor. They demonstrated that the repression of occludin translation by CUGBP1 was due the colocalization of CUGBP1 and occludin RNA in P-bodies (PBs) [151].

Abnormalities in RNA metabolism and AS are important players in complex disease phenotypes. It is known that CUGBP1 binds to $(CUG)_8$ containing RNA motifs. DM1 is genetically linked to a CUG expansion in 3´UTR of Dystrophia Myotonica protein kinase (DMPK). The overexpression of CUGBP1 has been reported in myotonic dystrophy type 1 (DM1) myoblasts, the heart, esophageal epithelial cells, skeletal muscle tissues, NSCLC, and some DM1 mouse model [204]. In addition to its role in embryonic and cardiac development, skeletal muscle and adipose tissue differentiation, and germ cell formation, CUGBP1 plays an important role tumour genesis [205,206,207,208,209].

1.4 miRNAs

miRNAs represent a new class of single-stranded RNAs of 18–22 nucleotides, which play a key regulatory role in gene expression at the post-transcriptional level [210]. They are conserved across species, expressed across cell types and active against a large proportion of the transcriptome. Since their discovery miRNAs have been shown to be involved in a wide range of biological processes such as cell cycle control, apoptosis and several developmental and physiological processes including stem cell differentiation, hypoxia,

cardiac and skeletal muscle development [211,212,213]. Furthermore, highly tissue-specific expression patterns and distinct temporal expression changes during embryogenesis suggest that miRNAs play a key role in the differentiation and maintenance of tissue identity. In addition to their important roles in healthy individuals, miRNAs have also been implicated in a number of diseases including cancer, heart diseases and neurological diseases. Lin-4 in *Caenorhabditis elegans* was the first identified miRNA. Lee *et al*. discovered that the *lin-4* gene did not encode a protein but rather a short non-coding RNA that contained sequences partially complementary to multiple sequences in the 3´UTR of the lin-14 mRNA [214]. Lin-4 regulates lin-14 gene expression by complementarily binding through base-pairing in the 3´UTR of the lin-14 mRNA and reduces the translation of the mRNA.

1.4.1 Biogenesis and regulation of miRNAs

Initially, canonical miRNA genes are transcribed into long primary transcripts (pri-miRNA) by RNA polymerase II (Fig. 11) [215]. The transcripts contain one or more hairpins, and the miRNAs are located in the double-stranded stem. RBP DiGeorge syndrome chromosomal region 8 (DGCR8) recognizes the pri-miRNA and cleaves it by interacting with the RNAse III Drosha [216,217]. This functional interaction of DGCR8 and Drosha is termed as microprocessor complex [218] (Fig. 11). Drosha cleaves at the basis of the hairpin within the pri-miRNA, resulting in a ~70 nt long hairpin molecule. This precursor miRNA (pre-miRNA) carries a two-nucleotide 3′ overhang of the RNase III-mediated cleavage that is recognized by the nuclear export factor Exportin-5 [219]. The pre-miRNA is exported to the cytoplasm by Ran-GTP dependent Exportin-5. In the cytoplasm, the RNase III enzym Dicer cleaves the pre-miRNA in complex with the double-stranded RNA-binding protein TRBP resulting in a double-stranded miRNA duplex [220,221]. Characteristically the duplex is 18–22 nt long, with one guide and a passenger strand. The guide strand is incorporated into the RNA-induced silencing complex (RISC), a large multiprotein miRNA ribonucleoprotein complex that is the effector compound in modulating target gene transcription. The RISC complex contains members of the Argonaute (Ago) protein family. They have an endonuclease activity directed against mRNA strands that are complementary to their bound miRNA fragment.

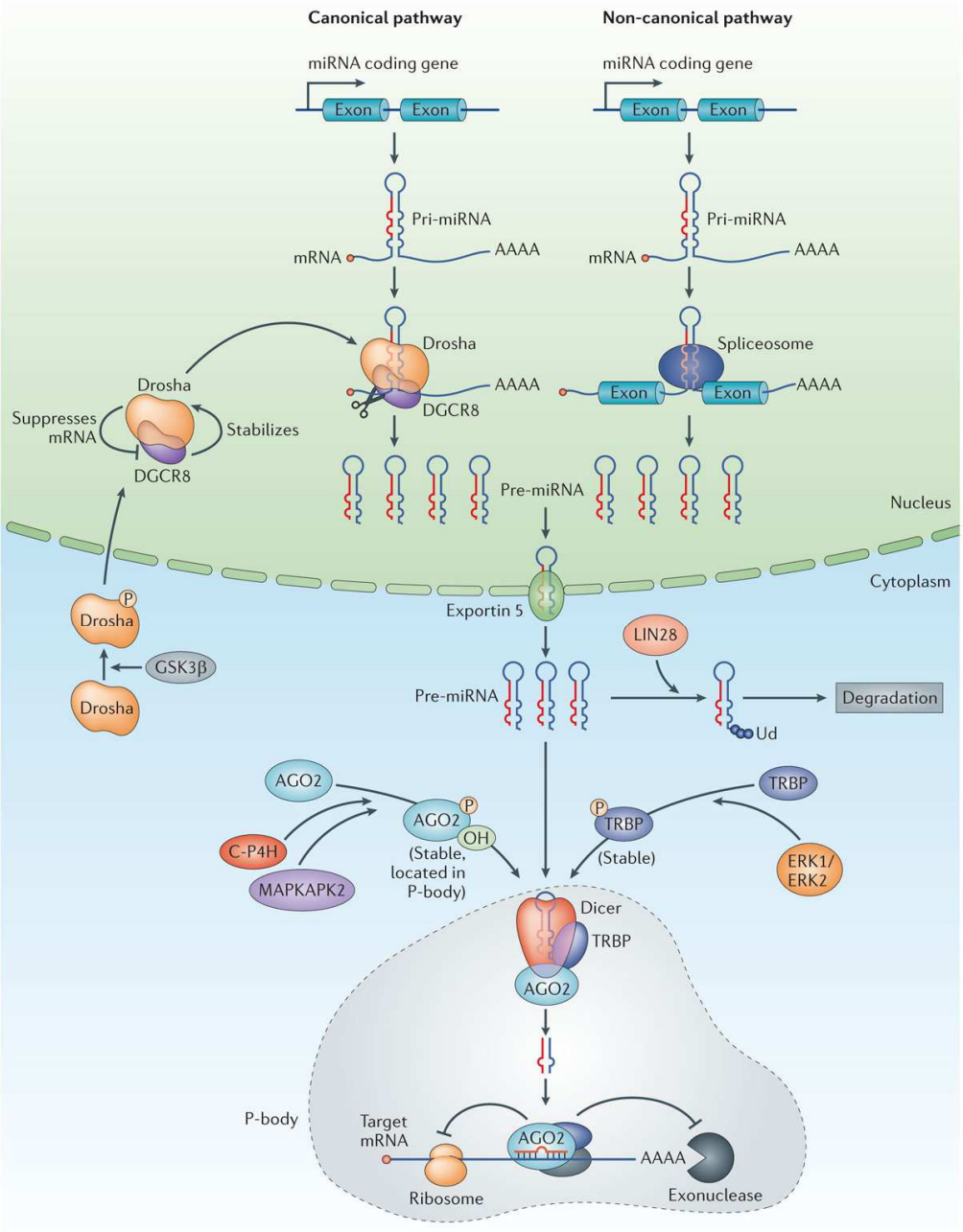

Fig. 11: Biogenesis of miRNAs. miRNAs are transcribed as pri-miRNAs by RNA-polymerase II. The pri-miRNAs are processed by Drosha into 70 nt long pre-miRNAs. Exportin-5 recognizes the structure and exports the pre-miRNA from the nucleus to the cytoplasm. Dicer processes the pre-miRNA into an imperfect double strand. The mature miRNA is incorporated into the RISC complex which is formed out of Ago proteins. The miRNA binds to the target mRNA where it can either regulate mRNA degradation, translational repression or deadenylation. Mirtrons are alternative precursors for miRNA biogenesis. The short hairpin introns use splicing to bypass Drosha cleavage, which is otherwise essential for the generation of canonical animal miRNAs, modified [222]

Selection of the guide strand from the dsRNA appears to be based primarily on the stability of the termini of the two ends [223]. The strand with lower stability base pairing of the 2–4 nt at the 5´-end of the duplex preferentially associates with RISC and thus becomes the active

miRNA. The guide strand is selected by Ago protein on the basis of stability of the 5´-end [223]. The remaining passenger strand is degraded as a RISC complex substrate. After integration into the active RISC complex, miRNAs exert their regulatory effects by binding to imperfect complementary sites within the 3´UTR of their mRNA targets. The formation of the double-stranded RNA, resulting from the binding of the miRNA, leads to translational repression.

A subclass of miRNAs, termed mirtrons, derives from short introns and enter the miRNA biogenesis pathway as Dicer substrates (Fig. 11). Mirtrons were first identified in *Drosophila melanogaster* and *C. elegans* and are a type of miRNAs that are located in the introns of the mRNA encoding genes [224,225]. Mirtrons are alternative precursors for miRNA biogenesis (Fig. 12). The short hairpin introns use splicing to bypass Drosha cleavage, which is otherwise essential for the generation of canonical animal miRNAs. Mirtrons are short intronic miRNA precursors representing an alternative, Drosha/DGCR8-independent miRNA biogenesis pathway, which relies on mRNA splicing and lariat debranching for the formation of pre-miRNA. The refolded stem loop pre-miRNA can be further processed by Dicer into mature miRNA and functions like classical miRNAs regulating gene expression, by either mRNA destabilization, inhibition of the translation or target mRNA cleavage [226].

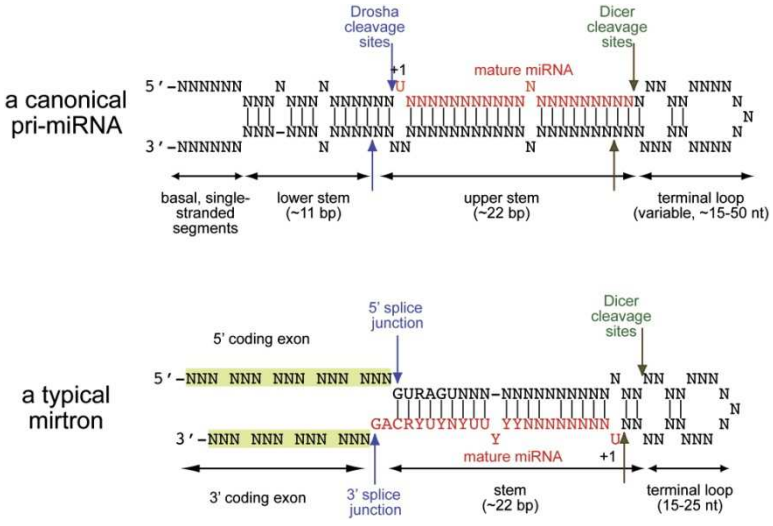

Fig. 12: Essential characteristics of pri-miRNAs and mirtrons [225]

It has been further demonstrated that miRNAs can be processed independently of Dicer. For example Ago2, can directly cleave miRNA precursors into mature miRNAs [227]. A third biogenesis strategy, similar to mirtron biogenesis, initiates from short introns (80-100 nt) but bypasses Dicer cleavage [228]. These short introns, termed as agotrons, are associated with

and stabilized by Ago proteins in the cytoplasm. Some agotrons are completely conserved in mammalian species, suggesting that they are of great functional importance.

1.4.2 Post-transcriptional gene regulation of miRNAs

In general, miRNAs post-transcriptionally regulate protein synthesis by base-pairing to partially complementary sequences in the 3´UTRs of target mRNAs but binding sites can also occur within the 5´UTR or the coding region [229,230,231], thus a plenty of mRNAs can be regulated by the same miRNA. The most common feature is perfect base-pairing between nucleotides 2 and 7 at the 5´end of the miRNA (seed region) and the target site. The miRNAs mediate mRNA repression by recruiting the miRNA-induced silencing complex (miRISC), a ribonucleoprotein complex, to target mRNAs. The core of the miRISC contains a miRNA-loaded Ago protein and GW182 [229]. The exact composition of the miRNA complex as well as the mechanisms used to control target gene expression are still uncertain**.** In animals miRNAs usually base-pair to their target mRNAs with imperfect complementarity, which predominantly leads to translational repression, although this may also induce mRNA destabilization [232,233]. However, several other mechanisms have been documented, including translational inhibition at the level of initiation and elongation, rapid degradation of the nascent protein and mRNA degradation. Vilmalraj *et al*. identified that the SMAD specific E3 ubiquitin protein ligase 1 (Smurf1) 3´UTR is directly targeted by miR-15b by that miR-15b promotes osteoblast differentiation by indirectly protecting transcription factor Runx2 from Smurf1 mediated degradation [234]. In this case miR-15b acts as a positive regulator for osteoblast differentiation. Stimulation of gene expression via a decoy mechanism was previously found for another miRNA, miR-328 [235,236]. It was shown that miR-328 acts as miRNA decoy for the poly(rC)-binding protein hnRNP E2, a global splicing factor and translation repressor thereby regulating myeloid cell differentiation. During monocyte maturation miR-328 was upregulated and antagonized hnRNP E2 which then leads to increased ROS production as well as monocyte adhesion and migration. Hence, the balance between hnRNP E2 and miR-328 is cruicial for hnRNP E2 inhibition and the concomitant upregulation of the expression of hnRNP E2 target genes.

1.4.3 Role of miRNAs in cancer and tumour development

Numerous studies demonstrated a highly specific miRNA expression profile during particular stages of tumour development. In particular, miRNAs are implicated in the process of stimulation of cellular invasion and metastasis, as well as predictors of poor prognosis of

breast cancer and lung cancer [237,238,239]. This indicates that miRNAs are a new class of genes involved in tumourigenesis [240]. Recent findings have linked the miRNA processing machinery to cancer pathogenesis. First, Dicer and Ago were found deleted in a certain subset of tumours, and Dicer protein levels were found to be reduced in poorly differentiated lung tumours with a significant impact on patient survival [241,242]. When cells exhibit abnormal growth and loss of apoptosis function, it usually results in cancer development and progression. Several recent studies indicate that miRNA regulates cell growth and apoptosis [212]. The expression of some miRNAs is decreased in cancer cells. These types of miRNAs are considered tumor suppressor genes. B cell chronic lymphocytic leukemia (CLL) is the most common adult leukemia in the western world and highly associated with loss of chromosomal region 13q14 [243]. It was demonstrated that expression of miR-16 and miR-15a was abolished or lost in 68% of CLL cases [244]. The tumor suppressing properties of these miRNAs are contributed to abnormal Bcl2 expression, an anti-apoptotic protein, which is overexpressed in CLL and thereby promoting cell survival [245]. Emerging evidence suggests that miR-let-7 may play a critical role in the pathogenesis of lung cancer [246]. In this study they observed reduced expression levels of miR-let-7 in both *in vitro* and *in vivo* lung cancer and they also observed that overexpression of miR-let-7 in A549 cell inhibited cancer cell growth. miR-let-7 negatively regulates the expression of rat sarcoma (RAS) and MYC by targeting their mRNAs for translation repression due to multiple complementary sites to miR-let-7 in their 3´UTR [247]. RAS and MYC have been implicated, together with p53, as important oncogenes in lung cancer. In lung cancer tissue levels of miR-let-7 were reduced whereas RAS protein was increased, suggesting miR-let-7 regulation of RAS as a mechanism for lung oncogenesis [247]. In contrast to miR-let-7, the expression of miRNA cluster miR-17–92 is significantly increased in lung cancer [248]. The cluster was shown to enhance cell growth in lung cancer. Interestingly, two predicted targets of the miR-17–92 cluster are two tumor suppressor genes *PTEN* and *RB2*. Whether the miR-17–92 is cluster directly involved in lung cancer development or controls lung cancer by targeting lung cancer suppressor genes is still unknown. Moreover, miR-19 has been identified as potent oncogene of the miR-17-92 cluster. It was shown that miR-19 promotes cellular growth and cancer by inhibiting the expression of phosphatase and tensin homolog (PTEN), a tumour suppressor [249]. miR-19 activates the Akt–mTOR pathway, thereby functionally antagonizing PTEN to promote cell survival. Recently, it was shown that the expression and function of the histone methyltransferase oncogene enhancer of zeste homolog 2 (EZH2) in cancer cell lines is limited by miR-101 [250,251,252]. Other links in cancer related miRNA

expression have been demonstrated by Michael *et al*, who showed that miR-143 and miR-145 are reduced in colorectal cancer [253]. However, the transcriptional level of the precursors of miR-143 and miR-145 was not altered in precancerous and neoplastic colorectal tissue, suggesting that altered transcription is not responsible for the reduced mature miRNA levels. These and other data show the important role of miRNA expression levels in the pathogenesis of human cancer.

2 Aims of this study

One of the key enzymes in the induced PG biosynthesis is mPGES-1. In the last decades it turned out that mPGES-1 and its product PGE_2 are crucial for tumour development and tumour progression. The promoter alone cannot account for the strong upregulation in these types of cancer. Until now nothing is known about post-transcriptional regulation of mPGES-1 by miRNAs or alternative splicing. Alternative splicing is a powerful mechanism of mammalian cells to regulate gene expression. However, dysregulation in splicing processes often correlates with diseases and tumour progression. Therefore, splicing patterns in different well-established cell lines for characterizing mPGES-1 were analyzed. The 3´UTR of mPGES-1 contains two GREs which could function as regulatory elements [254]. Recently, it was shown that GREs are binding sites for CUGBP1 [195]. To prove if mPGES-1 is regulated by CUGBP1, reporter gene assays, RT-PCR and REMSAs were performed. Furthermore, CUGBP1 has been demonstrated to act as potential destabilizing factor [177]. To address these issues, levels of CUGBP1 were manipulated in A549 and SF cells. Recently, it was demonstrated that besides its canonical function miR-328 is able to act as RNA decoy to hnRNP E2 [235]. Interestingly, mature miR-574-5p harbors GREs representing *bona fide* CUGBP1 binding sites. To address this mode of action, REMSAs were performed and miR-574-5p levels were manipulated. miR-574-5p was discovered as novel serum-based biomarker for early-stage NSCLC [239], therefore miR-574-5p levels in NSCLC tissues were analyzed. Furthermore, miR-574-5p enhances tumour progression via downregulating the checkpoint suppressor gene 1 in human lung cancer [255]. The tumourigenic properties of miR-574-5p were addressed by *in vivo* experiments in CD1 nude mice.

3 Materials & Methods

3.1 Cell culture

3.1.1 Cell types and cell culture conditions

The human lung adenocarcinoma cell line A549 (ATCC Manassas, VA, USA) and the cervical cancer cell line HeLa (DMSZ) were cultured in Dulbecco's modified Eagle medium (DMEM, Life technologies) with 10% (v/v) heat inactivated fetal bovine serum (Life technologies), 100 U/ml penicillin (PAA the Cell Culture Company) 100 µg/ml streptomycin (PAA the Cell Culture Company) and 1 mM sodium pyruvate (PAA the Cell Culture Company). Synovial fibroblasts of RA patients (kindly provided by Prof. P.-J. Jakobsson and Heidi Wähämaa) were cultured like A549 cells in 10% (v/v) heat inactivated fetal bovine serum (Sigma), additionally with 10 mM HEPES (Sigma Aldrich). A549 and HeLa cells were grown in T75 cell culture flasks under standard growth conditions (humidified atmosphere of 5% CO_2 at 37°C). SF cells were grown in T125 cell culture flasks under standard growth conditions (humidified atmosphere of 5% CO_2 at 37°C). When the cells were 70-90% confluent the medium was carefully removed and cells were washed with pre-warmed PBS. Cells were detached using pre-warmed Trypsin-EDTA (Invitrogen) at 37°C for 5 minutes. The reaction was stopped adding pre-warmed medium (1:1) to the cells and number of viable cells was examined by trypan blue staining (Biorad) and counted using Biorad TC10 automated cell counter. 0.5-1 million cells were transferred into a new culture flask. A549, Hela and SF cells were seeded as described in Tab. 2 .

Tab. 2: Cell density for different plate types

Plate type	Cell density	Medium (ml)
96-well	10.000	0.1
24-well	40.000	1
6-well	500.000	4

For the preparation of liquid nitrogen stocks cells were detached with pre-warmed Trypsin-EDTA, washed with pre-warmed PBS and resuspended in culture medium containing 10% (v/v) DMSO (Carl Roth). They were transferred into cryo vials (VWR) and stored at -80°C for 2 days. For long-term storage cryo vials were stored in liquid nitrogen.

3.1.2 Stimulation with IL-1β

A549 cells or synovial fibroblasts of RA patients were seeded at a density of 4 x 10^4 cells (e.g. 24-well plate) and cultured for 24 h before they were induced with IL-1β for further 24 h. A549 cells were stimulated with 5 ng/ml and synovial fibroblasts with 10 ng/ml IL-1β (Sigma Aldrich).

3.2. Transfection of HeLa, A549 and SF cells

3.2.1 Depletion of CUGBP1, UPF1 and GW182 using RNA interference

CUGBP1, GW182 and UPF1 were transiently depleted using siRNA oligonucleotides. 24 h prior to transfection, A549 cells were seeded at a density of 5 x 10^5 cells/well in a 6-well plate. 20 pmol/µl siRNA oligonucleotides were transfected using Lipofectamin2000® (Invitrogen) according to manufacturer's instructions. For UPF1 knockdown, MISSION® siRNA SASI_Hs01_00101017-19 (Sigma Aldrich) and for GW182 knockdown, MISSION® siRNA SASI_Hs01_00244664 (Sigma Aldrich) were used. For CUGBP1 knockdown a previously published siRNA (5´-GCUGUUUAUUGGUAUGAUU-3´) was used for the experiments [194]. As control a siRNA against GFP, naturally not expressed, was designed (5´-UCUCUCACAACGGGCAUUU-3´). Cells were harvested 24 h and 48 h after transfection. The efficiency of UPF1, CUGBP1 and GW182 knockdown was proven by qRT-PCR, Western blot analysis and Immunofluorescence staining, respectively.

3.2.2 Overexpression of miR-574-5p

The miRIDIAN hsa-miR-574-5p mimic (HMI0794, Sigma Aldrich) and negative control (HMC0002, Sigma Aldrich) were used for transient overexpression of miR-574-5p. 24 h prior to transfection A549 cells were seeded at a density of 5 x 10^5 per well in a 6-well plate. For miR-574-5p overexpression 20 pmol/µl mimics per well were transfected using Lipofectamin2000® (Invitrogen) according to the manufacturer´s instructions. The efficiency was assessed by qRT-PCR analysis.

The lentiviral particles Mission® lenti miR-574-5p (HLMIR0794, Sigma Aldrich), respectively Mission® lenti control (NCLMIR001, Sigma Aldrich) were used for generating the stable A549 miR-574-5p overexpression and control cell lines. 24 h prior to transduction, A549 cells were seeded at a density of 5 x 10^5 per well in a 6-well plate. Lenti viral particles were quickly thawn and added to A549 cells at an MOI of 0.83 for spinoculation (875 g, 32°C for 60 min). The transduced cells were grown for one day before 10 µg/ml puromycin (Sigma Aldrich)

was added for four days to select the transduced clones. The transduction efficiency was verified by qRT-PCR. The transduction of A549 cells for miR-574-5p overexpression was performed by Stefan Stein, Georg-Speyer Haus in Frankfurt.

3.2.3 Depletion of miR-574-5p by LNAs™

miR-574-5p was transiently depleted using LNAs™ from Exiqon (miR-574-5p-LNA™ inhibitor and a negative control MIMAT0004795). 24 h prior to transfection A549 were seeded at a density of 5 x 10^5 cells per well in a 6-well plate. 40 pmol/µl per well was transfected using Lipofectamin2000® (Invitrogen) according to manufacturer's instructions. The knockdown efficiency was assessed by qRT-PCR analysis.

3.3. DNA methods

3.3.1 *Escherichia coli* culture conditions

All media were autoclaved for 20 min at 120°C and 1 bar above atmospheric pressure. Heat-sensitive materials e.g antibiotics were filtered and then added to the autoclaved medium. In disc media 1.5% agar was added before autoclaving. For the cultivation of *Escherichia coli* (*E.coli)* strains Luria Broth medium (LB) was used. 10 g tryptone (Carl Roth), 10 g NaCl (Carl Roth) and 5 g Yeast extract (Carl Roth) were diluted in 1l Milli Q water (MQ). For selections 100 ug/ml ampicillin (Carl Roth) was added. Cultivation was carried out with shaking at 150 rpm and 37°C.

3.3.2 Preparation of chemo competent *E.coli* cells

100 ml of LB medium was inoculated with 5 ml of an overnight culture and shaked at 150 rpm at 37°C until OD_{600} 0.4-0.6 was reached. Cells were then incubated for 10 min on 4°C and harvested by centrifugation at 4000 rpm for 15 min. Cells were resuspended in sterile RF1 solution (50 mM $RbCl_2$, 20 mM $MnCl_2$ x 2 H_2O, 15 mM KAc, 5 mM $CaCl_2$, 1.63 M glycerine pH 5.8, all chemicals supplied from Carl Roth). Cells were subsequently incubated for 1 h at 4°C and harvested by centrifugation for 15 min at 4000 rpm and 4°C. *E.coli* cells were then resuspended in 2 ml RF2 solution (0.7 mM MOPS, 2 mM $RbCl_2$, 15 mM $CaCl_2$ x 2 H_2O, 1.63 M glycerin, pH 6.8, all chemicals supplied from Carl Roth). Cells were incubated for 15 min on ice and defined aliquots of the cell suspension were shock-frozen in liquid nitrogen and stored at -80°C until usage.

3.3.3 Spectrometric quantification of nucleic acids

The determination of the concentration and purity of nucleic acid aqueous solutions (dsDNA, ssDNA and RNA) was carried out by UV spectroscopic measurement using the NanoDrop ND-1000 spectrophotometer (Thermo Fischer).

3.3.4 Gel electrophoresis

Nucleic acid electrophoresis was used to separate DNA or RNA fragments by size and reactivity. Depending on the desired resolution agarose gels with a concentration of 1-3% (w/v) were prepared in TAE buffer (2 M Tris, 1 M Acetic acid, 1 mM EDTA, pH 8.3, all chemicals supplied from Carl Roth). The samples were mixed with 6x DNA loading buffer (10mM Tris-HCl pH 7.6, 60 mM EDTA, 60% Glycerin, and 0.03% Bromphenol blue, all chemicals supplied from Carl Roth) and separated at 8-10 V/cm gel length in 1x TAE buffer. As DNA standards Ultra Low Range DNA Ladder II (Peqlab) or 1 kb DNA ladder (Peqlab) were used. The gels were stained in ethidium bromide solution (Carl Roth) for 5 min.

3.3.5 DNA gel extraction

For purification of DNA fragments from agarose gels, the appropriate bands were excised and purified by QIAquick™ (Qiagen) gel elution Kit according to manufacturer's instructions.

3.3.6 Isolation of plasmid DNA

Plasmid DNA was isolated using QIAprep Spin Miniprep Kit (Qiagen) according to manufacturer’s instructions.

3.3.7 Polymerase chain reaction

The amplification of DNA segments was carried out using the polymerase chain reaction (PCR). The obtained DNA fragments were used for analysis, cloning or as a template for DNA sequencing. The *Taq*-DNA polymerase (New England Biolabs) or Q5® high-fidelity DNA polymerase (New England Biolabs) were used for PCR. The reaction proceeded in a thermocycler T100 (Biorad). A typical PCR reaction with 50 µl total volume (Tab. 3) contained the following components and has been conducted according to following program in Tab. 4.

Tab. 3: Standard PCR mastermix for *Taq*-polymerase or Q5-DNA polymerase*

Amount	Component
1 µl	Template DNA (chromosomal DNA), Plasmid-DNA ~1-2 ng/ µl
0.5 µl	Oligonucleotide fwd (100 pMol/ µl)
0.5 µl	Oligonucleotide rev (100 pMol/ µl)
3 µl	10x dNTP-Mix (2 mM dATP, dGTP, dCTP & dTTP)
5/10* µl	10x *Taq*-Pol. buffer / 5x Q5 reaction buffer*
0.5 µl	DNA-polymerase
ad 50 µl	H_2O

Tab. 4: Standard PCR program for *Taq*-polymerase or Q5-DNA polymerase*

Temperature		Time	Step
96 °C / 98 °C*		5 min/1 min*	Denaturation
96 °C / 98 °C*	31-34x	30 sec/10 sec*	Denaturation
52 °C		30 sec	Hybridization of oligo-nucleotides
72 °C		60/30* sec pro kb DNA fragment	DNA elongation
72 °C		5 min	final DNA elongation
4 °C		-	cooling

Hybridization temperatures were based on primer length and GC content. The extraction of DNA fragments from agarose gels was performed using the Qiaquick™ gel elution kit (Qiagen) or Qiaquick™ PCR purification Kit (Qiagen) according to the manufacturer's instructions.

3.3.8 Fragmentation of DNA using restriction endonucleases

Double-stranded DNA was fragmented with restriction enzymes (New England Biolabs) in manufacturer's specified reaction buffer. The amount of enzyme units as well as the duration of the restriction was adjusted to the amount of DNA and the characteristics of the nucleases. The required amount of restriction enzyme was calculated with Formula 1:

$$U = M_p \times \left(\frac{l_r \times n_p}{l_p \times n_r}\right)$$

Formula 1: Amount of restriction enzyme. U: enzyme units; m_p: mass of dsDNA [ng]; l_r: length of reference λ-DNA [48502 bp]; n_p: number of restriction sites within dsDNA; l_p: length of dsDNA [bp]; n_r: number of restriction sites within λ-DNA.

3.3.9 Ligation of DNA fragments

Ligation of DNA fragments proceeded after according to Sambrook and Russell established method [256]. For ligation vector and insert DNA were used in a molar ratio of 1:3. In Tab. 5 a standard ligation reaction is listed.

Tab. 5: Standard ligation

Component	Amount
T4 Ligase buffer (10x)	2 µl
ATP (1 mM final concentration)	1 µl
T4 DNA Ligase	2 µl
MQ	ad 20 µl

The T4 DNA Ligase (New England Biolabs) was used for ligation of amplified DNA inserts and the digested plasmid. The ligation was performed overnight at 16°C in a total volume of 20 µl. The ligation performance was controlled by reaction without insert.

3.3.10 Cloning and plasmid constructs

The pDL Dual Luciferase plasmid, the pCMV-MS and the pCUGBP1 overexpression plasmid were kindly provided by Julia Weigand [257]. mPGES-1 3´UTR cDNA was amplified from A549 cells using *Not*I-mPGES-1 3´UTR-forward and *Hind*III-mPGES-1 3´UTR-reverse primers (Tab. 6) and cloned into the pDL Dual Luciferase plasmid via *Not*I and *Hind*III restriction sites resulting in pDL_mPGES-1 3´UTR plasmid. Deletions of the two GU-rich elements were generated by site-directed mutagenesis PCR on mPGES-1 3´UTR plasmid. For deletion of the first GRE element the primers ΔGRE1_fw and ΔGRE1_rev (Tab. 6) were used resulting in the plasmid pDL_ΔGRE1_mPGES-1 3´UTR, followed by *Dpn*I (New England Biolabs) digestion. The deletion of the second GU-rich element was generated using ΔGRE2_fw and ΔGRE2_rev (Tab. 6) resulting in pDL_ΔGRE2_mPGES-1 3´UTR. The double deletion mPGES-1 3´UTR-ΔGRE1-ΔGRE2 was generated by mutagenesis PCR on the single mutant pDL_mPGES-1 3´UTR mGRE1 resulting in the plasmid pDL_ΔGRE1ΔGRE2_mPGES-1 3´UTR.

Tab. 6: Primers for cloning mPGES-1 3´UTR constructs

Primer name	5´-3´direction
mPGES-1 3`UTR-forward_*Not*I	AAGCGGCCGCCCAGCAGCTGATGCCTCCT
mPGES-1 3`UTR-reverse_*Hind*III	AAAGCTTTGCTGGGCCCAGCTGGCA
ΔGRE1_fw	TCCCCTTGATGGGGAATCCTTTCTCCTAGACCCGTGACC
ΔGRE1_rev	CGGGTCTAGGAGAAAGGATTCCCCATCAAGGGGA
ΔGRE2_fw	GCGCGTGTGGGTCTCTGGGCACAGTGGGCCTTTTCTTAGCCCCT TGGATTCCTGC
ΔGRE2_rev	GCAGGAATCCAAGGGGCTAAGAAAAGGCCCACTGTGCCCAGAGA C

For the *in vitro* transcription specific primers for plasmids pHDV_GRE1 and pHDV_GRE2 (Tab. 7) were used. For pHDV_GRE1 (GRE1_fwd and GRE1_rev) and pHDV_GRE2 (GRE2_fwd and GRE2_rev) were annealed and cloned via *EcoR*I and *Nco*I restriction sites into the high-copy-number plasmid pHDV [258]. In this way the HDV ribozyme was added to the 3´ end of GRE1 and GRE2 giving homogeneous 3´ends after *in vitro* transcription.

Tab. 7: Primers for REMSA constructs

Primer name	5´-3´direction
GRE1_fw	AAAAAAGAATTCTAATACGACTCACTATAGGTGTGTGTGTGCCCGTGT G
GRE1_rev	TTTTTTCCATGGCCGGCACATACACACACACATACACACACACGGGCA CACACACACCTATAGT
GRE2_fw	AAAAAAGAATTCTAATACGACTCACTATAGGGTGTGTGTGTGTGTG
GRE2_rev	TTTTACCATGGCCGGCCACACACACACACACACACACACACACACA CACACACACACACACCCTATAGTG

3.3.11 Transformation of *E.coli*

The transformation of the *E. coli* strains was performed by heat-shock method. The chemically competent cells were thawed on ice. In the case of ligation 10 µl mixture was transformed. For retransformation 0.5-1 µl plasmid DNA was used. The DNA was added to 100 µl competent cells and incubated for 30 minutes on ice. This was followed by a heat-shock (30-45 sec at 42°C). The mixture was briefly cooled on ice, 0.5 ml of LB medium was

added and cells were incubated for 1 h at 37°C and subsequently platted on LB plates with the appropriate selection marker.

3.3.12 Sequencing

The sequences of all plasmids were determined based on the method by Sanger reaction. The sequencing was performed by SRD (Scientific Research Development, Bad Homburg) and Seqlab (Göttingen).

3.4 RNA methods

3.4.1 RNA extraction and reverse transcription

Total RNA was extracted with TRIzol Reagent (Invitrogen) and treated with Turbo DNase (Ambion) for 5 min according to manufacturer's instructions. 1 µg of DNase-treated RNA was used for reverse transcription using High-Capacity RNA-to-cDNA Kit (Applied Biosystems) according to manufacturer's instructions. Usually 10 µl 2x RT buffer and 1 µg RNA dissolved in 9 µl MQ was mixed with 1 µl RT enzyme. miR-574-5p detection was performed using the Qiagen miScript system. 1 µg DNase digested RNA was used for reverse transcription according to the manufacturer's instructions. A standard mix for one reaction was 4 µl miScript HiSpec Buffer 5x, 2 µl miScript Nucleic Acid Mix 10x, reverse transcriptase 2 µl, 1 µg DNase digested RNA and H_2O ad 20 µl.

3.4.2 RT-PCR analysis

Primers mPGES-1 3´UTR forward (CCAGCAGCTGATGCCTCCTTG) and mPGES-1 3´UTR reverse (GCCCAGCTGGCAGACACTTCC) were used for specific amplification of mPGES-1 3´UTR. PCR was carried out using 2.5 U Taq polymerase (New England Biolabs) according to the manufacturer's instructions with the addition of 50 µM betaine (Sigma Aldrich). Cycle numbers were minimized for each series of experiments in order to keep the PCR reaction in the exponential phase and to avoid saturation effects. One tenth of each PCR sample was analyzed by gel electrophoresis on a ethidium bromide-stained agarose gel. QIAquick Gel Extraction Kit (Qiagen) was used for gel extraction of the RT-PCR products. PCR CloningPLUS Kit (Qiagen) was used to clone the isolated PCR fragments according to manufacturer's instructions. The selected recombinant plasmids were then sequenced.

3.4.3 Real-time quantitative RT-PCR (qRT-PCR)

1 µg of DNase-treated RNA was used for reverse transcription using High-Capacity RNA-to-cDNA Kit (Applied Biosystems) according to manufacturer's instructions. Real-time PCR was performed in Applied Biosystems StepOne Plus™ Real-Time PCR System (Applied Biosystem) using Power Syber Green PCR Master Mix (Applied Biosystems). A standard mix for one reaction was 10 µl 10x Sybergreen Mastermix, 1 µl cDNA (1:2 diluted), 3.75 µl forward Primer (1:50 diluted), 3.75 µl reverse Primer (1:50 diluted), and 1.5 µl H_2O. Actin was used as endogenous control to normalize variations in cDNA quantities from different samples. Each sample was set up in duplicates. Fold inductions were calculated using formula $2^{(-\Delta\Delta Ct)}$. The sequences for primer pairs are depicted in Tab. 8.

Tab. 8: Specific primers for qRT-PCR analysis using Sybergreen

Primer name	5´- 3´direction
GW182_Fwd	AATCTGGTGCAGCAAACTCC
GW182_Rev	AGTGTTTTGTGCAGGGGTTC
CUGBP1_Fwd	AAAGTCCTCCCAGGGATGCA
CUGBP1_Rev	AGCTTCCTGTCTTCCACTGCAT
3UTRisoform_Fwd	GTGCCCGTGTGTGTGTATGTGTGTGTGT
3UTRisoform_Rev	CCCAGCTGGCAGACACTTCCATTTAATGACT
COX-2_Fwd	CCGGGTACAATCGCACTTAT
COX-2_Rev	GGCGCTCAGCCATACAG
mPGES1_Fwd	TCCCGGGCTAAGAATGCA
mPGES1_Rev	ATTGGCTGGGCCAGAATTTC
Actin_Fwd	CGGGACCTGACTGACTAC
Actin_Rev	CTTCTCCTTAATGTCACGCACG

qRT-PCR of miR-574-5p expression was performed using the miR-574-5p specific primer (MS00043617, Qiagen). RNA U6 primer was used as endogenous control (MS00033740, Qiagen). miR-574-5p expression of NSCLC tissue samples were normalized to miRNA reverse transcription control using miRTC primer (MS00000001, Qiagen). Real-time PCR was performed according to the manufacturer's instructions. A standard mix for one reaction was 12.5 µl QuantiTect Syber Green Mastermix, 2.5 µl miScript Universal primer 10x, 2.5 µl U6 or miR-574-5p primer, 1 µl miScript cDNA (1000 ng) and 6.5 µl H_2O. Fold inductions were calculated using $2^{(-\Delta\Delta Ct)}$ values.

3.4.4 *In vitro* transcription

The GRE1 and GRE2 RNA was *in vitro* transcribed as described previously [259]. For large scale RNA synthesis the RNA was *in vitro* transcribed using of the linearized (*Hind*III) plasmids pHDV_GRE1 and pHDV_GRE2 (see 3.3.10). Isolated plasmids were linearized with *Hind*III (NEB) and purified by phenol (Carl Roth) treatment. The linear DNA (1-2 mg) was mixed with 200 mM Tris-HCl pH 8.0 (Sigma), 20 mM magnesium acetate (Sigma), 50 mM DTT (Carl Roth), 2 mM spermidine (Carl Roth), 4 mM each NTP (Carl Roth) and 15 ul T7 RNA polymerase (NEB). The transcription was incubated for 16 h at 37°C and then separated on a 15% denaturing Polyarcylamide (PAA) gel. The product band was excised, eluted overnight in 10 ml 300 mM sodium acetate pH 6.5, precipitated in ethanol/acetone (1:1) for 1 h at -20°C and centrifuged for 1 h at 8500 rpm. The RNA containing pellet was washed with 70% ethanol and resuspendend in 100 µl autoclaved MQ.

3.4.5 RNA electrophoretic mobility shift assay (REMSA)

Cytoplasmic extracts were prepared by lysing 4-6 million cells for 10 min on ice in 200 µl buffer containing 0.2% Nonidet P-40 (Sigma-Aldrich), 40 mM KCl (Sigma-Aldrich), 10 mM HEPES (pH 7.9) (Sigma-Aldrich), 3 mM $MgCl_2$ (Sigma-Aldrich), 1 mM DTT (Sigma-Aldrich), 5% glycerol (Sigma-Aldrich) and protease inhibitor (Roche). Nuclei were removed by centrifugation at 13300 rpm for 2 min and cytoplasmic extracts were immediately frozen on dry ice and stored at –80°C. The protein concentration of the extracts was determined by Bradford assay (see 3.5.1). GRE1 and GRE2 RNA probes were *in vitro* transcribed as described previously (3.4.4). The miR-574-5p (5´-UGAGUGUGUGUGUGUGAGUGUGU-3´) and mGRE1 (5´-GGUCACGGUCACGGUCACGGUCACGGUCACGGUCACGGU-3´) RNA probes were commercially synthesized by Sigma Aldrich. RNAs were end labeled with [γ^{32}P] ATP (6,000 Ci/mmol, Hartmann) using T4 polynucleotide kinase (Invitrogen) according to the manufacturer's instructions to produce a radioactively labeled probe with a specific activity of cpm/µg. EMSA assays were conducted by incubating cytoplasmic extracts with the ^{32}P-labeled RNA probe at room temperature for 30 min in a buffer containing 0.2% Nonidet P-40, 40 mM KCl, 10 mM HEPES (pH 7.9), 3 mM $MgCl_2$, 1 mM DTT, and 5% glycerol and 5 mg/ml heparin sulfate (Sigma-Aldrich). Each reaction contained 10-70 µg of cytoplasmic protein, and 10 fmol of radiolabeled RNA probe in a total volume of 15 µl for 20 min. Recombinant CUGBP1 protein was purchased by Abnova (H00010656-P01). Each sample was mixed with 5 µl 5x native loading buffer (50%, v/v, glycerol, 0.2% bromophenol blue, 0.5x TRIS-Borate-

EDTA buffer, Sigma-Aldrich). The mixtures were separated by electrophoresis under nondenaturing conditions on 6% polyacrylamide gels. The gels were analyzed on a Typhoon phosphorimager (Amersham Biosciences).

3.5 Protein methods

3.5.1 Protein concentration determination

The protein content was determined by Bradford assay (BioRad Laboratories). A standard curve was determined with BSA concentrations of 50-500 µg/ml. 10 µl of the different BSA concentrations, as well as 10 µl of the cell extract (0.5 µl probe + 9.5 µl MQ), were transferred on a 96-well plate and 190 µl of the Bradford reagent was added. The absorption at 595 nm was measured at a Tecan Infinte M 200 (Tecan Group). The protein concentration was calculated according to the determined standard curve.

3.5.2 Cell lysis

Cells were lysed in T-PER™ tissue protein extraction reagent (Life technologies) with EDTA-free protease inhibitor (Roche) for 30 min at 4°C. The protein content of the supernatant was determined by Bradford assay (BioRad Laboratories, see 3.6.1).

3.5.3 SDS-PAGE and Western Blot

60–120 µg protein lysate depending on the approach was separated by Sodium dodecyl sulfate polyacrylamide gel electrophoresis (SDS-PAGE) 12%, transferred to a HyBond ECL nitrocellulose membrane (Amersham) and blocked with Odyssey blocking buffer (*LI-COR*® Bioscience) for 1 h at room temperature. The membranes were then incubated over night at 4°C with primary antibodies that recognize mPGES-1 (Cayman and [260]), GAPDH (2118, Cell signaling), CUGBP1 (ab9549, Abcam), phosphorylated CUGBP1 (15903, Abnova), Lamin a/c (4777S, Cell signaling) and COX-2 (sc-1745, Santa Cruz). Membranes were washed with PBS (Invitrogen) pH 7.4/Tween20 0.1% (v/v) (Carl Roth) and incubated with infrared dye conjugated secondary antibodies (IRDye®, *LI-COR*® Bioscience) for 45 min at room temperature. Membranes were washed three times with PBS-Tween buffer. Visualization and quantitative analysis was carried out with the Odyssey Infrared Imaging System (*LI-COR*® Biosciences).

For separating nuclear and cytosolic fractions 0.5-1 million cells were lysed in 75 µl cytosolic extraction buffer containing 10 mM HEPES pH 7.9 (Sigma Aldrich), 1,5 mM $MgCl_2$ (Sigma

Aldrich), 10 mM KCl (Sigma Aldrich), EDTA-free protease inhibitor (Roche) on ice for 5 min. Afterwards samples were centrifuged for 3 min (6500 rpm). The supernatant contained the cytosolic fraction. The pellet was further resuspended in nuclear extraction buffer containing 20 mM HEPES pH 7.9, 1,5 mM $MgCl_2$, 0,42 M NaCl (Sigma Aldrich), 0,2 mM EDTA (Sigma Aldrich) 25 % glycerin (Sigma Aldrich) and protease inhibitor EDTA-free (Roche) for 15 min at -80°C. Samples were frozen and thawed at 37°C three times. Samples were centrifuged for 15 min at 13300 rpm. The supernatant contained the nuclear fraction.

Tab. 9: Dilution of antibodies

Primary antibody	Dilution
Actin	1:1000
CUGBP1	1:500
CUGBP1-P	1:250
GAPDH	1:1000
mPGES-1	1:250
Lamin a/c	1:1000
COX-2	1:200

3.6 Luciferase reporter gene assay

24 h prior to transfection, 4 × 10^4 HeLa cells per well were seeded in 24-well plates. 100 ng/well of mPGES-1 3´UTR constructs and 300 ng/well pCUGBP1 [257] or pCMV-MS as control, respectively, were used for transfection with Lipofectamin2000® (Invitrogen) according to the manufacturer´s instructions. After 48 h, cells were assayed for luciferase activity using the Dual-Glo™ Stop and Glow Luciferase Assay System (Promega) with a TECAN infinite M200 reader. *Renilla* luciferase activity was used to normalize the luciferase activity to the transfection efficacy.

3.7 Tetrazolium reduction assay

MTT (3-(4,5-dimethylthiazol-2-yl)-2,5-diphenyltetrazolium bromide) tetrazolium (Carl Roth) reduction assay was performed to investigate metabolic active and proliferating cells. 24 h prior transfection, A549 cells were seeded at a density of 10.000 cells per well in 96-well plates. (The mPGES-1 inhibitor CIII was kindly provided by Prof. P.-J Jakobsson). For the MTT cell proliferation assay 20 µl of 5 mg/ml MTT (in PBS) was added to the cells in culture and incubated for 4 h. The media was removed and 100 µl DMSO (Carl Roth) was added. The quantity of formazan was measured by recording changes in absorbance at 570 nm

using a plate reading spectrophotometer. As reference the wavelength of 630 nm was used to correct nonspecific background values.

3.8 Immunofluorescence staining of cells

5×10^5 A549 cells were seeded on cover slides 18 x 18 cm in 6-well plates and cultured before they were fixed using 500 µl 4% cold Paraformaldehyde (PFA, Carl Roth) for 15 min. Twice washed with PBS, followed by 5 min permeabilization with 500 µl 0.5% Triton X-100 (Sigma Aldrich). The cells were blocked with 1 ml 2% BSA in PBS (Sigma Aldrich) for 1 h. Primary antibodies GW182 (ab66009), CUGBP1 (ab9549), and DCP1a (ab70522), all purchased from Abcam, were diluted in blocking buffer and incubated with cells overnight at 4°C (Tab. 10). Cells were washed twice with PBS and incubated with secondary antibody (1:1000) goat anti-mouse IgG (Alexa Fluor® 594, ab150116) or goat anti-rabbit IgG (Alexa Fluor® 488, ab150077), respectively, from Abcam for 2 h at room temperature. Cells were stained with 4′,6-Diamidine-2′-phenylindole dihydrochloride (DAPI, Sigma Aldrich) for 2 min. Images were processed with 20 x magnitude using Axio Observer microscope (Zeiss, Jena, Germany) with LSM 510 Meta (Zeiss) image-processing software**.**

Tab. 10: Dilutions of antibodies

Primary antibody	Dilution
GW182	1:100
CUGBP1	1:500
DCP1a	1:1000

3.9 Prostaglandin E_2 levels in supernatants

Prostanoids from cell culture supernatants were extracted using a 30 mg 1cc HLB single extraction column (Waters Corporation, Milford, MA, USA). 1 ml methanol was used to pre-condition the column followed by a wash with 1 ml deionized water acidified with 0.05% formic acid. Sample was loaded to the column and was subsequently washed with 1 ml deionized water containing 5% methanol acidified with 0.05% formic acid. Sample was eluted into 1 ml methanol and evaporated under vacuum. For LC-MS/MS analysis samples were resolved in 50 µl deioinized water containing 7% acetonitrile (Merck Millipore) prior to analysis by Waters 2795 HPLC (Waters Corporation, MA, USA) coupled to a triple quadrupole mass spectrometer (Acquity TQ Detector, Water Corporation). Injection of 40 µl aliquots was made to a Synergi Hydro-RP column (100 mm x 2 mm i.d, 100 Å pore size and 2.5 µm particle size, Phenomenex, CA) with a 45 min stepwise linear gradient. As mobile

phase A, deionized water was used; acetonitrile acidified with 0.05% formic acid was used as mobile phase B. The first step with the duration of 9 min was followed by mobile phase B increased from 10% to 25%, then to 45% during 22 min in step two and moreover to 70% during 5 min in step three. 90% mobile phase B was applied as washing step and then re-equilibrated at 10 % mobile phase. Multiple reaction monitoring (MRM) mode was used for detection of analyses and quantified using internal standard calibration for PGE_2, PGD_2, $PGF_{2\alpha}$, TXB_2, 6-keto-$PGF_{1\alpha}$, 13,14-dihydro-15-keto-PGE_2 and 15-deoxy-$\Delta^{12,14}$ PGJ_2. Prostaglandin levels in supernatants were kindly analyzed by J. Raouf and H. Idborg, Karolinska Institut, Stockholm. Supernatants of the stable integrated A549 cell lines were kindly analyzed by Prof. P. Patrignanis Laboratory, University of Chieti, Italy.

3.10 Animal experiments

CD-1® Nude mice were purchased from (Charles River, Milan, Italy). The animals were housed in cages up to five mice each and acclimated for one week under conditions of controlled temperature (20±2°C), humidity (55±10%), and lighting (7:00 a.m. to 7:00 p.m.). For all experiments, mice were housed under specific pathogen-free conditions and allowed free access to food and water. Age-matched female (6-week-old to 8-week-old) were used for all experiments. A549 control cells or A549 miR-574-5p oe cells were resuspended in PBS ($5x10^6$/100µl) and then subcutaneously injected into both dorsal flanks of mice to establish a model of tumour-bearing mice. For the *in vivo* studies, the mPGES-1 inhibitor (CIII, 28575) was dissolved in 1% Tween 80 (Sigma-Aldrich) and 0.5% carboxymethylcellulose (Sigma-Aldrich) in 0.9% NaCl solution (vehicle) and administered every day (50 mg/kg, i.p.), once a day from tumour cell implantation until sacrifice (day 27, i.e. for 4 weeks). Control mice received A549 control cells (n=8) or A549 miR-574-5p oe cells (n=8) and were treated with vehicle, every day, once a day by i.p. injection from tumour cell implantation until sacrifice. A group of mice (n=6) received A549 control cells or A549 miR-574-5p oe cells (n=6) and were treated with CIII (50 mg/kg) every day, once a day by i.p. injection from tumour cell implantation until sacrifice. Tumour growth was monitored three times a week from tumour cell implantation until sacrifice by measuring its diameter with a digital calliper. Tumour volume (TV) was calculated by [$TV(cm^3)$ = length[D(cm)]×width [$d(cm)^2$]×0.44]. Body weight was monitored three times a week until sacrifice and tumour weight of dissected tumours was assessed at the sacrifice. Mice were sacrificed after 4 weeks from tumour cell implantation, 30 min after the last treatment. The experiments were performed in the lab of Prof. P. Patrignani University of Chieti, Italy.

3.11 Statistics

Results are given as mean + SEM of three independent experiments. Statistical analysis was carried out by Student's paired or unpaired t-test (two-tailed), respectively, for the time course experiments with 2-way ANOVA (Bonferroni post test) using GraphPad Prism 5.0. Differences were considered as significant for $p<0.05$ (indicated as * for $p<0.05$, ** for $p<0.01$ and ***for $p<0.001$).

4 Results

4.1 A novel mPGES-1 3´UTR splice variant regulated by CUGBP1

4.1.1 Identification and characterization of a novel mPGES-1 3´UTR variant

A pilot study of the P.-J. Jakobsson and D. Steinhilber groups revealed the existence of different splice variants of mPGES-1 mRNA in different cell lines analyzed by RT-PCR and sequence analysis. One of these splice variant was further investigated in synovial fibroblast from rheumatoid arthritis (RA) patients, adenocarcinoma cell line A549 and cervix carcinoma cell line HeLa, since they are well-established systems for characterizing mPGES-1 expression [70]. To investigate the existence of one of the mPGES-1 splice variants RT-PCR analysis was performed in these cell lines with specific primers (mPGES-1 3´UTR forward and reverse, chapter 3.4.2) covering the complete 3´UTR (Data from Meike Saul). The analysis revealed the presence of a novel short 3´UTR variant (Fig. 13 A). Sequence analysis demonstrated that mPGES-1 3´UTR isoform was generated by splicing out an intron, which removes the middle part of the 3´UTR (Fig. 13 B).

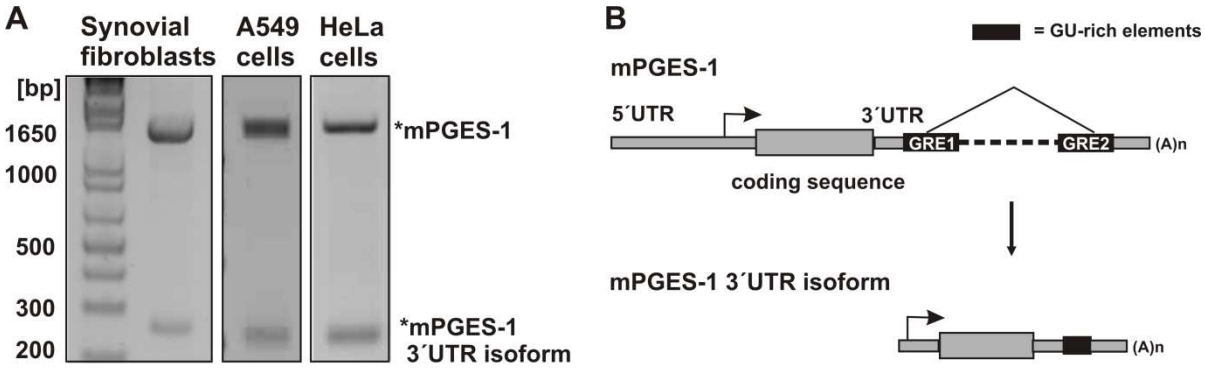

Fig. 13: Identification and characterization of a novel mPGES-1 3´UTR isoform. (A) RT-PCR products obtained with a primer pair (see chapter 3.4.2) covering complete mPGES-1 3´UTR in synovial fibroblasts of RA patients, A549 and HeLa cells separated on a 1% agarose gel. The existence of the PCR products were confirmed by at least one sequenced recombinant clone. (B) Schematic representation of the identified mPGES-1 3´UTR isoform. GU-rich elements (GREs) are indicated by black boxes.

4.1.2 CUGBP1 binds to GU-rich elements within mPGES-1 3´UTR

Interestingly, both intron boundaries are flanked by GU-rich elements (GREs) [254], GRE1 position chr9:129739418-129739456 39bp and GRE2 chr9:129738411-129738458 46bp, which may represent binding sites for the RNA-binding protein CUGBP1 [195]. It has been described for e.g. JunD and NDUFS2 that GU-repeat sequences are binding sites for

CUGBP1 [195,203]. To prove the binding affinity of CUGBP1 to GRE1 and GRE2 of mPGES-1 3´UTR, RNA EMSAs (REMSAs) were performed with radiolabeled RNA probes of GRE1 and GRE2. Therefore various cytosolic protein lysates of A549 cells with or without CUGBP1 overexpression (CUGBP1 oe) were prepared. The overexpression of CUGBP1 protein was confirmed by Western blot analysis and revealed a 3.5 fold induction (Fig. 14).

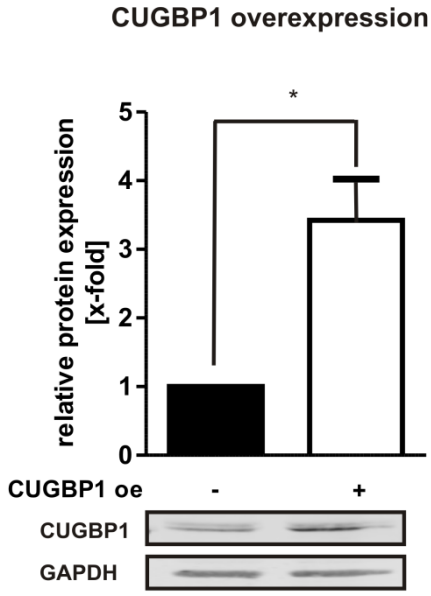

Fig. 14: Quantification of CUGBP1 overexpression in A549 cells via Western Blot analysis. A549 cells were transfected with 500 ng CUGBP1 overexpression plasmid or pCMV-MS control plasmid, respectively and collected 48 h after transfection. GAPDH was used as endogenous loading control. A representative Western blot of three idependent experiments is shown. The relative changes to control samples were given as mean + SEM of three independent experiments; t-test, $p^* < 0.05$.

Cytosolic extracts were incubated with radiolabeled GRE1 and GRE2 RNA probes. The shorter element (GRE1) was mutated to mGRE and used as negative control. The sequences are depicted in Fig. 15 A. Protein-RNA complexes were separated by a 6% native polyacrylamide gel. For GRE1 and GRE2, a shift could be observed using 10 µg cytosolic extract. For the mutated RNA probe mGRE no shift was detectable (Fig. 15 B). Additionally, REMSAs were performed using GRE-containing RNA probes and cytoplasmic lysates prepared from A549 cells, which were previously transfected with a CUGBP1 overexpression plasmid. As shown in Fig. 15 B, a protein-RNA complex was detected in response to CUGBP1 oe. The binding of GRE1 and GRE2 RNA probes was attributed to CUGBP1 since CUGBP1 oe led to a stronger RNA shift compared to control cells (Fig. 15 B). The shifts were abolished by addition excess amount of non-labeled RNA probes or using mGRE RNA probe (Fig. 15 C).

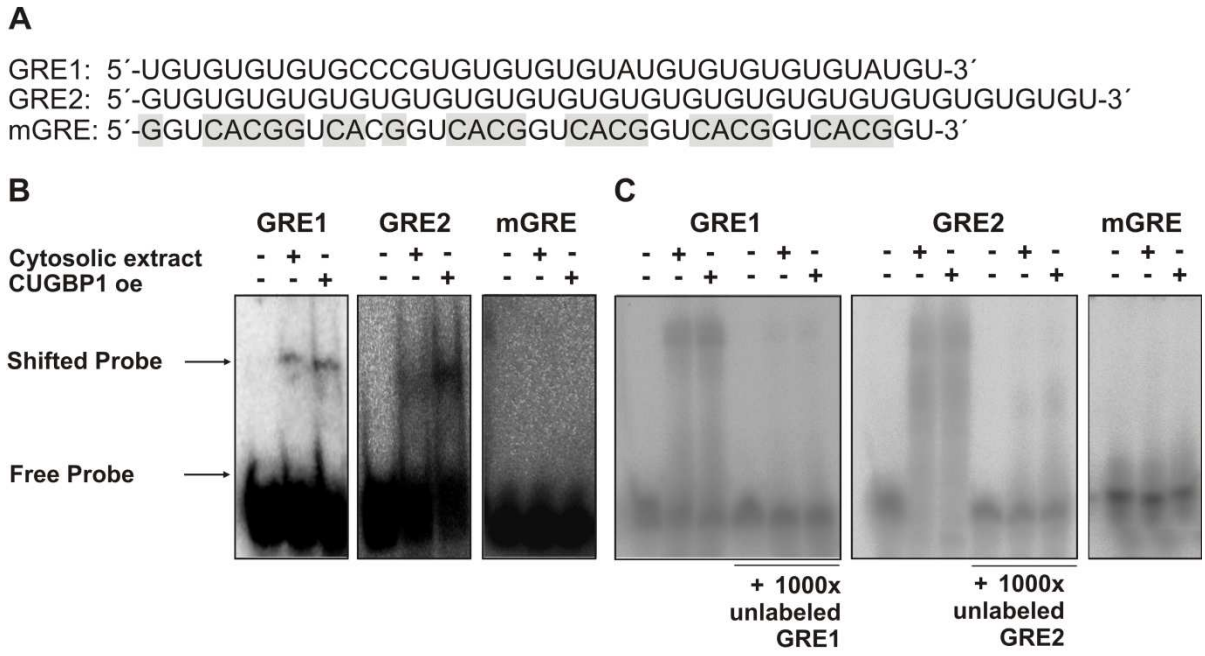

Fig. 15: CUGBP1 binds selectively to GU-rich elements of mPGES-1 3´UTR. (A) Sequences of GRE1, GRE2 and mutated mGRE. (B) REMSAs of radiolabeled GRE1, GRE2 and mGRE with 10 µg cytosolic protein. (C) REMSAs of radiolabeled GRE1, GRE2 and mGRE with 50 µg cytosolic protein. Unlabeled RNA was added for competitive shift of GRE1 and GRE2. RNA-protein complexes were separated by electrophoresis under non-denaturing conditions (6% PAA-Gel). Gels were analyzed on a phosphorimager. A representative REMSA of three idependent experiments is shown.

4.1.3 CUGBP1 mediates splicing and mRNA degradation of mPGES-1 3´UTR

Currently, nothing is known whether CUGBP1 regulates mPGES-1 expression, but it has been shown that CUGBP1 associates with mPGES-1 mRNA in mouse myoblast cells [261]. It has been described that binding of CUGBP1 to GREs leads to alternative splicing in the nucleus [180,194,262]. Therefore, the next step was to investigate whether splicing of mPGES-1 3´UTR is regulated by CUGBP1. Hence, reporter gene assays with different mPGES-1 3´UTR constructs in response to CUGBP1 oe were performed in HeLa cells. HeLa cells were transfected with CUGBP1 oe plasmid (see 3.3.10) or pCMV-MS control plasmid, respectively, to quantify CUGBP1 oe in HeLa cells. CUGBP1 protein expression was increased to 8.5-fold in HeLa cells after 48 h compared to control level (Fig. 16 A). Then HeLa cells were cotransfected with the wildtype mPGES-1 3´UTR reporter plasmid and CUGBP1 oe plasmid in increasing ratios to identify optimal working concentration for the luciferase reporter gene assay. The reporter gene assay demonstrated a significant reduction of luciferase activity of mPGES-1 3´UTR by CUGBP1 oe compared to control for each ratio (Fig. 16 B), assuming that there might be an event of splicing. The optimal ratio

1:3 (mPGES-1 3´UTR construct: CUGBP1 oe construct) was used for further experiments as luciferase activity was significantly reduced to ~70%.

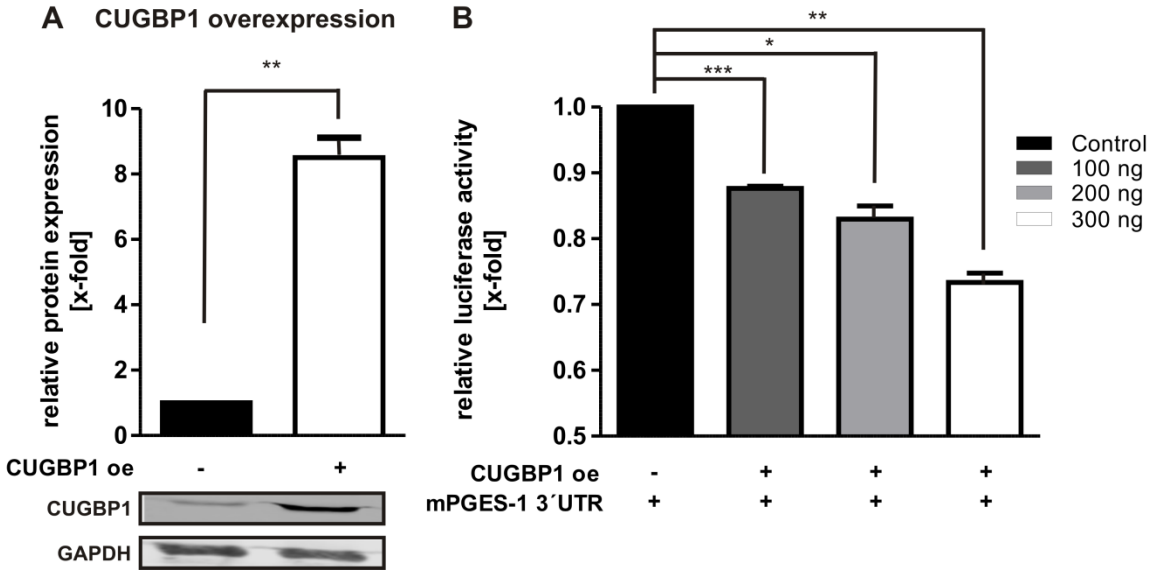

Fig. 16: Quantification of CUGBP1 overexpression and mPGES-1 3´UTR reporter gene assay in HeLa cells. (A) For CUGBP1 oe HeLa cells were transfected with 500 ng CUGBP1 oe plasmid or pCMV-MS control plasmid, respectively and collected 48 h after transfection. GAPDH was used as loading control. A representative Western blot of three independent experiments is shown. The relative changes to control samples were given as mean + SEM of three independent experiments; t-test, p* < 0.05; **p < 0.01. (B) CUGBP1 oe regulates mPGES-1 3´UTR gene expression dose-dependently. Reporter gene assay of mPGES-1 3´UTR construct (100 ng) in HeLa cells subjected to CUGBP1 oe in different concentrations. The relative changes to control samples were given as mean + SEM of three independent experiments; t-test, p* < 0.05; **p < 0.01, ***for p<0.001.

It was then interesting to elucidate if GU-rich elements have an influence on splicing mPGES-1 3´UTR, therefore HeLa cells were cotransfected with different mPGES-1 3´UTR reporter gene constructs and the CUGBP1 oe plasmid. In addition to the wildtype mPGES-1 3´UTR containing plasmid, three additional plasmids were designed with sequential deletion of the GRE elements and the double deletion. The decreased luciferase activity of mPGES-1 3´UTR in response to CUGBP1 oe was abolished by the sequential and the double deletion of GREs (Fig. 17 A). The luciferase activity was restored up to control level. RT-PCR analysis primer pairs covering mPGES-1 3´UTR (see chapter 3.4.2) confirmed the reporter gene assay results, as no mPGES-1 3´UTR isoform PCR splice product could be detected by the sequential or double deletion of GREs (Fig. 17 B). These data suggest mPGES-1 3´UTR splicing was mediated by CUGBP1 whereby both GREs are essential for splicing.

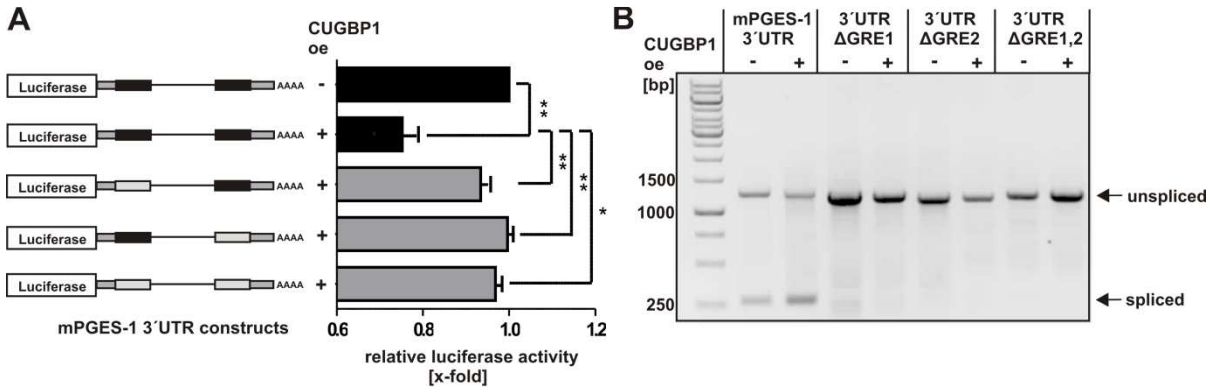

Fig. 17: CUGBP1 is responsible for mPGES-1 3´UTR splicing. (A) Reporter gene assay of mPGES-1 3´UTR constructs in HeLa cells subjected to CUGBP1 oe (ratio 100:300 ng). The black boxes indicate GREs within mPGES-1 3´UTR, whereas the grey boxes indicate deleted GREs. The relative changes were given as mean + SEM of minimum three independent experiments; t-test, $p^* < 0.05$; $^{**}p < 0.01$, ***for $p < 0.001$. (B) RT-PCR analysis using primer pair (see chapter 3.4.2) covering mPGES-1 3´UTR in HeLa cells, previously transfected with mPGES-1 3´UTR constructs with CUGBP1 oe or pCMV-MS control, respectively. RT-PCR products were separated on a 1% agarose gel. A representative gel of three independent experiments is shown.

The reporter gene assay in HeLa cells demonstrated a decreased luciferase activity for mPGES-1 3´UTR in response to CUGBP1 oe suggesting that mRNA stability might be affected by the GREs and CUGBP1 binding. Therefore, mRNA stability of mature mPGES-1 and splice variant mRNA was addressed by comparing mRNA levels in A549 cells treated with actinomycin D. Actinomycin D is a peptide antibiotic that inhibits RNA synthesis. As shown in Fig. 18 A exposure to actinomycin D treatment resulted in a substantial decrease in the amount of mPGES-1 isoform mRNA in contrast to mature mPGES-1 mRNA. Previously, Rattenbacher *et al*. demonstrated that GU-rich containing mRNA transcripts are rapidly degraded by CUGBP1-dependent recruiting of PARN deadenylases [195]. Alternatively, the 3´UTR isoform is also an NMD target by placing the natural stop codon in front of an EJC rendering it into a PTC [263]. To determine which mechanism is responsible for mRNA degradation of 3´UTR isoform UPF1 knockdown experiments were performed in A549 cells. The siRNA-mediated knockdown of the crucial NMD factor UPF1 led to a 73% reduction of UPF1 protein using siRNA C (Fig. 18 B). No significant changes in mRNA expression of mPGES-1 and the 3´UTR variant were observed with the inhibition of NMD factor UPF1 (Fig. 18 C), assuming that mRNA decay of mPGES-1 3´UTR is UPF1 independent and mRNA degradation of mPGES-1 splice variant is mediated by CUGBP1. Taken together these data indicate that CUGBP1 negatively influences mPGES-1 3´UTR isoform mRNA stability via binding to GU-rich elements, however the mature mPGES-1 mRNA transcript is not affected.

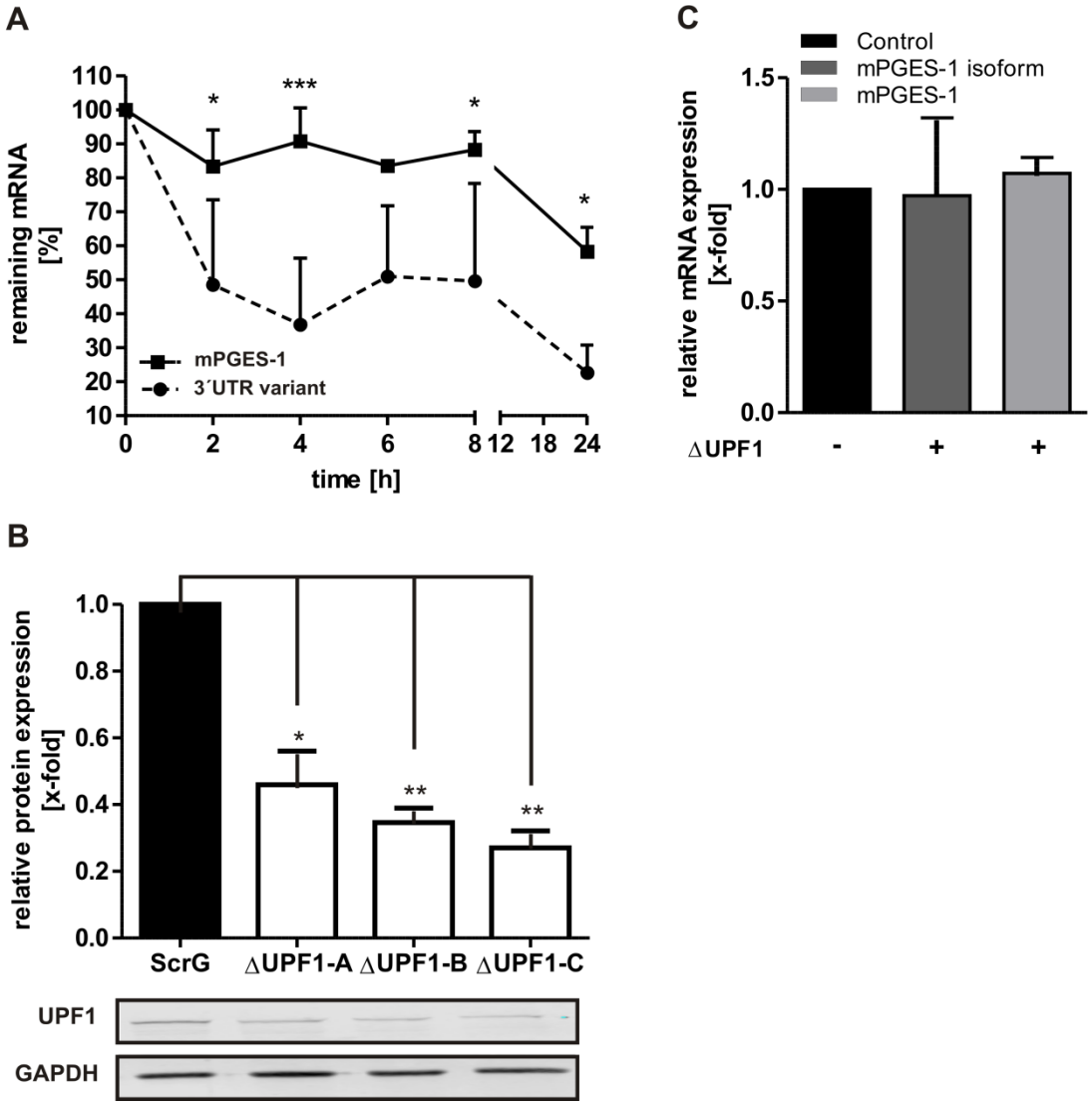

Fig. 18: mRNA decay of mPGES-1 3´UTR is UPF1 independent. (A) Remaining mPGES-1 3´UTR isoform and mPGES-1 mRNA expression 24 h after actinomycin D treatment (2 µg/ml) at indicated time points. Relative changes were given as mean + SEM of three independent experiments; two way ANOVA, Bonferroni post test, *$p < 0.05$, **$p < 0.01$, ***for $p<0.001$. Actin was used as control. (B) Quantification of UPF1 knockdown in A549 cells via Western Blot analysis. A549 cells were transfected with 20 pmol/ul siRNA or control siRNA, respectively and collected 24 h after transfection. GAPDH was used as loading control. A representative Western blot of three idependent experiments is shown. The relative changes were given as mean + SEM of minimum three independent experiments; t-test, p* < 0.05; **$p < 0.01$, ***for $p<0.001$. (C) Effect of NMD inhibition by UPF1 knockdown on mPGES-1 3´UTR isoform and mPGES-1 mRNA expression 24 h after transfection. Actin was used as control. Relative changes are given as mean + SEM of three independent experiments; t-test.

4.1.4 Depletion of CUGBP1 stabilizes 3´UTR variant and mPGES-1 protein expression

CUGBP1 is a multifunctional protein whereupon its functions are determined by its cellular localization and phosphorylation status. In the cytosol, it regulates translation efficiency and mRNA stability [195] whereas nuclear located CUGBP1 is involved in the regulation of alternative splicing [194]. Here in this study it was demonstrated that CUGBP1 mediates

mPGES-1 3´UTR splicing and degradation of 3´UTR isoform (Fig. 17). Mature mPGES-1 mRNA was not affected, although it contains the two GRE elements in its 3´UTR, suggesting that cytosolic CUGBP1 might regulate translation. Treatment with cytokines e.g. IL-1β can highly induce mPGES-1 expression [11]. To investigate mPGES-1 mRNA and protein expression pattern regulated by CUGBP1, the protein was depleted using RNAi. As shown in Fig. 19 the siRNA-mediated knockdown (ΔCUGBP1) lead to a ~80% reduction of CUGBP1 protein expression in A549 cells using Western blot analysis.

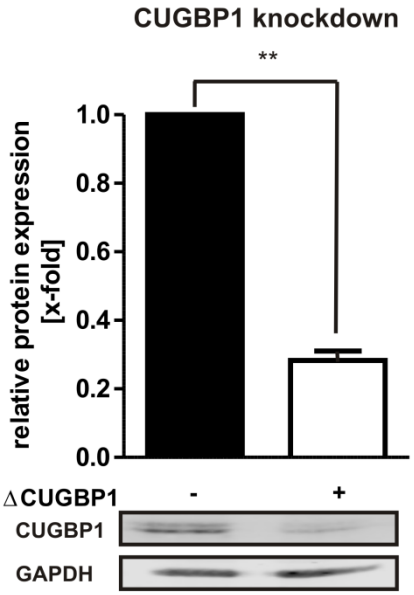

Fig. 19: Quantification of CUGBP1 knockdown in A549 cells via Western Blot analysis. A549 cells were transfected with 20 pmol/µl siRNA or a control siRNA, respectively and collected 24 h after transfection. GAPDH was used as loading control. A representative Western blot of three idependent experiments is shown. The relative changes were given as mean + SEM of minimum three independent experiments; t-test, $p^* < 0.05$; $^{**}p < 0.01$.

Time course experiments in A549 cells were performed to address the effect of CUGBP1 on mPGES-1 mRNA and protein expression. The mPGES-1 expression was induced by stimulating the cells with 5 ng/ml IL-1β for 24 h, afterwards the medium was changed and IL-1β depleted. The cells were then cultivated for further 24 h to find the natural downregulation mechanisms. At defined time points, samples were collected for mRNA, protein and PGE_2 analysis. The time course experiments revealed that the mRNA of mPGES-1 3´UTR isoform was 8.7 fold induced in response to ΔCUGBP1 compared to the control after IL-1β stimulation (Fig. 20 A). The 3´UTR isoform mRNA expression was increased to 7.6 fold until 9 h after medium change, which indicates that CUGBP1 acts as mRNA decay factor for the mPGES-1 3´UTR isoform [177,264]. The mature mPGES-1 mRNA in contrast was less

affected by ΔCUGBP1 (Fig. 20 B), even after medium change without cytokine stimulus. A slight increase in mPGES-1 mRNA expression by ΔCUGBP1 compared to control was observed. A similar expression pattern was determined for mPGES-1 protein expression, differing only in a stronger upregulation in response to ΔCUGBP1 (Fig. 20 C). After IL-1β stimulation mPGES-1 protein expression increased up to 5.8 fold induction (ΔCUGBP1) compared to 2.8 fold for the control. Depletion of CUGBP1 led to 6.9 fold induction in contrast to 4.0 fold for mPGES-1 protein 24 h after cultivation without stimulus.

Also PGE_2 levels in supernatants were measured to investigate changes in product formation downstream of mPGES-1. Interestingly, the enzymatic product of mPGES-1 was significantly upregulated to ~50 fold in response to ΔCUGBP1 after IL-1β induction, but rapidly decreased after IL-1β depletion in contrast to mPGES-1 mRNA and protein level (Fig. 20 D). It has been demonstrated that PGE_2 regulation by mPGES-1 sometimes acts in concert with COX-2 [61]. Therefore, the COX-2 mRNA and protein level was monitored during this time course to investigate decreasing PGE_2 level and whether CUGBP1 had also an influence on COX-2 expression. qRT-PCR and Western blot analysis of the time course experiment revealed that mRNA (Fig. 20 E) as well as protein (Fig. 20 F) expression of COX-2 was markedly induced by IL1-β stimulation after 24 h, but after IL-1β depletion a strong downregulation of COX-2 expression was observed. ΔCUGBP1 had no influence on COX-2 expression. These data suggest that CUGBP1 acts as decay factor for mPGES-1 3´UTR mRNA regulating mPGES-1 protein expression independent from COX-2.

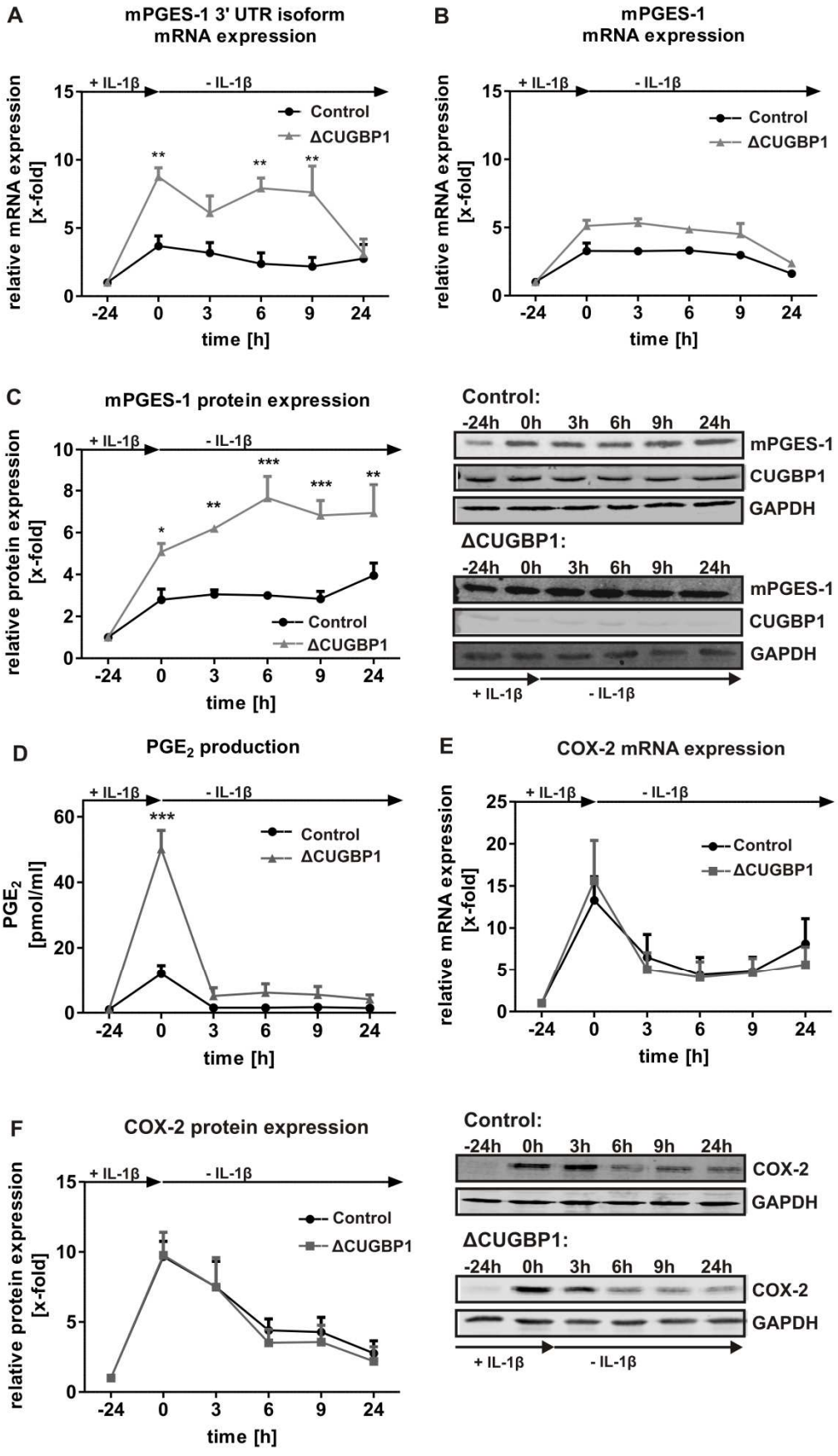
A
mPGES-1 3' UTR isoform mRNA expression
relative mRNA expression [x-fold]
+ IL-1β
- IL-1β
Control
ΔCUGBP1
time [h]
B
mPGES-1 mRNA expression
C
mPGES-1 protein expression
relative protein expression [x-fold]
Control:
ΔCUGBP1:
mPGES-1
CUGBP1
GAPDH
D
PGE2 production
PGE2 [pmol/ml]
E
COX-2 mRNA expression
F
COX-2 protein expression
COX-2

Fig. 20: Effect of CUGBP1 knockdown on mPGES-1 and COX-2 expression. A549 cells were transfected with 20 pmol/µl siRNA or control siRNA, respectively and incubated with 5 ng/ml IL-1β for 24 h. Afterwards cell culture medium was replaced by cell culture medium without IL-1β. The cells were cultured for further 24 h.Samples were collected at different time points. qRT-PCR analysis of (A) mPGES-1 and (B) mPGES-1 3´UTR isoform mRNA expression. Actin was used as control. (C) Western blot analysis of mPGES-1 expression (D) LC-MS/MS analysis of PGE_2 level. (E) qRT-PCR analysis of COX-2 mRNA expression. Actin was used as control. (F) Western blot analysis of COX-2 protein expression level. For Western blot analysis GAPDH was used as loading control. A representative blot of three independent experiments is shown. The relative changes were given as mean + SEM of three independent experiments, two way ANOVA, Bonferroni post test, *$p < 0.05$, **$p < 0.01$, ***for $p<0.001$.

Kojima *et al*., demonstrated that mPGES-1 was induced in cultured synovial fibroblasts obtained from RA patients, upon stimulation by pro-inflammatory cytokines such as IL-1β and TNF-α [38]. It was interesting to elucidate if CUGBP1 depletion showed similar effects on SF cells of RA patients. To address these issues SFs of five patients (SF0246, SF0252, SFHW, SF5, SF2) were cultured for 24 h and transfected with CUGBP1 siRNA and a control siRNA, respectively. During cultivation SF5 showed an abnormal phenotype and was not used for further analysis. The knockdown of CUGBP1 in SF2 did not show a reduction of CUGBP1 mRNA, maybe due to low transfection efficiency. The siRNA-mediated knockdown of CUGBP1 of the remaining SF cells lead to ~59% reduction of CUGBP1 mRNA (Fig. 21 A). According to the results in A549 cells there were no significant changes in IL-1β induced mPGES-1 mRNA expression levels (10 ng/ml) in response to ΔCUGBP1 (Fig. 21 C). Interestingly, IL-1β induced induction of mPGES-1 3´UTR isoform demonstrated a slightly increase in response to ΔCUGBP1 (Fig. 21 C). Preliminary data in SF0246 showed that CUGBP1 protein was slightly reduced after IL-1β stimulation, whereas mPGES-1 protein was slightly increased after stimulation (Fig. 21 B). These data stand in line with the A549 results and suggest that CUGBP1 is responsible for GU-mediated mRNA decay and degradation of the mPGES-1 3´UTR isoform in SF cells. Additionally, the data indicates that CUGBP1 might repress mPGES-1 protein translation.

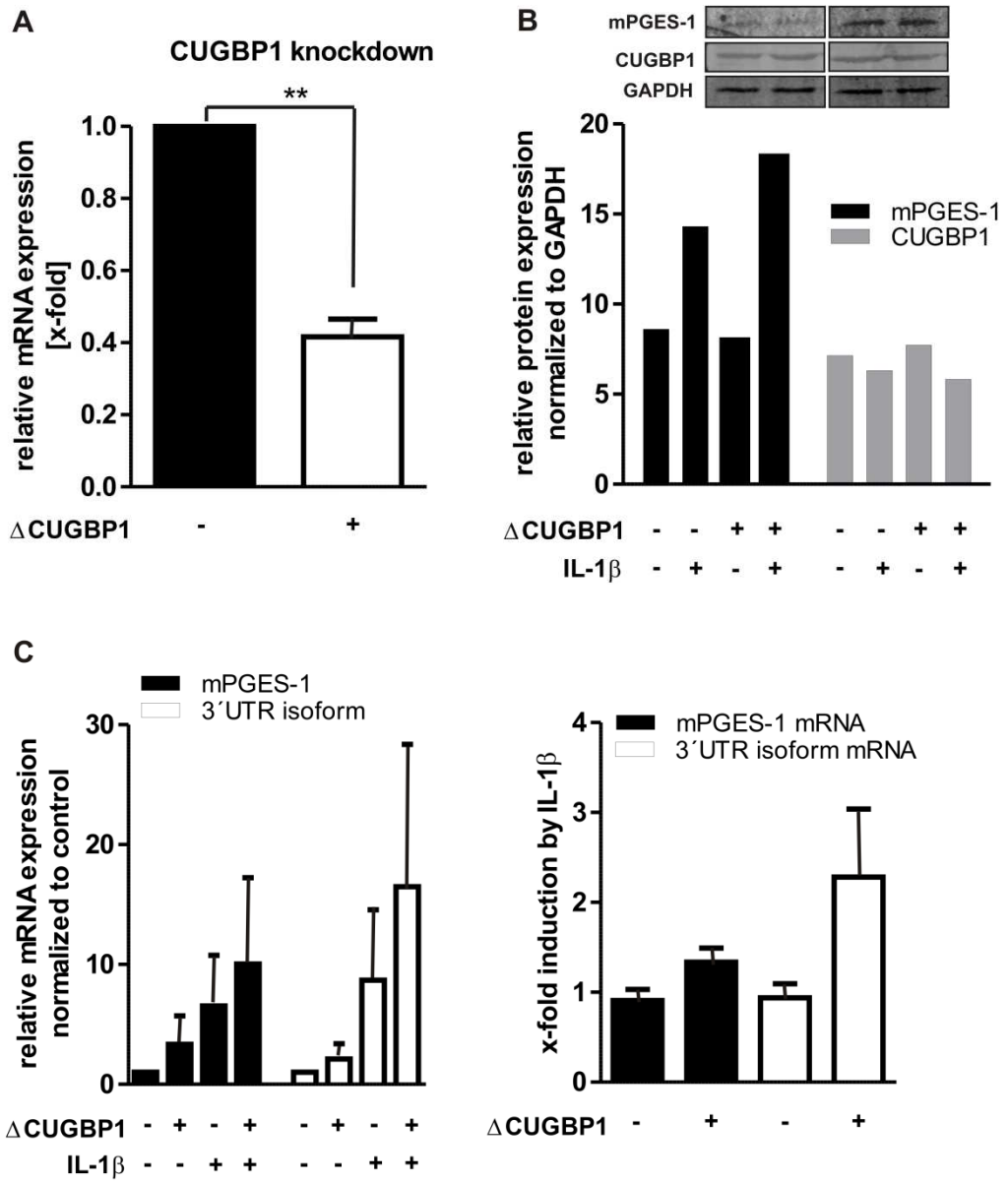

Fig. 21: Effect of CUGBP1 knockdown on induced mPGES-1 and mPGES-1 3´UTR expression in SF cells of RA patients. SF-0246, SF-0252 and SF-HW were transfected with 20 pmol/µl siRNA or control siRNA, respectively. 24 h after transfection cells were incubated with 10 ng/ml IL-1β for further 24 h. (A) qRT-PCR analysis of CUGBP1 mRNA expression. Actin was used as control. (B) Western blot analysis of CUGBP1 and mPGES-1 protein expression in SF-0246 with depleted CUGBP1 levels. SF-0246 was transfected with 20 pmol/µl siRNA, or a control siRNA respectively. 24 h after transfection cells were incubated with 10 ng/ml IL-1β for further 24 h. GAPDH was used as loading control. (C) qRT-PCR analysis mPGES-1 and mPGES-1 3´UTR isoform mRNA expression in SF-0246, SF-0252 and SF-HW in response to ΔCUGBP1. Actin was used as control. The relative changes were given as mean + SEM of three independent experiments; t-test, $p^* < 0.05$; $^{**}p < 0.01$.

4.1.5 mPGES-1 protein translation is repressed by CUGBP1 overexpression

A549 cells were transfected with the CUGBP1 overexpression plasmid (500 ng) for 48 h to investigate the effects of CUGBP1 overexpression on mPGES-1 expression pattern. The

time course experiment 48 h after transfection (see Chapter 4.1.4) could not be analyzed because long-term overexpression of CUGBP1 led to a decreased cell viability in A549 cells (Fig. 22). Trypan blue, a diazo dye, was used to selectively stain dead cells [265]. The measurement of cell viability demonstrated that CUGBP1 overexpressing A549 cells showed less viable cells during this time course compared to the control. Therefore samples for qRT-PCR and Western blot analysis were collected 48 h after transfection and an additional incubation with IL-1β for 24 h.

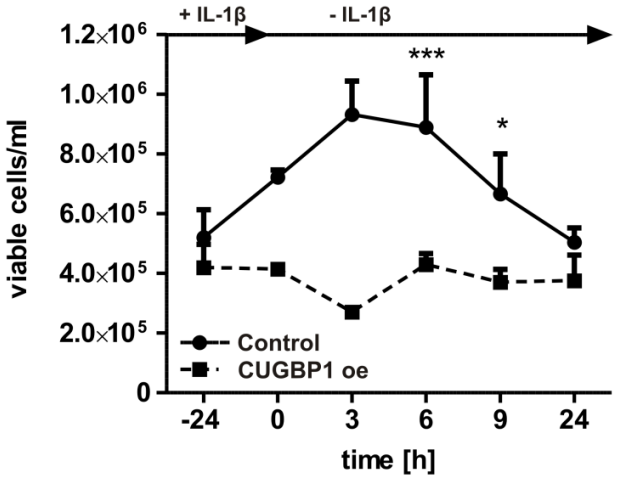

Fig. 22: Cell viability of A549 cells analyzed by Trypan blue measurement. A549 cells were transfected with 500 ng CUGBP1 oe plasmid or pCMV-MS control plasmid, respectively and collected at different time points. 48 h after transfection the cells were induced with 5 ng/ml IL-1β for further 24 h. Samples were collected at different time points. The relative changes were given as mean + SEM of minimum three independent experiments; two way ANOVA, Bonferroni post test, *$p < 0.05$, **$p < 0.01$, ***for $p<0.001$.

qRT-PCR analysis demonstrated that CUGBP1 oe did not alter mPGES-1 mRNA expression levels with and without IL-1 β stimulation (Fig. 23 A). However, IL-1β mediated induction of mPGES-1 3´UTR isoform was slightly decreased compared to control (Fig. 23 A) but not significantly reduced. In contrast to this, it could be shown that IL-1β mediated induction of mPGES-1 protein was significantly repressed by CUGBP1 oe (Fig. 23 B). These experiments indicate that CUGBP1 functions as destabilizing factor for mPGES-1 3´UTR isoform and as a translational repressor for mPGES-1 protein expression.

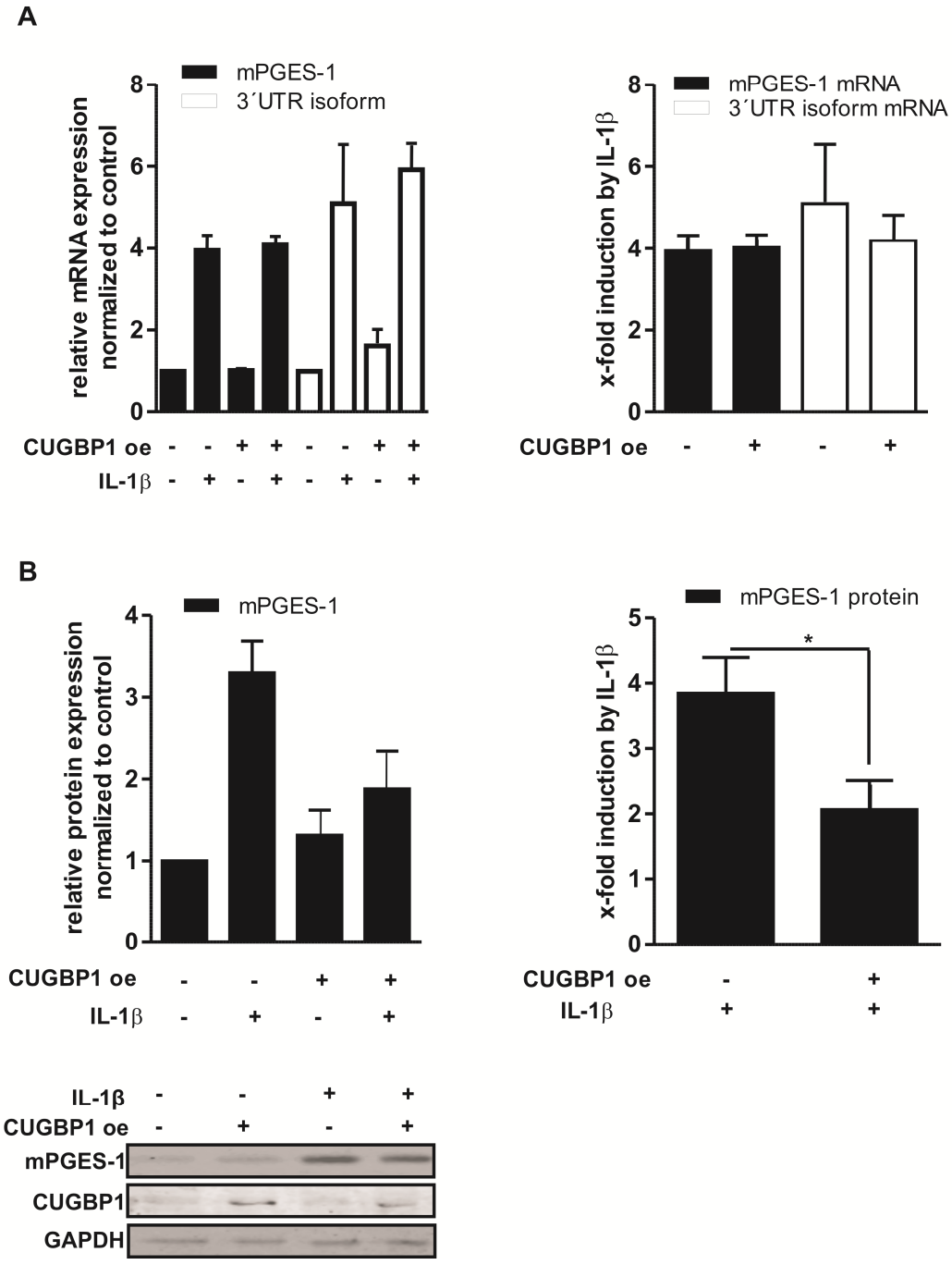

Fig. 23: Effect of CUGBP1 oe on IL-1β mediated induction of mPGES-1 expression. A549 cells were transfected with 500 ng CUGBP1 oe plasmid or pCMV-MS control, respectively and induced 48 h after transfection with 5 ng/ml IL-1β for further 24 h. (A) qRT-PCR analysis of mPGES-1 and mPGES-1 3´UTR isoform mRNA expression in response to CUGBP1 oe. Actin was used as control. (B) Western blot analysis of mPGES-1 protein expression in response to CUGBP1 oe. GAPDH was used as loading control. A representative Western blot of three idependent experiments is shown. The relative changes were given as mean + SEM of minimum three independent experiments; t-test, $p^* < 0.05$.

4.1.6 GW182 acts in concert with CUGBP1 and is crucial for mPGES-1 protein expression

Studies in mammalian cells have revealed that mRNA decay intermediates accumulate at P-bodies (PBs) when normal decay is blocked suggesting that PBs are sites of decapping and 5´-3´degradation [266,267,268]. Kedersha *et al*. showed that mRNA-decapping enzyme 1a (DCP1a) [269] and glycine-tryptophan protein (GW182) [270] are components of PBs [269,270]. Moreover, Yu *et al.* showed that translation repression of target mRNA was due to colocalization of CUGBP1 and tagged mRNA in PBs [151,271]. To verify the hypothesis that CUGBP1 might repress mPGES-1 translation by recruiting mPGES-1 mRNA to PBs, the distribution of CUGBP1 and the PB component DCP1a was examined by immunofluorescence stainings. Immunofluorescence analysis demonstrated extensive colocalization of CUGBP1 and DCP1a (Fig. 24 A). The stainings showed that CUGBP1 was rather located in the nucleus than in the cytosol. It has been shown that depletion of the PB marker GW182 can disrupt PBs formation and stability. Therefore, GW182 (ΔGW182) was depleted to determine whether GW182 is linked to translation repression mediated by PBs. Immunoflourescence stainings showed a slight decrease of GW182 expression for ΔGW182 cells after 24 h compared to the control cells (Fig. 24 B). This was also confirmed by qRT-PCR. The knockdown of GW182 led to a ~55% reduction of GW182 mRNA expression (Fig. 24 C). It has been demonstrated that GW182 is partly involved in miRNA biosynthesis and knockdown can influence miRNA maturation for some miRNAs. As an example, for miR-575-5p no significant changes could be detected in response to ΔGW182 (Fig. 24 D). As expected the mature mPGES-1 mRNA was not affected by ΔGW182 (Fig. 24 E), whereas the protein expression was significantly induced in A549 cells with depleted GW182 (Fig. 24 F), suggesting that GW182 and PB formation is crucial for mPGES-1 protein translation. These data indicate the important role of CUGBP1 as translational repressor for mPGES-1 expression in combination with PB formation mediated by GW182. However, it remains unclear how exactly mPGES-1 protein expression is increased by ΔCUGBP1, whether only due to mRNA turnover or due to PB formation or a combination of both.

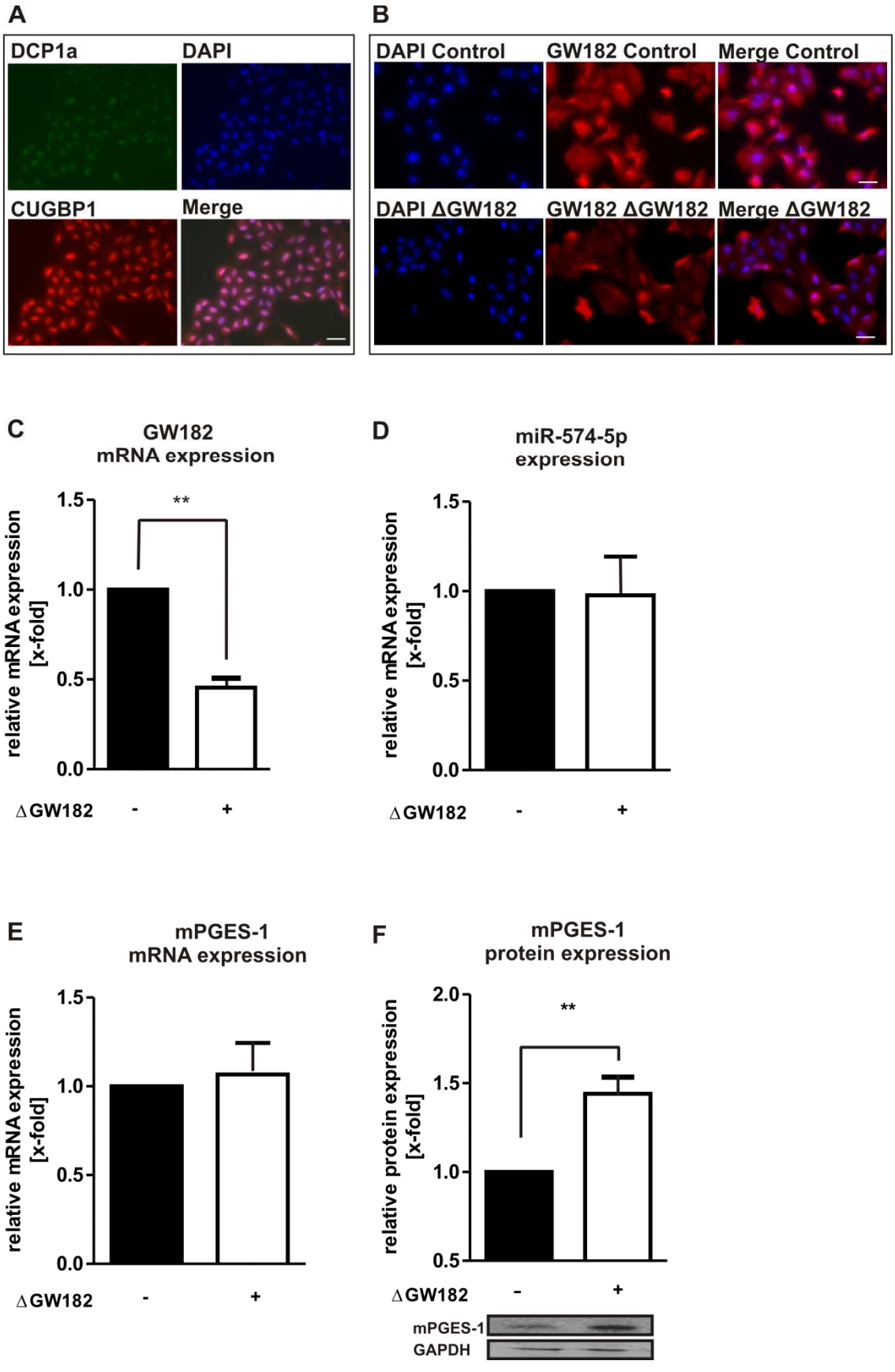
A
DCP1a
DAPI
CUGBP1
Merge
B
DAPI Control
GW182 Control
Merge Control
DAPI ΔGW182
GW182 ΔGW182
Merge ΔGW182
C
GW182
mRNA expression
relative mRNA expression
[x-fold]
1.5
1.0
0.5
0.0
**
ΔGW182
-
+
D
miR-574-5p
expression
relative mRNA expression
[x-fold]
1.5
1.0
0.5
0.0
ΔGW182
-
+
E
mPGES-1
mRNA expression
relative mRNA expression
[x-fold]
1.5
1.0
0.5
0.0
ΔGW182
-
+
F
mPGES-1
protein expression
relative protein expression
[x-fold]
2.0
1.5
1.0
0.5
**
ΔGW182
-
+
mPGES-1
GAPDH

Fig. 24: CUGBP1 colocalizes with the PB marker DCP1a and PB formation is crucial for mPGES-1 protein translation. (A) Fluorescence analysis of CUGBP1 colocalization with PB protein DCP1a. Alexa Fluor 594® was detecting CUGBP1, Alexa Fluor® 488 detecting DCP1a and DAPI detecting nuclei. Scale bar represents 100 µM. (B) Fluorescence analysis of GW182 knockdown in A549 cells 24 h after transfection (20 pmol/µl). Alexa Fluor® 594 was detecting GW182 and DAPI detecting nuclei. Scale bar represents 100 µM. (C) qRT-PCR analysis of siRNA-mediated knockdown of GW182 in A549 cells 24 h after transfection. Actin was used as control. (D) miR-574-5p mRNA expression during ΔGW182 24 h after transfection. U6 was used as endogenous control. (E) qRT-PCR analysis of mPGES-1 mRNA expression level during GW182 knockdown 24 h after transfection. Actin was used as control. (F) Western Blot analysis of mPGES-1 protein expression. GAPDH was used as loading control. A representative Western blot of three independent experiments is shown. The relative changes were given as mean + SEM of minimum three independent experiments; t-test, $p^* < 0.05$; $^{**}p < 0.01$.

4.1.7 CUGBP1 overexpression inhibits the proliferation of A549 cells

It has been demonstrated that proliferation in Lewis lung carcinoma cells was reduced by siRNA-mediated knockdown of mPGES-1, indicating the critical role of mPGES-1 in cancer progression and tumour growth [33]. Decreased cell viability was observed in response to CUGBP1 oe in A549 cells analyzed by Trypan blue measurement (Fig. 22). To investigate the influence of CUGBP1 on A549 cell proliferation MTT cell proliferation assays were performed. First the influence of IL-1β stimulation on cell proliferation was analyzed. Therefore, A549 cells were seeded and stimulated with and without IL-1β for 24 h (Fig. 25 A). The induction with IL-1β did not significantly change the cell proliferation after 24 h compared to the unstimulated control cells. Interestingly, IL-1β induced cell proliferation was significantly increased in response to ΔCUGBP1, whereas CUGBP1 oe significantly decreased A549 cell proliferation (Fig. 25 B).

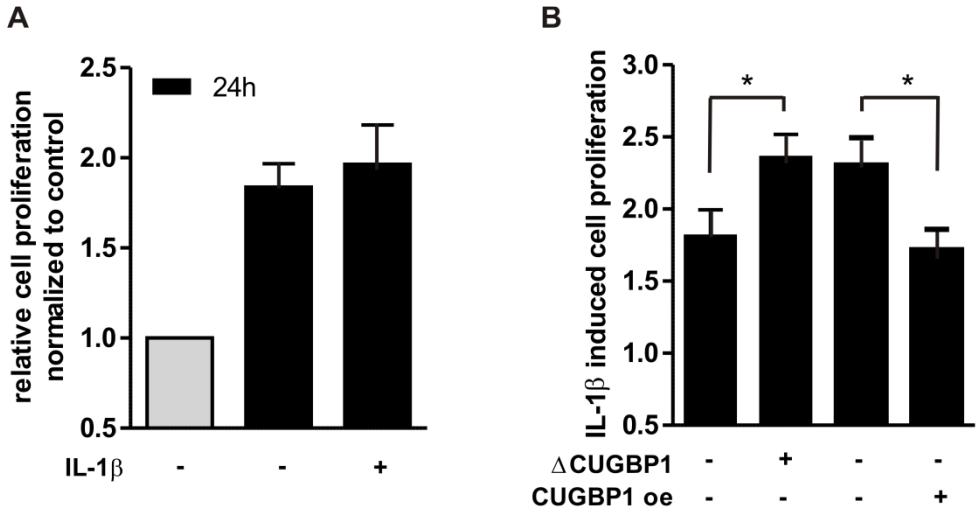

Fig. 25: Effect of CUGBP1 overexpression and knockdown on IL-1β induced cell proliferation. MTT cell proliferation assay was performed in A549 cells (A) induced with (5 ng/ml) and without IL-1β for 24 h, (B) ΔCUGBP1 and CUGBP1 oe. A549 cells were transfected with 500 ng CUGBP1 plasmid or pCMV-MS control, respectively for CUGBP1 oe or 20 pmol/µl siRNA for ΔCUGBP1. The cells were induced with IL-1β for 24 h after 24 h transfection for ΔCUGBP1 or 48 h for CUGBP1 oe. The relative changes were given as mean + SEM of three independent experiments; t-test, $p^* < 0.05$.

The MTT cell proliferation analysis suggests that CUGBP1 negatively influence cell proliferation.

4.1.8 Expression pattern and localization of CUGBP1 in A549 and SF cells

The function of CUGBP1 is regulated by its cellular localization and phosphorylation status [203]. In Fig. 24 A, it was shown that CUGBP1 is located in the nucleus and the cytosol. It was observed that CUGBP1 protein is higher expressed in the nucleus than in the cytosol. To investigate whether changes in localization, expression level or phosphorylation status of CUGBP1 influenced mPGES-1 expression, CUGBP1 mRNA and protein level was observed during the defined time course. No significant changes could be determined neither in the mRNA expression nor in the protein expression level of CUGBP1 (Fig. 26 A), CUGBP1 was constitutively expressed on mRNA and protein level even after IL-1β depletion.

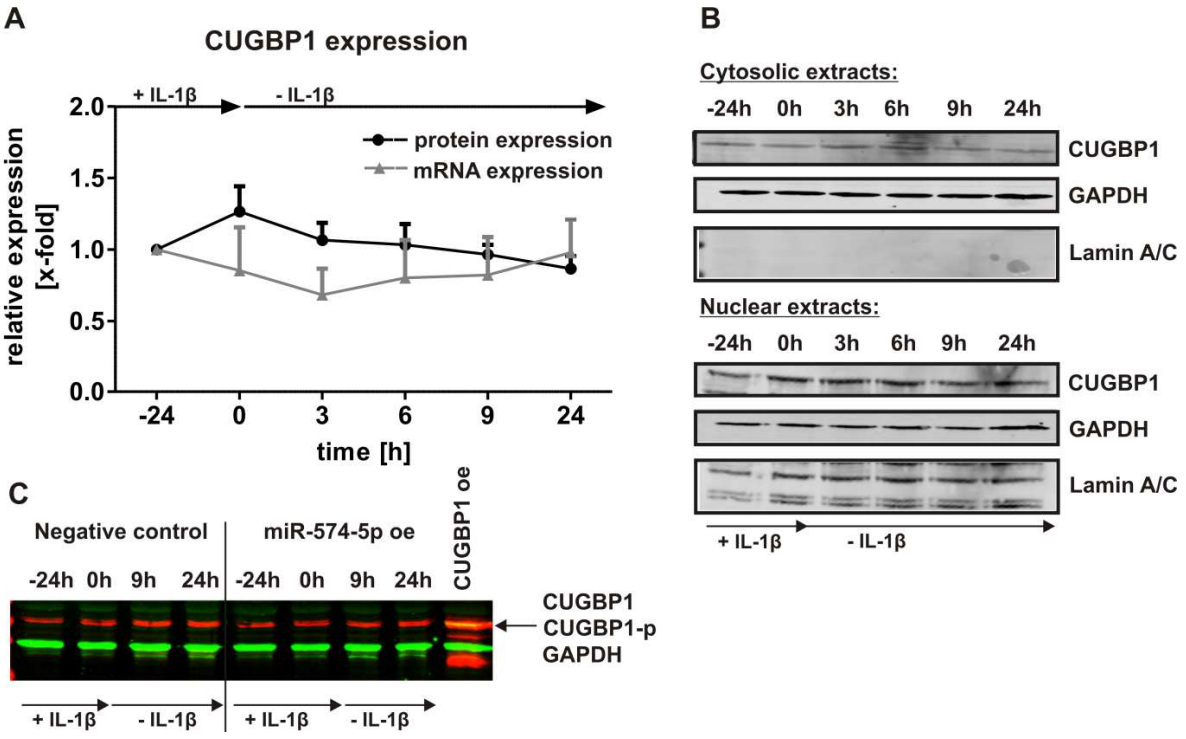

Fig. 26: Expression levels and localization of CUGBP1 during time course experiment. A549 cells were induced with 5 ng/ml IL-1β for 24 h. Afterwards cell culture medium was replaced by medium without IL-1β and the cells were cultured for further 24 h. Samples were collected at different time points. (A) qRT-PCR and Western blot analysis were performed to analyze the CUGBP1 expression profile. Actin was used as control for qRT-PCR and GAPDH was used as control for Western blot analysis. Two way ANOVA, Bonferroni post test. (B) Western blot analysis of cellular localization of CUGBP1 during time course experiment in the cytosolic fraction and the nuclear fraction. Lamin A/C was used a nuclear loading control. GAPDH is located in the nucleus and the cytosol. (C) Western Blot analysis of phosphorylation of CUGBP1 (CUGBP1-p) during time course experiment. Red bands represent the fluorescense at 680 nm and green bands the flourescence at 800 nm. A representative Western blot of three independent experiments is shown. For Western Blot analysis GAPDH was used as loading control. The relative changes were given as mean + SEM of minimum three independent experiments.

4 Results

Western blot analysis was performed to confirm the localization of CUGBP1 in nucleus and cytosol during the time course. Lamin A/C was used as nuclear control as it is thought to be involved in nuclear stability, chromatin structure and gene expression and thus an appropriate endogenous control for nuclear proteins, whereas GAPDH is ubiquitously expressed in the nucleus and the cytosol [272]. Localization during the time course was determined by Western blot analysis and exhibited that CUGBP1 is located both in the nucleus and cytosol (Fig. 26 B), which stands in line with the staining results in Fig. 24 [151,262,273]. CUGBP1 was just slightly phosphorylated if overexpressed in A549 cells, suggesting that most of CUGBP1 protein was active in its deadenylation functions (Fig. 26 C). Time course experiments in A549 cells revealed that CUGBP1 mRNA and protein expression levels were not altered. The analysis of CUGBP1 expression in SF cells confirmed these data and revealed that CUGBP1 was constitutively expressed on mRNA level in response to IL-1β treatment (Fig. 27).

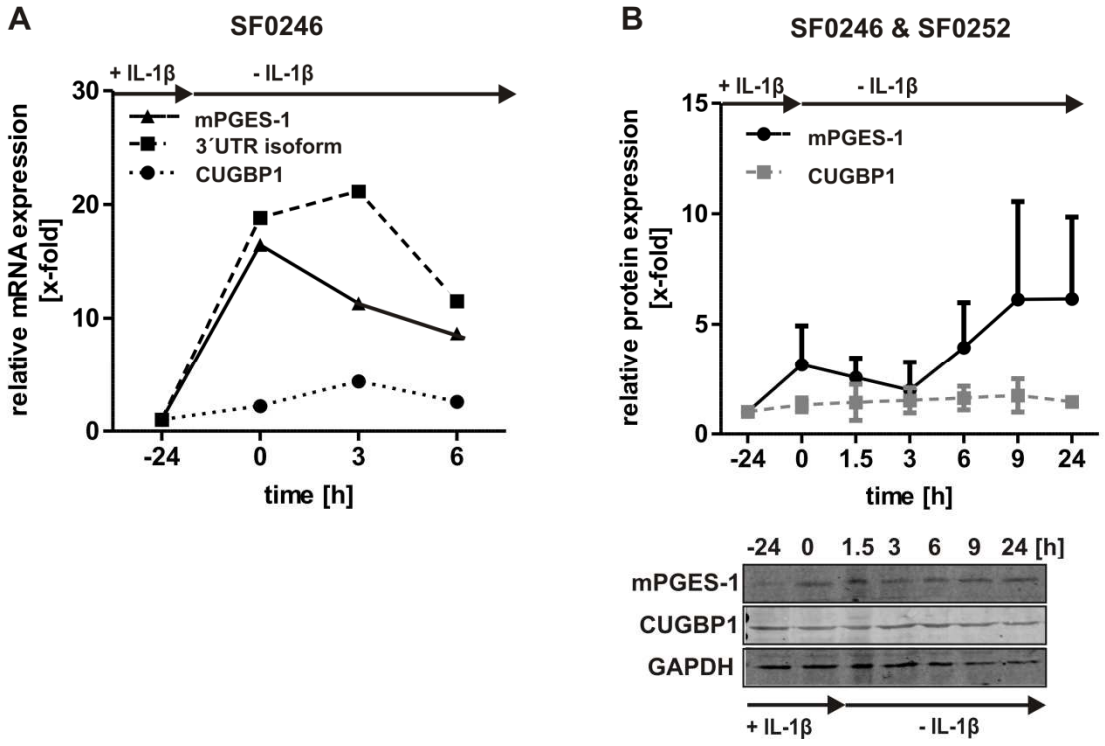

Fig. 27: Time course experiments in SF cells. SF cells were induced with 10 ng/ml IL-1β for 24 h. Afterwards cell culture medium was replaced by medium without IL-1β and the cells were cultured for further 24 h. Samples were collected at different time points. (A) qRT-PCR of mPGES-1, CUGBP1 and mPGES-1 3´UTR mRNA in SF0246. Actin was used as control. (B) Western blot analysis of mPGES-1 and CUGBP1 protein expression. A representative Western blot of two independent experiments is shown. For Western Blot analysis GAPDH was used as loading control. The relative changes were given as mean + SEM of one respectively two independent experiments.

In stimulated SF0246 cells mPGES-1 and mPGES-1 3´UTR isoform mRNA were increased after IL-1β treatment, but rapidly decreased after IL-1β depletion (Fig. 27 A). Protein expression was analyzed in SF0246 and SF0252. As shown in Fig. 27 B mPGES-1 protein was increased after stimulation, followed by a reduction after IL-1β depletion, whereas no changes in CUGBP1 protein expression were observed.

4.2 miR-574-5p acts as direct decoy to CUGBP1

4.2.1 CUGBP1 binds to mature miR-574-5p

The various effects of CUGBP1 on mPGES-1 expression could not fully be explained by its localization, expression levels or phosphorylation status, assuming that an additional regulation may exists. Eiring *et al*. demonstrated that miR-328 can act as RNA decoy to hnRNP E2 [235]. It binds to hnRNP E2 and inhibits its translational repressor activity which leads to directly increased expression of hnRNP E2 target genes [236]. Interestingly, GU-rich repeat elements are present in the mature form of miR-574-5p representing *bona fide* CUGBP1 binding sites (Fig. 28). miR-574-5p, an intronic miRNA, is encoded by gene *FAM114A1* and located on the short arm of chromosome 4 (4.p14) in humans on the forward strand sense. The alignment of GRE1, GRE2 of mPGES-1 3´UTR and the miR-574-5p showed high sequence similarities indicating a potential binding of miR-574-5p to CUGBP1.

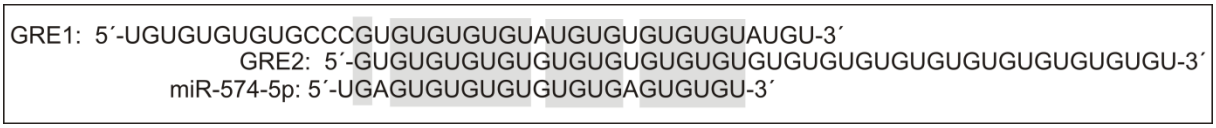

Fig. 28: Alignment of RNA sequences of GRE1, GRE2 and miR-574-5p. Sequence homologies (100%) are shaded in grey.

To determine whether CUGBP1 binds to mature miR-574-5p REMSAs were performed using radiolabeled miR-574-5p RNA (Fig. 29). As shown in Fig. 29 A, protein-miR-574-5p complexes were detected in response to increasing amounts of cytosolic extracts of A549 cells. The shift of the miR-547-5p RNA probe can be attributed to CUGBP1 because overexpression of CUGBP1 led to a stronger RNA shift compared to control cells (Fig. 29 B). This shift was abolished by adding excess amount of non-labeled miR-574-5p RNA probe (Fig. 29 B). These data indicated that CUGBP1 can bind to the mature form of miR-574-5p. In order to verify these results, an additonal experiment was performed using purified recombinant CUGBP1 protein (0.08 µg). A protein-RNA complex was observed located above the cytosolic/nuclear protein RNA complex. This difference in size was due to the

difference in molecular weight of the recombinant protein (~78 kDa) compared to ~50 kDa wildtype CUGBP1 (Fig. 29 C) .

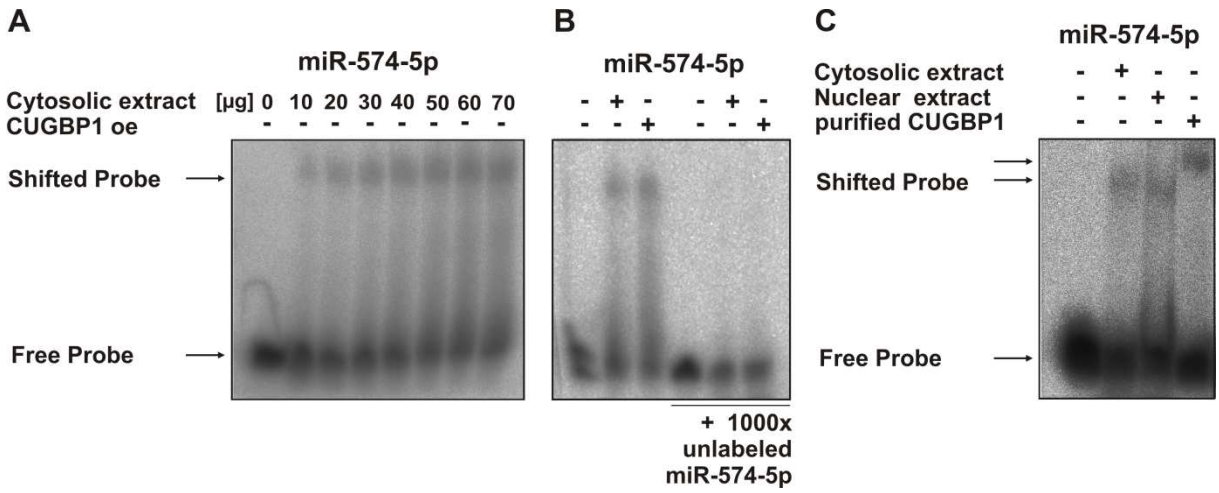

Fig. 29: CUGBP1 binds to mature miR-574-5p. (A) Radiolabeled miR-574-5p RNA probe with 10-70 µg cytosolic A549 lysates. (B) REMSA of radiolabeled miR-574-5p with 50 µg cytosolic protein. Unlabeled RNA was added for competitive shift of miR-574-5p. (C) Radiolabeled miR-574-5p RNA probe with 10 µg cytosolic, or nuclear A549 lysates or 0.08 µg purified recombinant CUGBP1 protein. RNA-protein complexes were separated by electrophoresis under non-denaturing conditions (6% PAA-Gel). Gels were analyzed on a phosphorimager. A representative REMSA of three idependent experiments is shown.

4.2.2 miR-574-5p expression is upregulated by IL-1β treatment in A549 cells

In this study it was shown that CUGBP1 exerts several functions on mPGES-1 expression that could not completely be explained by its translocation and expression pattern. The results in Fig. 29 clearly demonstrated that miR-574-5p binds to CUGBP1, which suggests that an additional regulation mechanism by the interactions with this miRNA might exist. To gain first insights into miR-574-5p expression pattern during the time course experiment miRNA expression was analyzed. Fig. 30 shows that miR-574-5p expression was increased after 24 h upon IL-1β stimulation. In contrast to mPGES-1 mRNA expression, miR-574-5p levels decreased rapidly after IL-1β depletion. This data suggest that the miR-574-5p may be cytokine-dependently regulated.

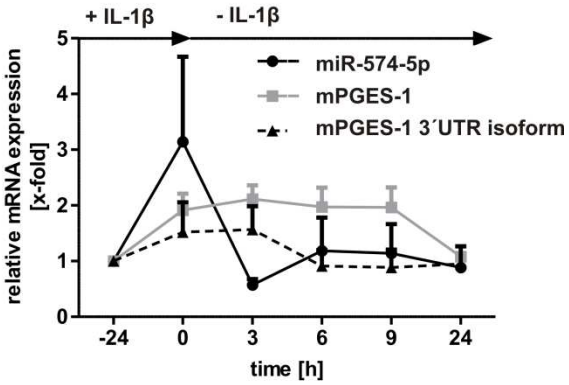

Fig. 30: qRT-PCR analysis of miR-574-5p, mPGES-1 and mPGES-1 3´UTR mRNA expression in A549 cells. A549 cells were incubated with 5 ng/ml IL-1β for 24 h. Afterwards cell culture medium was replaced by medium without IL-1β and the cells were cultured for further 24 h. Samples were collected at different time points. For miR-574-5p expression U6 was used as endogenous control. For mPGES-1 and mPGES-1 3´UTR Actin was used as control. The relative changes were given as mean + SEM of minimum three independent experiments; two way ANOVA, Bonferroni post test.

4.2.3 Effects of changes in miR-574-5p expression level in A549 lung cancer cells

In order to study the role of miR-574-5p on mPGES-1, miR-574-5p expression levels in A549 cells were varied. miR-574-5p was overexpressed using miRNA mimics in A549 cells for 24 h (see chapter 3.2.2). The overexpression was assessed by qRT-PCR (Fig. 31) and led to ~120 fold increase of miR-574-5p using U6 as endogenous control.

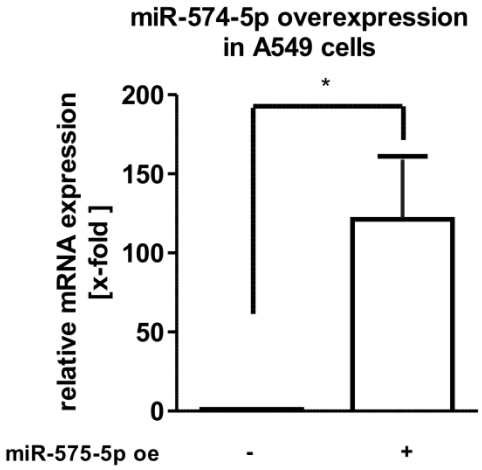

Fig. 31: Quantification of 574-5p-mimcs mediated overexpression in A549 cells via qRT-PCR analysis. The cells were transfected with 20 pmol/µl miR-574-5p mimics or negative control, respectively and collected 24 h after transfection. U6 was used as endogenous control. The relative changes were given as mean + SEM of minimum three independent experiments; t-test, $p^* < 0.05$.

It was demonstrated that miR-574-5p and mPGES-1 were induced by IL-1β treatment after 24 h (Fig. 30) and miR-574-5p was notably downregulated without IL1-β. Therefore, the

influence of miR-574-5p oe 24 h after IL-1β stimulation was investigated. qRT-PCR analysis revealed an increase of IL-1β mediated induction of mPGES-1 3´UTR isoform in response to miR-574-5p oe (Fig. 32 A).

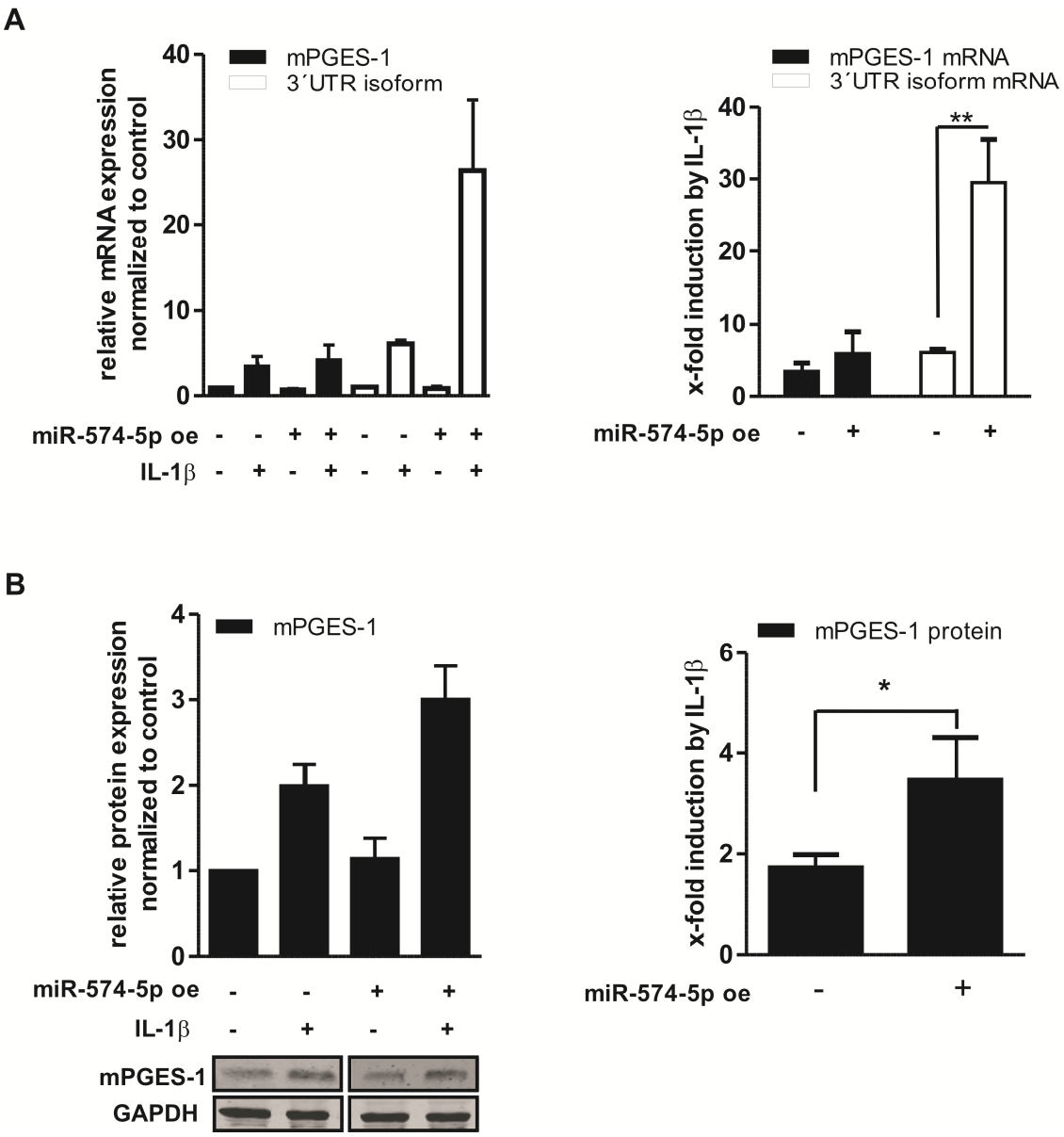

Fig. 32: Effect of miR-574-5p oe on mPGES-1 induction by IL-1β. 24 h after mimics transfection (20 pmol/µl) A549 cells were induced with 5 ng/ml IL-1β for further 24 h. (A) qRT-PCR analysis of mPGES-1 and mPGES-1 3´UTR mRNA expression in response to miR-574-5p oe. Actin was used as control for mPGES-1 and mPGES-1 3´UTR mRNA expression. U6 was used as endogenous control for miR-574-5p expression. (B) Western blot analysis of mPGES-1 protein expression overexpressing miR-574-5p. A representative Western blot of three independent experiments is shown. For Western blot analysis GAPDH was used as loading control. The relative changes were given as mean + SEM of minimum three independent experiments; t-test, $p^* < 0.05$; $^{**}p < 0.01$.

In contrast to that, the mature mPGES-1 mRNA transcript was not affected by IL-1β mediated induction in response to miR-574-5p oe (Fig. 32 A). On protein level a significant upregulation on IL-1β mediated induction of mPGES-1 was observed in response to miR-574-5p oe (Fig. 32 B), indicating that miR-574-5p oe inhibited CUGBP1-mediated 3´UTR mRNA degradation and mPGES-1 protein translational repression in the cytosol. However, the increased level of mPGES-1 3´UTR variant indicates that the alternative splicing mediated by CUGBP1 in the nucleus is not affected by the mature miR-574-5p. It was interesting to elucidate if decreased levels of miR-574-5p showed the opposite effects on mPGES-1 expression. Next miR-574-5p expression was depleted using specific miR-574-5p LNAs™ (see chapter 3.2.3). The knockdown efficiency of miR-574-5p was assayed by qRT-PCR and revealed a significant reduction (~ 90%) in A549 cells after 24 h (Fig. 33).

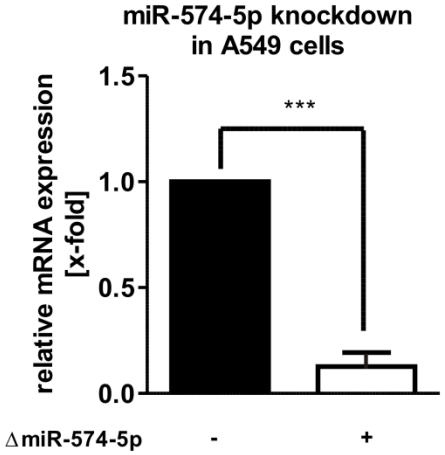

Fig. 33: qRT-PCR analysis of LNA-mediated knockdown of miR-574-5p. A549 cells were transfected with 40 pmol/µl LNAs™ and collected 24 h after transfection. The relative changes were given as mean + SEM of minimum three independent experiments; t-test, p* < 0.05; **p < 0.01, ***for p<0.001.

As shown in Fig. 34 A, induced mPGES-1 mature mRNA expression was not affected by ΔmiR-574-5p, whereas induced mPGES-1 3´UTR isoform was significantly reduced in response to ΔmiR-574-5p (Fig. 34 A).

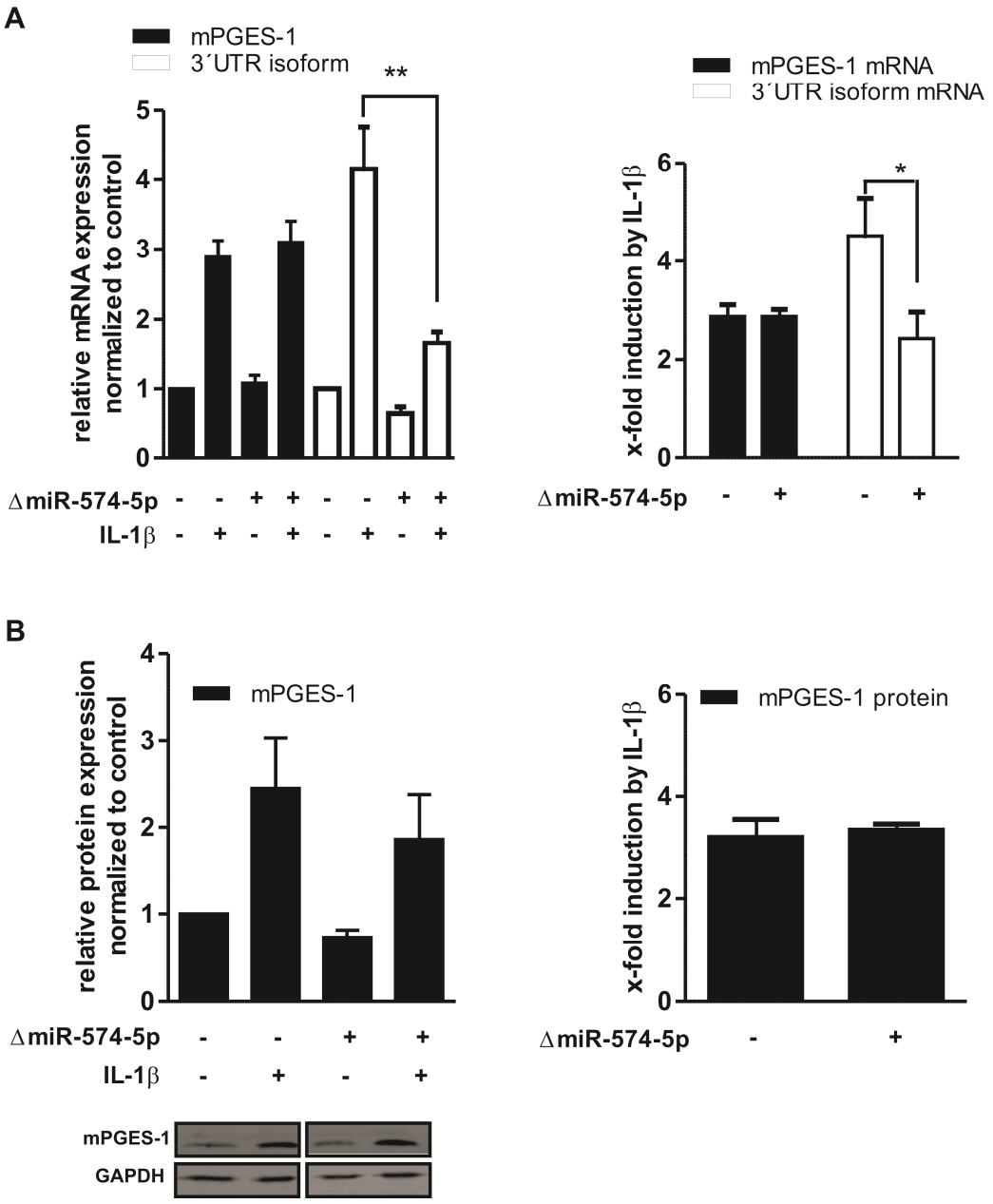

Fig. 34: Influence of ΔmiR-574-5p on induced mPGES-1 expression. A549 cells were transfected with miR-574-5p LNA™ (40 pmol/µl) and 24 h after transfection induced with 5 ng/ml IL-1β for 24 h. (A) qRT-PCR analysis of mPGES-1 and mPGES-1 3´UTR mRNA expression. Actin was used as control. (B) Western blot analysis of mPGES-1 protein expression. A representative Western blot of three independent experiments is shown. For Western blot analysis GAPDH was used as loading control. The relative changes were given as mean + SEM of minimum three independent experiments; t-test, $p^* < 0.05$; $^{**}p < 0.01$.

Comparable to the mRNA level, the IL-1β induced mPGES-1 protein expression was not affected in response to ΔmiR-574-5p (Fig. 34 B). However, relative protein expression showed a slight decrease in mPGES-1 protein level. These experiments stand in line with the results obtained with miR-574-5p oe and CUGBP1 oe suggesting that mPGES-1 expression

in the cytosol is regulated by the interaction between miR-574-5p and CUGBP1. The results obtained in Fig. 25 demonstrated that ΔCUGPB1 led to a significant increase of IL-1β induced cell proliferation, whereas CUGBP1 overexpression decreased significantly A549 cell proliferation. In the next step, it was interesting to elucidate if miR-574-5p oe shows a similar effect on A549 cell proliferation as ΔCUGBP1. miR-574-5p was overexpressed in unstimulated A549 cells and led to no significant changes in cell proliferation (Fig. 35 A). Interestingly, miR-574-5p mimics in stimulated cells revealed a significant up regulation in IL-1β induced cell proliferation (Fig. 35 B), whereas a knockdown of miR-574-5p led to a significant decrease in induced cell proliferation (Fig. 35 B). The data suggest that CUGBP1 acts as a proliferation inhibitor and miR-574-5p acts as a direct decoy to CUGBP1 by inhibiting its functions.

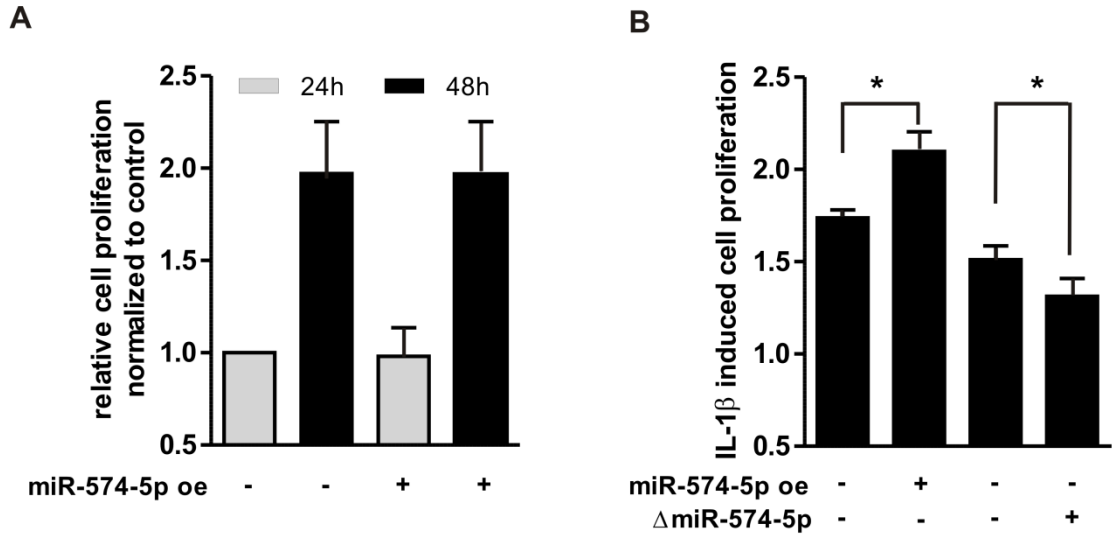

Fig. 35: Effect of miR-574-5p overexpression (20 pmol/µl) and knockdown (40 pmol/µl) on IL-1β induced cell proliferation in A549 cells analyzed by MTT cell proliferation assay. MTT cell proliferation assay was performed in A549 cells 24 h after transfection induced with and without IL-1β (5 ng/ml) for 24 h with (A) miR-574-5p oe w/o IL-1β (B) miR-574-5p oe and ΔmiR-574-5p with IL-1β. The relative changes were given as mean + SEM of minimum three independent experiments; t-test, $p^* < 0.05$.

Next it was investigated whether the effect of mPGES-1 regulation alone is responsible for the changes in proliferation mediated by CUGBP1 and miR-574-5p. Therefore, a MTT cell proliferation assay was performed using an mPGES-1 inhibitor (CIII) or DMSO control, respectively [53,57]. As shown in Fig. 36 treatment with the mPGES-1 inhibitor led to no significant changes in A549 cell proliferation neither for the control nor for ΔCUGBP1/miR-574-5p oe. Determination of cell viability analyzed in Fig. 22 demonstrated a decreased cell viability of CUGBP1 overexpression cells. The MTT cell proliferation analysis indicate that

there might be an additional pathway that is regulated by the interplay of CUGBP1 and miR-574-5p, as mPGES-1 regulation alone is not responsible for changes in cell proliferation. This stands in line with the results in Fig. 25 that IL-1β treatment led to an increased mPGES-1 expression but not an increased cell proliferation.

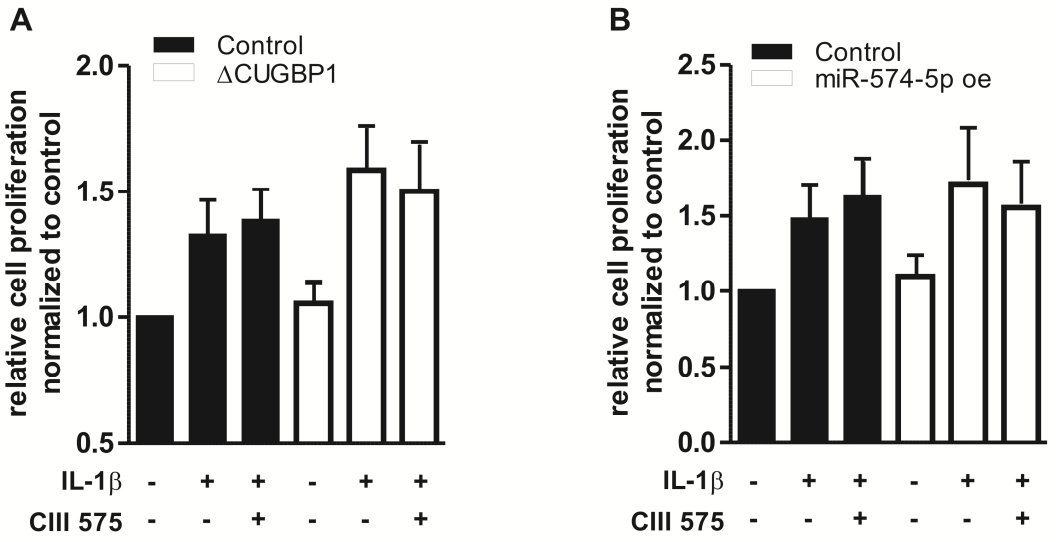

Fig. 36: Cell proliferation in A549 cells treated with 10 µM mPGES-1 inhibitor (CIII) in combination with ΔCUGBP1 (20 pmol/µl) and miR-574-5p oe (20 pmol/µl) analyzed by MTT cell proliferation assay. MTT cell proliferation assay was performed in A549 cells 24 h after transfection induced with IL-1β (5 ng/ml) for further 24 h with (A) ΔCUGBP1 (B) miR-574-5p overexpression. The relative changes were given as mean + SEM of four independent experiments; t-test.

4.3 miR-574-5p promotes lung tumour growth *in vivo*

4.3.1 Characterization of the stable miR-574-5p oe A549 cell line

It is known that tumour invasion and metastasis is regulated by miR-574-5p in non-small cell lung cancer [274]. Furthermore, it was shown that mPGES-1 expression and PGE_2 formation determines tumour growth of lung cancer cells *in vivo* [70]. To gain more detailed insights into the mechanisms behind the tumour progression linked with miR-574-5p *in vivo* and to unravel potential links with enhanced PGE_2 synthesis, miR-574-5p was stably overexpressed in the human A549 lung cancer cell line using lentiviral particles. The stable transfection was more useful due to long-term gene expression required in the mouse xenocraft model, which was established in cooperation with the lab of Prof. Paola Patrignani (University Chieti, Italy). The overexpression of miR-574-5p was assessed by qRT-PCR analysis. miR-574-5p was significantly upregulated to ~33 fold (Fig. 37 A), but much lower than transient miR-574-5p oe. Since there can be variations between stable and transient transfection due to a number of factors like position, site of integration and copy number, the stable cell line was

characterized. On mRNA level no significant changes could be observed for IL-1β induced mPGES-1 and mPGES-1 3´UTR isoform (Fig. 37 C). However, MTT cell proliferation assay did not show an increase in A549 cell proliferation in response to miR-574-5p (Fig. 37 B) in contrast to observations in transient A549 miR-574-5p oe cells.

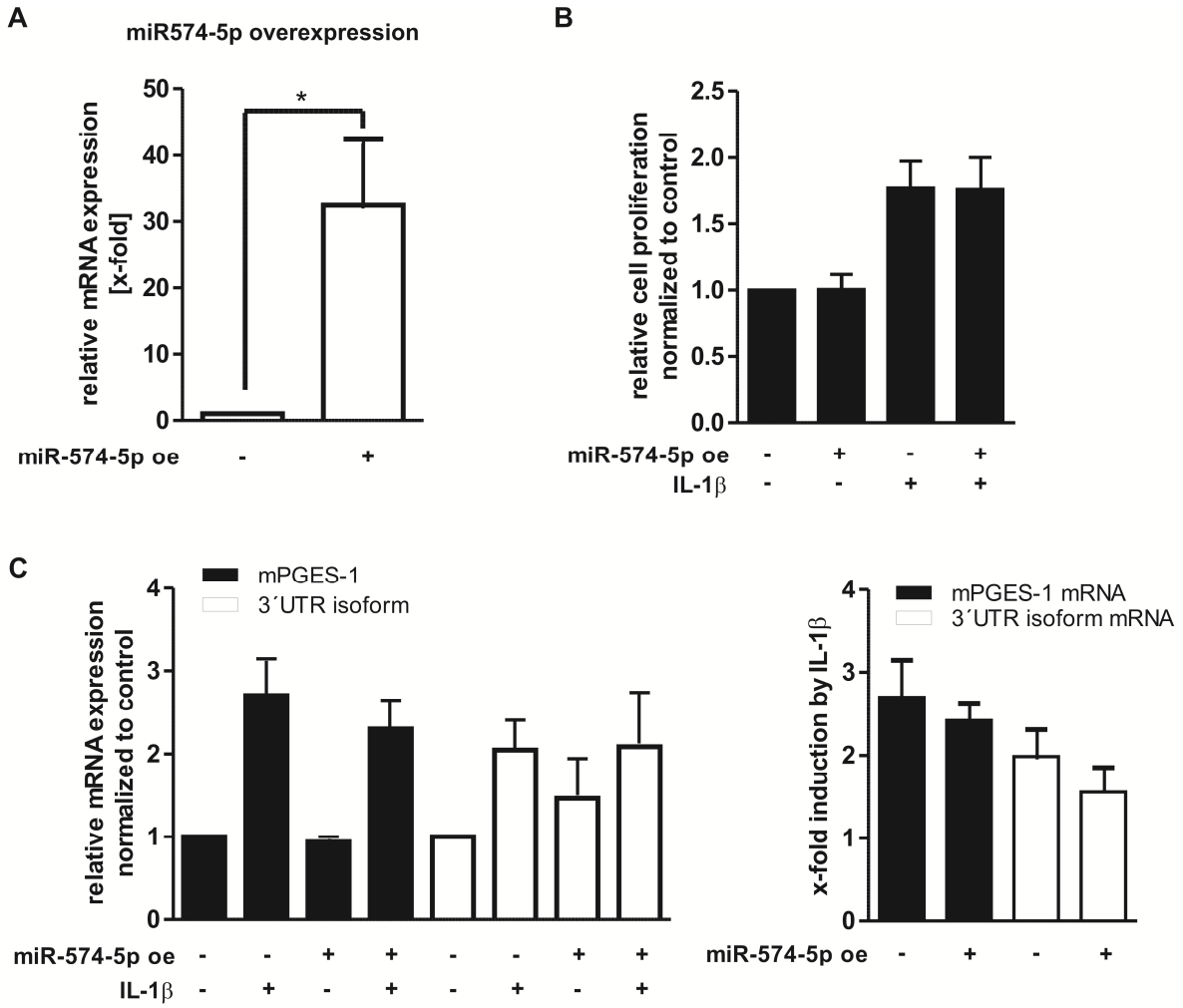

Fig. 37: Characterization of stable miR-574-5p oe A549 cell line. (A) qRT-PCR analysis of miR-574-5p-overexpressing A549 cell line. U6 was used as endogenous control. The relative changes to control samples were given as mean + SEM of five independent experiments. (B) MTT cell proliferation assay. MTT cell proliferation assay was performed in A549 cells induced with IL-1β (5 ng/ ml) for 24 h. (C) qRT-PCR analysis of mPGES-1 3´UTR and (C) mPGES-1 mRNA expression in response to miR-574-5p oe. Actin was used as control. The relative changes were given as mean + SEM of three independent experiments. The relative changes were given as mean + SEM of three independent experiments; t-test, $p^* < 0.05$.

4.3.2 miR-574-5p enhances lung tumour growth *in vivo*

Together with our cooperation partner in Italy (Prof. Paola Patrignani and her lab members, University Chieti) mPGES-1 protein expression and PGE_2 production in stable A549 miR-

547-5p cells was analyzed. It was shown that A549 miR-574-5p oe cells produced enhanced PGE_2, which was associated with increased mPGES-1 protein expression in response to IL-1β treatment (Fig. 38 A/B). This supported the theory that the dysregulated mPGES-1 expression in miR-574-5p oe cells explained enhanced PGE_2 production *in vitro*.

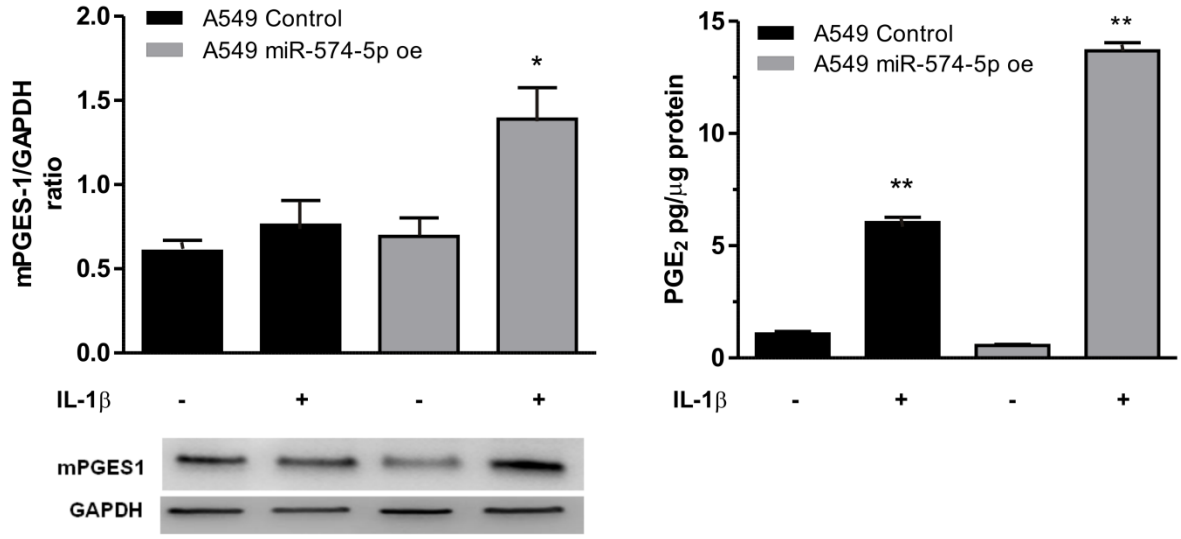

Fig. 38: miR-574-5p increases mPGES-1 protein and PGE_2 production. (A) Stably transduced A549 cells were stimulated with IL-1β (5 ng/ml) for 24 h. mPGES-1 protein expression in stable A549 miR-574-5p oe and control cells. GAPDH was used as loading control. A representative Western blot of three idependent experiments is shown. (B) PGE_2 production in A549 control and miR-574-5p oe cells. The relative changes to control samples were given as mean + SEM of three independent experiments, t-test, $p^* < 0.05$, $^{**}p < 0.01$.

For deeper insights into the mechanisms behind the tumour progression linked with miR-574-5p *in vivo* demonstrated by Zhou *et al.* [275], CD-1® Nude mice were chosen to address the potential tumourigenic effect of miR-574-5p. These experiments were performed in the lab of Prof. Paola Patrignani in Italy. PGE_2 measurements demonstrated a significant increase in PGE_2 production in A549 miR-574-5p oe cells in response to IL-1β, which was attributed to upregulation of mPGES-1 expression in response to miR-574-5p oe. Therefore, the selective mPGES-1 inhibitor CIII [53] was used to evaluate whether the stimulation of tumour growth by miR-574-5p *in vivo* is due to increased PGE_2 formation. A549 control cells or A549 miR-574-5p oe cells were resuspended in PBS and then subcutaneously (s.c.) injected into both dorsal flanks of mice to establish a model of tumour-bearing mice (Fig. 39 A). Tumour growth and weight was recorded over 4 weeks.

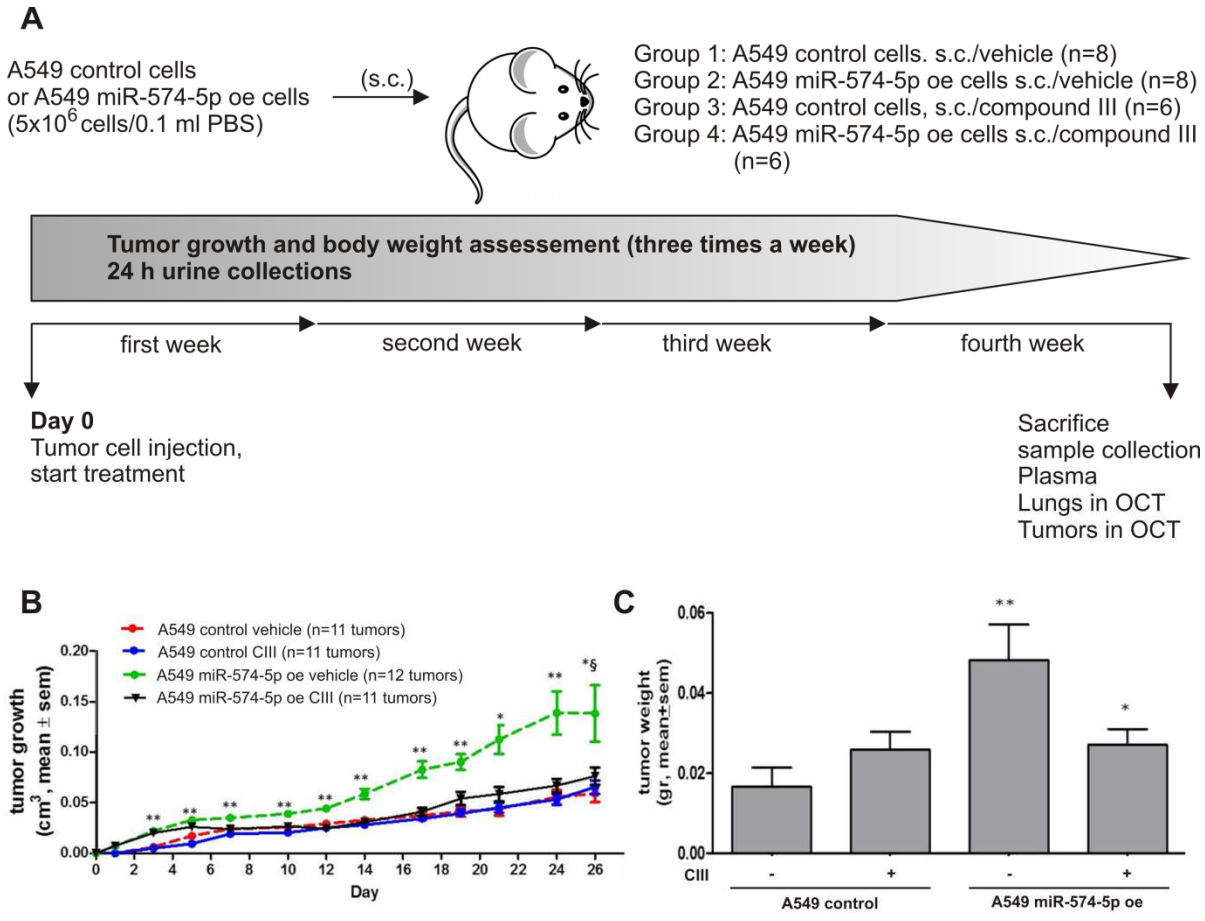

Fig. 39: miR-574-5p promotes tumour growth *in vivo*. (A) Experimental design of mouse experiments. CD-1® Nude Mice were housed under specific pathogen-free conditions. A549 control cells or A549 miR-574-5p oe cells were s.c. injected into both dorsal flanks of mice. The mPGES-1 inhibitor (CIII) or vehicle control, respectively were administered every day, until sacrifice. Control mice received A549 control cells or A549 miR-574-5p oe cells and were treated with vehicle, once every day by i.p. injection from tumour cell implantation until sacrifice. A group of mice received A549 control cells or A549 miR-574-5p oe cells and were treated with CIII once every day, by i.p. injection from tumour cell implantation until sacrifice. Tumour growth and body weight were monitored from tumour cell implantation until sacrifice. Mice were sacrificed after 4 weeks from tumour cell implantation, 30 min after the last treatment. Plasma, Lungs and tumours were collected for further analysis. (B & C): Nude mice with A549 control cells (A549 control) or A549 cells overexpressing miR-574-5p (A549 miR-574-5p oe) ($5x10^6$/100µl PBS). A549 control cells-injected or miR-574-5p oe cells-injected mice were treated with vehicle or with CIII (50mg/kg) once every day by i.p. injection from tumour cell implantation until sacrifice. (B) PGE_2 measurement after sacrifice (B) tumour growth (C) tumour weight. At each experimental time-point, **p<0.001 vs. A549 control vehicle and A549 miR-574-5p oe CIII 50mg/kg, i.p. *p<0.01 vs. A549 control vehicle; §p<0.05 vs. A549 miR-574-5p oe CIII 50mg/kg, i.p. ANOVA analysis and Newman-Keuls multiple comparison test.

Cells overexpressing miR-574-5p exhibited enhanced tumourigenic ability compared to control cells starting from day 3 after tumour cell implantation (Fig. 39 B). The treatment with the mPGES-1 inhibitor CIII prevented this effect. In mice injected with A549 control cells, treatment with the mPGES-1 inhibitor CIII did not significantly affect tumour growth *in vivo*. At the day of sacrifice the animals were killed and the tumours dissected and weighted. Accordingly to the volume, the weight of the tumours was significantly enhanced in mice

injected with A549 miR-574-5p oe cells compared to the mice injected with A549 control cells (Fig. 39 C). Moreover, the treatment with the mPGES-1 inhibitor CIII every day from tumour cell implantation until sacrifice significantly prevented this effect. In mice injected with A549 control cells, the treatment with the mPGES-1 inhibitor CIII did not significantly affect tumour weight at sacrifice. These results indicate that A549 miR-574-5p oe cells and elevated PGE_2 levels in this cell type are associated with enhanced tumour growth *in vivo* in nude mice.

4.4 miR-574-5p is upregulated in tumours of NSCLC patients stage II-III

Recently, miR-574-5p has been described as a potential important serum-based biomarker for early-stage non-small cell lung cancer cells (NSCLC) I-II [239]. In that microarray of Foss *et al*. miR-574-5p was upregulated to 2.17 fold in serum normalized to control. Keller and coworkers demonstrated a 3.59 fold upregulation of miR-574-5p in blood cells from lung tumour in response to blood cells from healthy controls [276]. In IL-1β stimulated A549 cells with transient miR-574-5p overexpression the proliferation was increased (Fig. 35). To reveal novel tumour-related miR-574-5p expression in NSCLC miR-574-5p expression in tumour and non-tumour, lung tissue of four NSCLC patients was analyzed. (The samples were kindly provided by Dr. R. Savai, Max Planck Institute for Heart and Lung Research in Bad Nauheim, Germany). Three of them were histological categorized as adenocarcinoma and one as squamous carcinoma. In tumours there was a significant increase in miR-574-5p expression assessed by qRT-PCR (T:24.5-28.2 Ct values) (NT:28-33.5 Ct values) (Fig. 40).

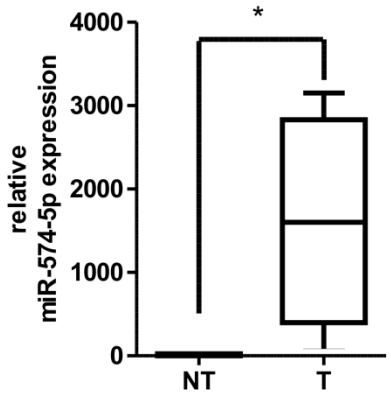

Fig. 40: miR-574-5p expression is upregulated in tumours of NSCLC patients. qRT-PCR analysis of miR-574-5p expression. miRTC was used as endogenous control. The relative changes to control samples were given as mean + SEM of four independent experiments; t-test, $p^* < 0.05$.

The expression values were normalized to miRTC control, which permits a suitable assessment of reverse-transcription performance. It has been shown that miRNAs expression levels can be differently regulated in lung cancer [277,278]. Therefore, a selection of other miRNAs was tested as endogenous control. U6, miR-16 and Snord-72 were no valid controls as their expression level changes in lung cancer. qRT-PCR analysis of U6, miR-16 and Snord-72 revealed a strong regulation in the lung cancer tissue of the patients. The different miR-574-5p expression profiles between NSCLC and healthy tissue and between the subtypes/stages of NSCLC may have potential implications in the pathogenesis of this cancer. This preliminary data demonstrated that there may be an association between miR-574-5p upregulation in NSCLC and survival in lung cancer patients.

5 Discussion

5.1 CUGBP1 regulates mPGES-1 expression multifunctional via alternative splicing, mRNA turnover and translational repression

There is huge evidence addressing increased prostaglandin production in tumour development and progression. Elevated levels of mPGES-1 and PGE_2 have been found in different types of cancers, including prostate cancer, colon cancer and non-small cell lung cancer (NSCLC) [11,65]. Different studies demonstrated that the mPGES-1 promoter alone cannot account for the strong induction of mPGES-1 by cytokines suggesting that additional post-transcriptional mechanisms might be involved such as alternative splicing, mRNA turnover or translational control. It is known that the expression of mPGES-1 can be controlled by several transcription factors (Egr-1, NF-κB, AP-1) and MAP kinases [279,280]. Moreover, it was shown that the 3´UTR of mPGES-1 contains two GREs which could function as *cis* regulatory elements recruiting *trans*-acting factors which may regulate mRNA level, translation or localization [254]. Until now nothing is known if alternative splicing is involved in the upregulation of mPGES-1 expression observed in inflammation and cancer.

Since defects in splicing are often correlated with diseases and involved in the progression of cancer [116,117], changes in the splicing patterns of mPGES-1 3´UTR in A549 cells, HeLa cells and synovial fibroblast from RA patients were investigated. Analysis of mPGES-1 splicing pattern in these cell lines revealed the existence of a ~300 bp alternatively spliced 3´UTR transcript (Fig. 13). Sequence analysis of this mPGES-1 3´UTR isoform exhibits that the middle part of mPGES-1 3´UTR was spliced out (NM_004878.4). Interestingly, both sites of mPGES-1 3´UTR intron are flanked with a GRE representing binding sites for RNA-binding protein CUGBP1 [195]. In this study, it was demonstrated that CUGBP1 binds sequence specifically to both GREs of mPGES-1 3´UTR.

Multiple regulatory functions of CUGBP1 on mRNA processing including mRNA splicing, destabilization and translation of mRNAs have been reported so far [151]. In line with that, we have shown that CUGBP1 is responsible for mPGES-1 3´UTR splicing and both GREs within the 3´UTR are necessary for alternative splicing (Fig. 17). The GREs were responsible for decreased luciferase activity analyzed by reporter gene assays. The effect was abolished by the sequential and double deletion of the GREs. Furthermore, RT-PCR analysis confirmed these data as there was no 3´UTR splice product detectable by the sequential or

double deletion of GREs. These data suggest mPGES-1 3´UTR splicing was mediated by CUGBP1 whereby both GREs are essential for splicing. These findings correspond with published data. It was shown that aberrant regulation of insulin receptor (INSR) was due to alternative splicing (skipping of exon 11) mediated by CUGBP1 [281]. Furthermore, CUGBP1 binds to a GU-rich sequence in intron 2 of muscle-specific chloride channel 1 (CLCN1) in DM1, which leads to intron retention and a PTC-containing mRNA transcript that is rapidly degraded [188,189]. However, additional studies are required to clarify the exact mechanism by which CUGBP1 binding to its RNA targets regulates alternative splicing events. It could also involve conformational changes in the RNA structure or competition with other splicing factors to promote or repress the spliceosome formation. Furthermore, mPGES-1 3´UTR has predicted binding sites for hnRNP E2, HuR and muscleblind-like splicing regulator (MBNL) 1, which play a role in many regulatory processes. It was shown that abnormal alternative splicing of CLCN1 and INSR caused myotonia and insulin resistance and was due to an imbalance of the two RNA-binding proteins MBNL and CUGBP1 that act in an antagonistic manner. In addition, it has been shown that MBNL1 binds directly to CUG and CCUG repeat RNAs [282,283]. Also, it has been shown that competition between CUGBP1 and HuR modulates MYC translation and intestinal epithelium renewal [284]. Competition of CUGBP1 and calreticulin in the regulation of p21 translation determines cell fate [200]. ABLIM1 splicing is abnormal in skeletal muscle of patients with DM1 and regulated by the interplay between MBNL, CELF1, 2 and 6 and PTBP1 [285]. It seems that aberrant alternative splicing mediated by CUGBP1 occurs in the nucleus [286]. Repression of nuclear CUGBP1 activity could rescue CUGBP1-regulated alternative splicing defects in skeletal muscle models of myotonic dystrophy [287].

The reporter gene assays in HeLa cells demonstrated that CUGBP1 binding to GREs in the mPGES-1 3´UTR reduced gene expression maybe mediated by reduced mRNA stability. Indeed, actinomycin D treatment to address mRNA stability resulted in a substantial decrease in the amount of mPGES-1 isoform mRNA, in contrast to mature mPGES-1 mRNA, which still contains two GREs in the 3´UTR (Fig. 18). This data suggest that CUGBP1 might preferably regulate mRNA stability of the mPGES-1 3´UTR isoform. Highly conserved GU-rich elements composed of a consensus sequence UGUUUGUUUGU or GU-repeat sequence can be targeted by CUGBP1 and have been identified as sequence elements enriched in the 3´UTR of short-lived transcripts, which encode important regulators of cell

cycle and apoptosis [177]. It has been shown that cytosolic GU-containing mRNA transcripts are rapidly degraded by CUGBP1 dependent recruitment of PARN deadenylases [264,288]. CUGBP1 interacts with PARN in HeLa cytosolic cell extracts to promote deadenylation of Fos and TNF transcripts [264]. Furthermore, siRNA-mediated knockdown of CUGBP1 in HeLa cells and myoblasts led to the stabilization of a set of normally rapidly degraded transcripts bound by CUGBP1 to GREs and GU-repeats [177,195,261].

mRNA transcripts with premature termination codons are highly instable and rapidly degraded by mRNA decay mechanisms such as NMD. The spliced mPGES-1 3´UTR isoform contains a PTC and is therefore a potential NMD target [263]. UPF1 knockdown experiments were performed to inhibit NMD and to determine whether CUGBP1 or UPF1-mediated mRNA decay pathways is responsible for 3´UTR isoform degradation. No changes in mRNA expression of mPGES-1 and the 3´UTR splice variant were observed depleting UPF1, suggesting that UPF1-independent mRNA degradation of mPGES-1 isoform is mediated by CUGBP1, which recruits PARN to cytosolic GU-containing transcripts (Fig. 18). Interestingly, mature mPGES-1 3´UTR transcript is not affected by GU-mediated mRNA decay, suggesting that there are additional regulatory mechanisms that prevent the correctly spliced mature transcript from GU-mediated mRNA decay in the cytosol. This observation stands in line with CUGBP1 overexpression where only a slight decrease of 3´UTR isoform was observed but mature mPGES-1 mRNA was not affected (Fig. 23). Taken together, these data suggest that (i) nuclear CUGBP1 acts as splice factor for mPGES-1 3´UTR by binding to both GREs, thereby inducing alternative splicing in the 3´UTR, (ii) cytosolic CUGBP1 acts together with PARN as RNA destabilizing factors by binding to the GU consensus sequence of mPGES-1 3´UTR isoform, (iii) cytosolic CUGBP1 preferably seems to reduce dysregulated 3´UTR isoform, whereas correctly spliced mPGES-1 mRNA is not degraded or maybe stabilized by other RBPs. Until now, whether these functions of CUGBP1 are directly linked together or compartmentally independently regulated remains unclear. There can be a network of additional regulation mechanisms and RBPs that regulate mPGES-1 mRNA turnover and translation.

Time course experiments in A549 cells were performed with ΔCUGBP1 to address the potential destabilizing effect of CUGBP1 on mPGES-1 expression in an inflammatory context. Depletion of CUGBP1 significantly increased mPGES-1 3´UTR isoform mRNA expression, whereas mature mPGES-1 mRNA was less affected. These data demonstrate the destabilizing effect of CUGBP1 on the splice variant. However, mPGES-1 protein

expression was also upregulated by ΔCUGBP1 (Fig. 20) and in contrast downregulated in response to CUGBP1 oe (Fig. 23). CUGBP1 depletion had a stronger effect on mPGES-1 protein than on mRNA expression, suggesting that (i) mRNA turnover increases mPGES-1 protein and (ii) CUGBP1 may additional acts as translational repressor for mPGES-1. This stands in line with the results of Yu and coworkers who demonstrated that CUGBP1 acts as translational repressor for occludin [151]. In this study, they showed that CUGBP1 binds to 3´UTR of occludin through increasing recruitment of tagged occludin mRNA to processing bodies (PBs). Consistent with these findings, CUGBP1 has also been shown to repress CDK4 translation by increasing CDK4 mRNA translocation to PBs [289]. Furthermore, CUGBP1 and HuR regulate E-cadherin translation by altering recruitment of E-cadherin mRNA to PBs thereby modulating epithelial barrier function [271]. To prove the hypothesis that CUGBP1 might repress translation of mPGES-1 mRNA due to recruiting mPGES-1 mRNA in PBs the distribution of CUGBP1 and PBs was examined by immunofluorescence staining. CUGBP1 extensively colocalizes with the prominent PB marker DCP1a (Fig. 24). To investigate whether PB formation plays a crucial role in mPGES-1 translation GW182 was silenced, which is crucial for PB formation [270]. As expected the mature mPGES-1 mRNA was not affected by GW182 knockdown, whereas the protein expression was significantly increased (Fig. 24), indicating an important role of CUGBP1 acting as translational repressor for mPGES-1 protein expression in combination with PB formation mediated by PB marker GW182. The exact mechanisms by which PBs repress the translation of resident mRNAs need to be further investigated. It remains still unclear how exactly mPGES-1 protein is increased by CUGBP1 depletion. Whether it is only due to mRNA turnover, PB formation or a combination of both needs to be further investigated. PBs contain many proteins that are associated with RISC complex and mRNA decay: All four Ago proteins, GW182, RCK and MOV10 (two RNA helicases), DCP1 and DCP2 (decapping enzymes), CCR4–CAF-1–Not complex (mRNA deadenylation factors), Dhh1/RCK/p54, Pat1, Scd6/RAP55, Edc3, and the LSm1–7 complex (activators of decapping) and XRN-1 (exonucleases) [290,291,292]. Further studies investigating Ago or RCLK protein would be helpful to understand the exact regulation of PB recruitment, association with mRNA turnover and translation.

PGE_2 is highly expressed at sites of inflammation and cancer and though it might be involved in the progression an onset of many types of cancer. It is known that genetic deletion of mPGES-1 reduced the synthesis of inducible PGE_2 and markedly suppressed intestinal tumour formation in $Apc^{\Delta 14}$ mice [71]. Therefore, PGE_2 formation was analyzed in response

to ΔCUGBP1. Like mPGES-1 protein expression PGE_2 release was also significantly increased by CUGBP1 knockdown, assuming that mPGES-1 protein upregulation increases its enzymatic product PGE_2 (Fig. 20). Contrary to mPGES-1 protein expression, PGE_2 levels were significantly reduced after IL-1β depletion, suggesting that COX-2 or PGH_2 might be affected by CUGBP1. mPGES-1 expression is often concomitantly induced in response to COX-2 overexpression, thus, contributing to the efficient generation of PGE_2 [11]. COX-2 has no binding site for CUGBP1. Hence, CUGBP1 knockdown had no influence on COX-2 expression levels. The downregulation of PGE_2 was attributed to the strong decrease in COX-2 mRNA and protein expression after IL-1β depletion, leading to decreased PGH_2 levels (Fig. 20). These data demonstrate the specific regulation of mPGES-1 expression by CUGBP1.

To sum up CUGBP1 has multiple functions on mPGES-1 expression. Here, it was demonstrated that CUGBP1 is responsible for mPGES-1 3´UTR splicing. Besides its role as splice factor, CUGBP1 binds to GREs within 3´UTR of short-lived transcripts and promotes GU-dependent mRNA decay of the spliced 3´UTR isoform. Furthermore, it was shown that CUGBP1 represses mPGES-1 translation, obviously by recruiting mPGES-1 mRNA to PBs.

5.2 New insights into CUGBP1-dependent mPGES-1 regulation in RA

RA is a systemic autoimmune disease primarily affecting the joints of patients and leading to their progressive destruction. This joint destruction is a unique and most prominent symptom of RA that not only distinguishes the disease from other arthritic conditions [293]. RA is associated with typical symptoms such as pain and inflammation. During active RA immune cells like monocytes, macrophages, mast cells, T and B cells infiltrate the synovial joints. The immune cells interact in a complex manner, which leads to the release of pro-inflammatory mediators [294] (Fig. 41). High levels of pro-inflammatory cytokines including TNFα, IL-1β and IL-17 can be detected in fluids and synovium in the joints of RA patients. It is known that these mediators play an important role in the initiation and development of RA [295]. Furthermore, they are associated with the production of biologically active lipid mediators like PGE_2. It has been shown that mPGES-1 in contrast to cPGES and mPGES-2 is markedly

upregulated in synovial tissue from RA patients [296]. These findings suggest that increased levels of mPGES-1 during active RA play a major role in the production of PGE_2, while mPGES-2 and cPGES may rather have a minor role. Until today selective COX-2 inhibitors are extensively used for the treatment of RA [297]. But several clinical trials demonstrated that some COX inhibitors, except ASS and Naproxen, increase the risk of cardiovascular events [24]. In order to reduce the side effect of COX inhibitors, selective suppression of mPGES-1-derived PGE_2 production seems to be an attractive therapeutic alternative. It was shown that mPGES-1 deletion in mice leads to significant decrease in PGE_2 levels and increases in PGI_2 with no alterations in blood pressure or thrombosis [75].

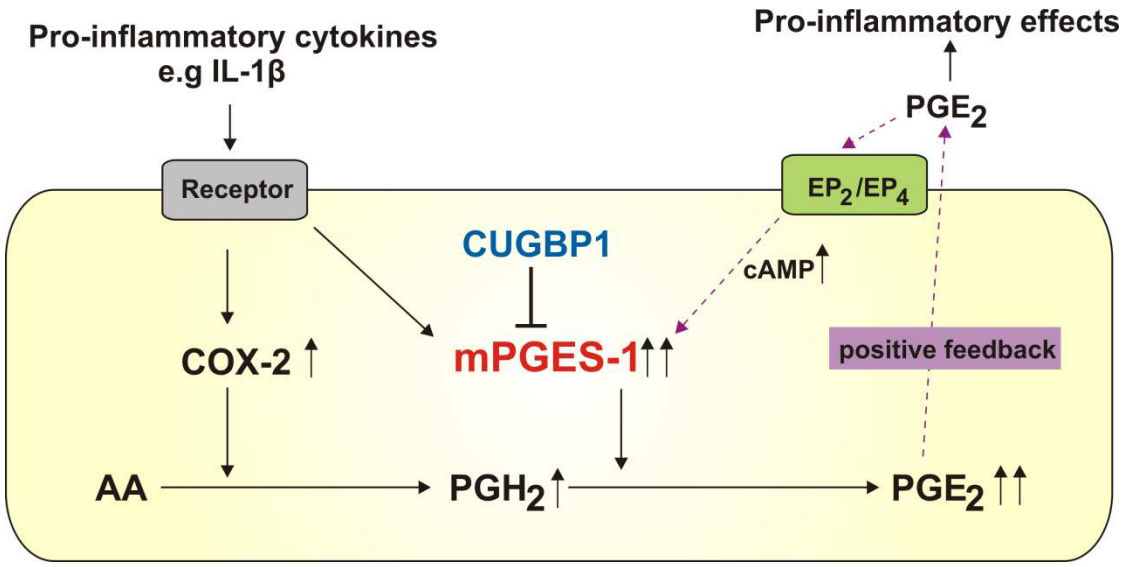

Fig. 41: Model of regulation of mPGES-1 expression in rheumatoid synovial fibroblasts. COX-2 and mPGES-1 are induced by stimulation of pro-inflammatory cytokines e.g. IL-1β. Abundant PGE_2 production at the inflammation sites of RA is caused by the coordinated upregulation of mPGES-1 and COX-2. PGE_2 enhances mPGES-1 expression associated with increase of cyclic AMP (cAMP) via the EP2 and EP4 receptors. The positive feedback regulation of mPGES-1 expression by PGE_2 may play an important role in the vicious circle of inflammation associated with RA, modified [298].

Investigation of mPGES-1 splicing pattern in SF cells demonstrated the presence of the mPGES-1 3´UTR isoform that may be correlated to the inflammatory status of synovial fibroblasts derived from RA patients. In the model cell line A549, it was shown that CUGBP1 is responsible for mPGES-1 expression regulation by alternative splicing and GU-mediated mRNA degradation of the spliced mPGES-1 3´UTR isoform. CUGBP1 levels were manipulated to investigate the influence of CUGBP1 on mPGES-1 expression in SF cells. According to the results in A549 cells the siRNA-mediated knockdown of CUGBP1 did not alter mPGES-1 mRNA levels (Fig. 21), whereas the destabilizing effect of CUGBP1 on the 3´UTR isoform was abolished. Preliminary data showed that mPGES-1 protein was slightly

increased in SF0246 by ΔCUGBP1. However, the knockdown efficiency of CUGBP1 was weaker than in A549 cells. The results would match with those in A549 cells that translation repression of mPGES-1 is mediated by CUGBP1. With these results it will be interesting to elucidate further approaches in CUGBP1-dependent mPGES-1 regulation and PGE_2 production as they may be important in RA development and treatment.

5.3 CUGBP1 is constitutively expressed and not regulated via its translocation

CUGBP1 is a multifunctional protein and involved in different molecular processes with specific functions in different cellular compartments [109,186]. Therefore, it was investigated how CUGBP1 is localized, regulated and expressed in A549 cells to unravel the multiple influence of CUGBP1 on mPGES-1 expression. Investigation of mRNA and protein expression levels of CUGBP1 in A549 cells and in RASF revealed that CUGBP1 is constitutively expressed and not regulated by cytokine IL-1β or altering mPGES-1 expression levels (Fig. 26 & Fig. 27). Immunofluorescence stainings and Western blot analysis showed that CUGBP1 is located in the nucleus as well as in the cytoplasm, which stands in line with previous work of Timchenko and coworkers [109].

CUGBP1 function is not only dependent from its localization but also by its phosphorylation status [202,203]. CUGBP1 protein expression was increased in the muscle of myotonic dystrophy (DM) patients and DM mouse models in which nuclear CUGBP1 was stabilized by PKC-mediated phosphorylation [199,281]. Until now it is not known how PKC is activated. In addition, phosphorylation of CUGBP1 is altered by activation of GSK3β signaling in DM [181]. However, the mechanism of PKC and GSK3β activation by expanded repeat RNAs remains unclear. It was shown that for binding to the G/C rich element of p21 and C/EBPβ mRNAs, CUGBP1 has to be hyperphosphorylated and accumulated in the nucleus [200,204]. In contrast, the cytosolic deadenylation activity to GREs is activated by dephosphophorylation [202]. The deadenylation activity leads to a degradation of the target mRNA and consequently a decreased synthesis of the encoded protein by removal of the translation template. In accordance with this, analysis of phosphorylation status of CUGBP1 revealed no phosphorylation in A549 cells, HeLa cells and RASF during time courses or CUGBP1oe/ΔCUGBP1 experiments (data not shown). CUGBP1 was just slightly phoshorylated in A549 cells when it was overexpressed (Fig. 26). It was shown that regulation of CUGBP1 expression may be crucial in NSCLC tissue, where CUGBP1 was highly expressed and there its overexpression was associated with the progression of

NSCLC [205,208,209]. The various effects of CUGBP1 on mPGES-1 expression could not fully be explained by its cellular translocation, changes in expression levels or phosphorylation status of CUGBP1, suggesting that an additional regulation mechanism may exists.

The capacity of CUGBP1 to bind to one or more GU-rich elements could depend on the presence or absence of other proteins in a multimeric functional complex. The association with these cofactors could be affected by the hyper- or dephosphorylation status of CUGBP1 or by the expression of the cofactor(s). Hence, the change between G/C-rich binding associated with translational control, possibly via eIF2 binding [299], and GU-rich binding associated with deadenylation and mRNA degradation appears to be controlled by signaling pathways that activate or inactivate appropriate kinases. Until now the amino acids whose phosphorylation is required for G/C-rich binding and those that must be dephosphorylated to activate the deadenylation process have not been identified. Therefore, whether these binding and functional characteristics are mutually exclusive cannot be decided yet.

5.4 miR-574-5p acts as RNA decoy to CUGBP1

Previously, a new mechanism for miRNAs has been identified for miR-328. It has been shown that miR-328 can bind to a regulatory repressing protein thereby acting as decoy leading to activation of gene expression [235,236]. This is, in contrast to the classical function of miRNAs as silencers. miR-574-5p harbors the GU-rich elements (GREs) in its mature form thereby representing *bona fide* binding sites for the RNA-binding CUGBP1 (Fig. 28). Therefore, we hypothesized that miR-574-5p may act as RNA-decoy for CUGBP1. We could demonstrate that CUGBP1 binds specific to miR-574-5p, assuming that there may be a regulation of mPGES-1 by the interaction of miR-575-5p and CUGBP1 (Fig. 29). Interestingly, different studies demonstrated that upregulation of miR-574-5p confer with an enhanced tumour progression in human lung cancer, which correlates with an elevated mPGES-1 expression level in this type of cancer [300]. In addition to this, miR-574-5p has been described as a serum-based miRNA biomarker for early stage NSCLC [239]. We demonstrated that miR-574-5p and mPGES-1 mRNA were upregulated by IL-1β treatment after 24 h and notably downregulated in response to IL-1β removal (Fig. 30). Furthermore, miR-574-5p levels in A549 cells were manipulated to investigate the effects of the balance between miR-574-5p and CUGBP1 on mPGES-1 expression. Overexpression of miR-574-5p in A549 cells using miR-574-5p mimics supported the theory that miR-574-5p acts a direct

decoy for CUGBP1 binding. During IL-1β mediated induction mPGES-1 3´UTR isoform was significantly induced in response to miR-574-5p oe. The mature induced mPGES-1 transcript was not affected by miR-574-5p overexpression, whereas IL-1β induced mPGES-1 protein expression was significantly upregulated (Fig. 32). Additionally, knockdown of miR-574-5p in A549 cells led to a significant decrease of IL-1β induced mPGES-1 3´UTR isoform, where in contrast the mature mPGES-1 mRNA was not affected (Fig. 34). Unfortunately, a decrease of induced mPGES-1 protein expression was not detected, which could be due cell homoeostasis. If miR-574-5p is not present in A549 cells there is no need for CUGBP1 to reduce mPGES-1 protein levels.

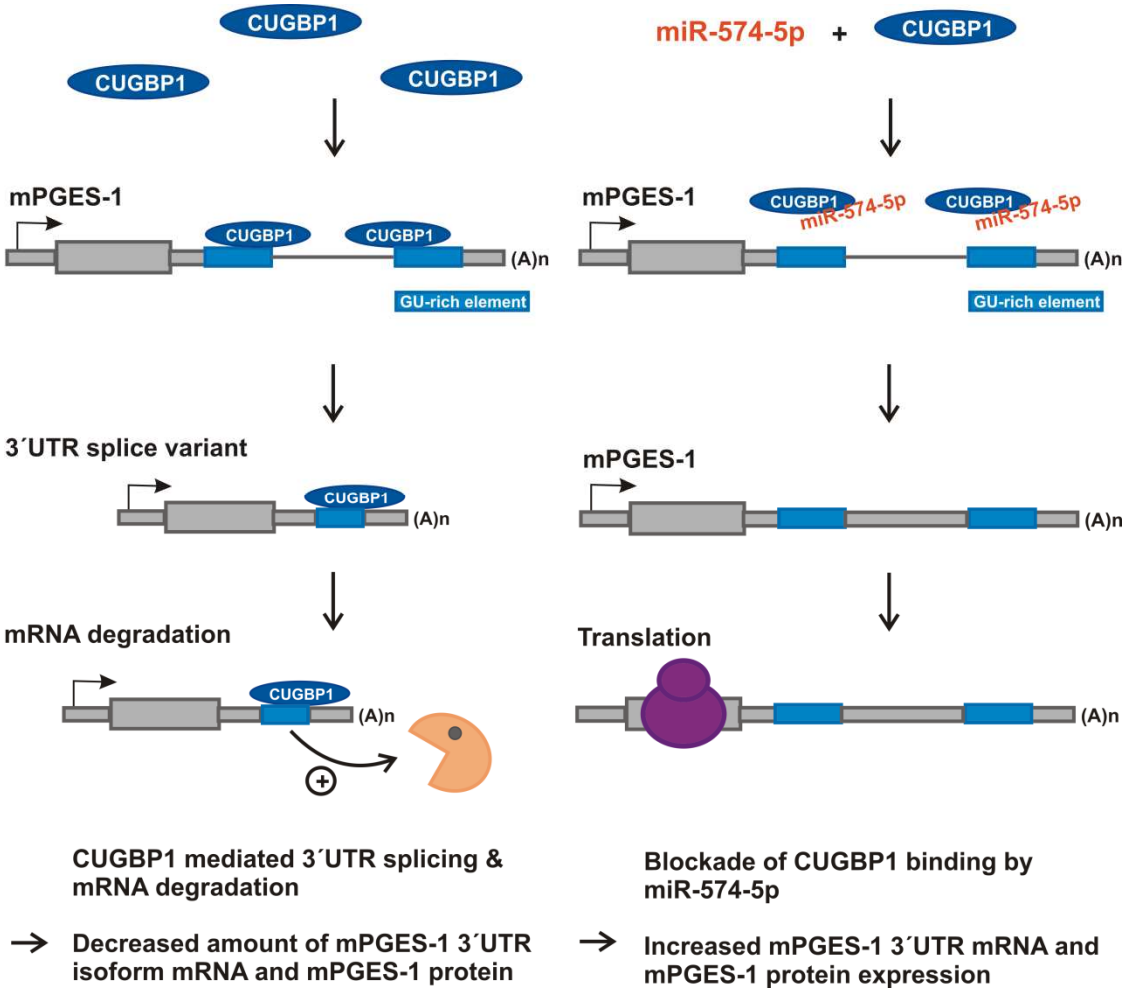

Fig. 42: Model of the interaction between miR-574-5p and CUGBP1 on mPGES-1 expression.

5 Discussion

Taken together our study revealed that miR-574-5p has a perfect binding site for CUGBP1 and acts as RNA decoy to CUGBP1 as it is illustrated in the model in Fig. 42. The stimulatory effects of miR-574-5p on mPGES-1 expression suggested a mechanism that does not follow the canonical function of miRNAs to inhibit gene expression via binding to the 3´UTR of the target gene and stands in line with previous results of Saul *et al*. 2016 [236].

5.4.1 A549 cell proliferation is regulated by the balance of CUGBP1 and miR-574-5p

Cell proliferation, migration and invasion are commonly required for metastatic progression [301,302]. Assays that determine metabolic activity are suitable for analyzing proliferation, viability and cytotoxicity. The reduction of tetrazolium salts MTT and WST to colored formazan compounds only occurs in metabolically active cells [303]. Actively proliferating cells increase their metabolic activity while cells exposed to toxins will have decreased activity [304]. Since overexpression of mPGES-1 and its product PGE_2 are known to promote tumour growth acting via EP_2 receptor and by that stimulate cell proliferation, apoptosis and angiogenesis it was interesting to elucidate whether miR-574-5p stimulates A549 cell proliferation. miR-574-5p promotes NSCLC migration and invasion *in vitro* but it did not affected A549 cell proliferation [275]. This stands in line with the results shown in Fig. 35. No significant cell proliferation changes were observed in unstimulated A549 in response to miR-574-5p oe. Interestingly, an increase in IL-1β induced cell proliferation was observed in response to miR-574-5p oe, suggesting that inducing cytokine-dependent targets like mPGES-1 and miR-574-5p increase proliferation upon stimulation. CUGBP1 has been described to inhibit A549 cell proliferation [209]. In this study of Gao *et al*. a WST assay was used for the determination of the number of viable cells in cell proliferation. Contrary, trypan blue measurements revealed decreased cell viability in response to CUGBP1 oe in A549 cells during time courses (Fig. 22). These data were confirmed by MTT assays which demonstrated a significant decrease in IL-1β induced proliferation in response to CUGBP1 oe and a significant increase by depleting CUGBP1 (Fig. 25). It is known that the immunomodulatory cytokines, including IL-1β, TNF-α, and interferon-gamma (IFN) modulate the growth response in nonimmune cells and regulate cellular metabolism by inducing gene expression of biologically active molecules [305]. Interestingly, stable A549 miR-574-5p oe cells did not show increased cell proliferation (Fig. 37). The exact involvement of CUGBP1 and miR-574-5p in cell migration and tumor invasion needs to be further investigated, since mPGES-1 may not be the only common target involved in cell proliferation.

5 Discussion

5.5 miR-574-5p promotes lung tumor growth *in vivo* and may be a novel potent biomarker for NSCLC

A function of miRNAs as oncogenes or tumour suppressors has been extensively described [249]. Compelling evidences have demonstrated that dysregulated miRNAs affect proliferation, apoptosis, tumour metastasis and angiogenesis. Although miRNAs have multiple targets, their function in tumourigenesis remains unclear and could be due to their regulation of few specific targets [306]. A growing number of miRNAs have been shown to target genes which play a key role in lung cancer progression [307,308]. miR-224 promotes tumor progression in NSCLC by shifting the equilibrium of the partially antagonist functions of SMAD4 and TNFAIP1 toward enhanced invasion and growth [309]. miR-221 and miR-222 are involved in the development and progression of lung cancer by targeting PTEN and TIMP3 tumor suppressor genes [310,311]. Overexpressed miR-221/222 inhibits apoptosis and promotes cell migration by down-regulating PTEN and TIMP3**.** Recently, miR-574-5p has been described as one important serum-based biomarker for early-stage NSCLC [239]. The expression of miR-574-5p was significantly increased in serum samples obtained from patients with early-stage NSCLCs. Furthermore, it is known that tumour invasion and metastasis is regulated by miR-574-5p in lung cancer but the mechanisms behind these observations are unclear [274,275]. A549 cells which stable express miR-574-5p showed a strong increase in mPGES-1 expression and PGE_2 formation. Since PGE_2 is known to promote tumour growth by binding to EP_2 receptor and stimulates thus cell proliferation, apoptosis and angiogenesis we were interested to see if miR-574-5p stimulates tumour growth via a PGE_2-dependent mechanism. Additionally, it is known that PGE_2 reduction by selective COX-2 inhibitors suppress the growth of established tumours including head and neck, colorectal, stomach, lung, breast, and prostate tumours [69,312]. Recently, two clinical studies showed an upregulation of miR-575-5p in blood and sera of lung tumours, demonstrating the important role as a potent biomarker for this cancer type. In the present study analysis of four NSCLC patients showed a significant upregulation of miR-574-5p in tumours compared to control, suggesting that miR-547-5p may play a critical role in tumour growth and development. This hypothesis was confirmed in a xenograft mouse model where injection of A549 cells overexpressing miR-574-5p into nude mice led to a highly significant induction of tumour growth and weight compared to A549 control cells which could be blocked with the selective mPGES-1 inhibitor CIII. The data suggest that miR-574-5p exhibits oncogenic properties and promotes tumour growth via the induction of mPGES-1-derived PGE_2 synthesis. miR-574-5p may play a major role in the regulation of mPGES-1 dependent

5 Discussion

PGE_2 release in lung cancer and tumour growth. Therefore, miR-574-5p might offer a novel therapeutic target in treatment of lung cancer.

6 Summary

The terminal PGE synthase mPGES-1 converts PGH_2 derived from the precursor arachidonic acid into the pro-tumourigenic PGE_2 and is the key enzyme in the induced prostaglandin biosynthesis. mPGES-1-derived PGE_2 causes inflammation including swelling, fever and inflammatory pain. Therefore, mPGES-1 is a potential target for the development of novel anti-inflammatory drugs that can reduce symptoms of inflammation hopefully without causing severe cardiovascular side effects as traditional NSARs or selective COX-2 inhibitors may do. Here in this study, the regulation of mPGES-1 mRNA expression by post-transcriptional mechanisms such as alternative splicing or mRNA stability was investigated. A novel mPGES-1 3´UTR variant was identified in the non-small lung cancer cell line A549 and other cell types. This isoform is generated by splicing out a part of the 3´UTR. Here we could show that CUGBP1 binds to the GREs in the 3´UTR of mPGES-1. It was demonstrated that mPGES-1 3´UTR mRNA splicing and its subsequent degradation was mediated by CUGBP1 binding to GREs flanking both intron boundaries. This way of post-transcriptional regulation of mPGES-1 3´UTR by CUGBP1-dependent alternative splicing and rapid mRNA degradation is a powerful mechanism to reduce the amount of mRNA and protein. Additional, CUGBP1 repressed mPGES-1 translation obviously by recruiting mPGES-1 mRNA into P-bodies. We have shown that CUGBP1 exerts several functions on mPGES-1 mRNA and protein. Furthermore, we unraveled an additional regulatory level on mPGES-1 expression by a miRNA. MiRNAs are small non-coding RNAs and bind to the 3´UTR of their target mRNA in a sequence-specific manner controlling the expression of target genes either by translational repression or mRNA degradation. Recently, a new regulatory mechanism has been discovered when it was found that miR-328 acts as a RNA decoy to modulate translational repressor activity of hnRNP E2 by direct binding. In this study, we identified a second miRNA which exerts such new regulatory mechanisms. miR-574-5p harbors a binding site for CUGBP1 and acts as RNA decoy to CUGBP1. CUGBP1 binds to mature miR-574-5p thereby preventing the mPGES-1 3´UTR isoform from GU-mediated mRNA decay and mPGES-1 protein from translation repression mediated by CUGBP1. We assume that miR-574-5p plays a key role in the regulation of PGE_2 biosynthesis in inflammatory reactions by inhibiting CUGBP1 controlled mRNA decay and translation repression of mPGES-1. It is known that dysregulation of miRNAs contribute to the onset of cancer. Here it was shown that miR-574-5p is cytokine-dependent upregulated, suggesting its important role

in inflammation and micro environment of tumours. Indeed, in tumour tissue of NSCLC patients' miR-574-5p was significantly upregulated. We could show that the balance of CUGBP1 and miR-574-5p regulates cell proliferation and mPGES-1-dependent PGE_2 synthesis. This hypothesis was confirmed in a xenograft mouse model where injection of A549 cells overexpressing miR-574-5p into nude mice led to a highly significant induction of tumour growth and weight compared to A549 control cells. This effect could be blocked with the selective mPGES-1 inhibitor CIII. Based on these results we proofed that miR-574-5p is an oncogene and may play a major role in the regulation of mPGES-1-dependent PGE_2 release in lung cancer and tumour growth. Therefore, miR-574-5p might offer a novel therapeutic target in treatment of lung cancer.

7 Zusammenfassung

Die terminale PGE-Synthase mPGES-1 konvertiert PGH_2, welches von der Arachidonsäure geliefert wird, in das tumorigene PGE_2. In der induzierten Prostaglandin Biosynthese ist PGE_2 eines der wichtigsten Enzyme. Es ist verantwortlich für Entzündungen, Schwellungen, Fieber und Schmerz. Für die Pharmaforschung stellt mPGES-1 ein potenzielles Zielmolekül dar, um neue anti-inflammatorische Medikamente zu entwickeln, welche die kardiovaskulären Nebenwirkungen von NSARs nicht mehr besitzen. In dieser Studie wurde die post-trankriptionelle Regulation der mPGES-1 untersucht. Hierbei wurde eine neue mPGES-1 3´UTR Variante in der NSCLC Zelllinie A549 und anderen Zelllinien gefunden, die durch alternatives Spleißen des 3´UTR generiert wurde. Hierbei wurde ein Teil des 3´UTRs durch Spleißen entfernt, was zum rapiden mRNA dieser 3´UTR Isoform führte. Es konnte gezeigt werden, dass sowohl für das Spleißen wie auch für den Abbau der mRNA CUGBP1 verantwortlich ist. Diese Art der post-transkriptionellen Regulation des mPGES-1 3´UTR durch CUGBP1-abhängiges alternatives Spleißen und mRNA-Abbau ist ein wirksamer Mechanismus, um die Menge an mRNA und Protein zu reduzieren. Zusätzlich reprimiert CUGBP1 die Translation von mPGES-1, indem es mPGES-1 mRNA in sogenannte *P-bodies* rekrutiert. Somit konnte in dieser Arbeit gezeigt werden, dass CUGBP1 mehrere Funktionen auf die mRNA und das reife Protein von mPGES-1 ausübt und somit die Expression reprimiert. Darüber hinaus konnte wir einen weiteren Regulationsmechanismus für die mPGES-1 aufgedeckt werden. MiRNAs sind kleine nicht-kodierende RNAs, die sequenzspezifisch an den 3´UTR binden und durch Repression der Translation oder mRNA Abbau die Expression ihrer Zielgene kontrollieren. Kürzlich wurde jedoch ein neuer Interaktionsmechanismus von miRNAs endeckt. miR-328 agiert als „RNA Köder“ für hnRNP E2 und verhindert so die Bindung von hnRNP E2 and die mRNA und dadurch kommt es zur Translationsrepression. In dieser Studie identifizierten wir eine zweite miRNA, die einen solchen neuen regulatorischen Mechanismus ausübt. Die miR-574-5p besitzt eine Bindestelle für CUGBP1. CUGBP1 bindet an die reife miR-574-5p und verhindert dadurch den mRNA Abbau der 3´UTR Variante und die Repression der mPGES-1 Translation. Durch die Inhibierung der CUGBP1-vermittelten Reduktion der mPGES-1 Expression nimmt die miR-574-5p eine wichtige Rolle in der Regulation der PGE_2 Biosynthese in entzündlichen Reaktionen ein. Oft wird die Dysregulation von miRNAs in Verbindung gebracht mit der Krebsentstehung und Krankheiten. Hier konnte gezeigt werden, dass miR-574-5p

7 Zusammenfassung

zytokinabhängig hochreguliert wurde, was dafür spricht, dass diese miRNA eine wichtige Rolle in Mikromilieu von Tumoren und Entzündungen spielt. In der Tat war die Expression der miR-574-5p in Tumorgewebe von NSCLC Patienten signifikant hochreguliert. Zusätzlich konnten wir zeigen, dass die Balance von CUGBP1 und miR-574-5p die Zellproliferation und die mPGES-1 abhängige PGE_2 Synthese reguliert, welche für die Tumorproliferation wichtig ist. Diese Hypothese wurde in einem Xenograft-Mausmodell bestätigt. Die Injektion von A549 Zellen, mit stabiler miR-574-5p Überexpression, kam es zu einer signifikanten Induktion des Tumorwachstums verglichen mit der Kontrollgruppe. Dieser Effekt konnte mit dem selektiven mPGES-1-Inhibitor CIII blockiert werden. Die Ergebnisse haben gezeigt, dass miR-574-5p onkogene Eigenschaften besitzt, die das Tumorwachstum fördern. Die miR-574-5p spielt eine wichtige Rolle in der mPGES-1 abhängigen PGE_2 Freisetzung in Lungenkrebs und Tumorwachstum und stellt deshalb ein potenzielles, therapeutisches Zielmolekül in der Behandlung von Lungenkrebs dar.

8 References

1. Whitelaw A, Parkin J (1988) Development of immunity. Br Med Bull 44: 1037-1051.
2. Unanue ER, Beller DI, Calderon J, Kiely JM, Stadecker MJ (1976) Regulation of immunity and inflammation by mediators from macrophages. Am J Pathol 85: 465-478.
3. Hamberg M, Svensson J, Wakabayashi T, Samuelsson B (1974) Isolation and structure of two prostaglandin endoperoxides that cause platelet aggregation. Proc Natl Acad Sci U S A 71: 345-349.
4. Ferraris VA, DeRubertis FR (1974) Release of prostaglandin by mitogen- and antigen-stimulated leukocytes in culture. J Clin Invest 54: 378-386.
5. Smith JB, Ingerman C, Kocsis JJ, Silver MJ (1973) Formation of prostaglandins during the aggregation of human blood platelets. J Clin Invest 52: 965-969.
6. Horton EW (1963) Action of Prostaglandin E1 on Tissues Which Respond to Bradykinin. Nature 200: 892-893.
7. Crunkhorn P, Willis AL (1971) Cutaneous reactions to intradermal prostaglandins. Br J Pharmacol 41: 49-56.
8. Birrell GJ, McQueen DS, Iggo A, Coleman RA, Grubb BD (1991) PGI2-induced activation and sensitization of articular mechanonociceptors. Neurosci Lett 124: 5-8.
9. Collins AJ, Cosh JA (1970) Temperature and biochemical studies of joint inflammation. A preliminary investigation. Ann Rheum Dis 29: 386-392.
10. Rather LJ (1971) Disturbance of function (functio laesa): the legendary fifth cardinal sign of inflammation, added by Galen to the four cardinal signs of Celsus. Bull N Y Acad Med 47: 303-322.
11. Jakobsson PJ, Thoren S, Morgenstern R, Samuelsson B (1999) Identification of human prostaglandin E synthase: a microsomal, glutathione-dependent, inducible enzyme, constituting a potential novel drug target. Proc Natl Acad Sci U S A 96: 7220-7225.
12. Brown EM, MacLeod RJ (2001) Extracellular calcium sensing and extracellular calcium signaling. Physiol Rev 81: 239-297.
13. Funk CD (2001) Prostaglandins and leukotrienes: advances in eicosanoid biology. Science 294: 1871-1875.
14. Balsinde J, Balboa MA, Insel PA, Dennis EA (1999) Regulation and inhibition of phospholipase A2. Annu Rev Pharmacol Toxicol 39: 175-189.
15. Xie WL, Chipman JG, Robertson DL, Erikson RL, Simmons DL (1991) Expression of a mitogen-responsive gene encoding prostaglandin synthase is regulated by mRNA splicing. Proc Natl Acad Sci U S A 88: 2692-2696.
16. Kujubu DA, Fletcher BS, Varnum BC, Lim RW, Herschman HR (1991) TIS10, a phorbol ester tumor promoter-inducible mRNA from Swiss 3T3 cells, encodes a novel prostaglandin synthase/cyclooxygenase homologue. J Biol Chem 266: 12866-12872.
17. Chandrasekharan NV, Simmons DL (2004) The cyclooxygenases. Genome Biol 5: 241.
18. Fosslien E (1998) Adverse effects of nonsteroidal anti-inflammatory drugs on the gastrointestinal system. Ann Clin Lab Sci 28: 67-81.
19. Hawkey CJ (2000) Nonsteroidal anti-inflammatory drug gastropathy. Gastroenterology 119: 521-535.
20. Whelton A, Hamilton CW (1991) Nonsteroidal anti-inflammatory drugs: effects on kidney function. J Clin Pharmacol 31: 588-598.
21. Chan CC, Boyce S, Brideau C, Charleson S, Cromlish W, et al. (1999) Rofecoxib [Vioxx, MK-0966; 4-(4'-methylsulfonylphenyl)-3-phenyl-2-(5H)-furanone]: a potent and orally active cyclooxygenase-2 inhibitor. Pharmacological and biochemical profiles. J Pharmacol Exp Ther 290: 551-560.

8 References

22. Scott DG, Watts RA (2005) Increased risk of cardiovascular events with coxibs and NSAIDs. Lancet 365: 1537.
23. Fitzgerald GA (2004) Coxibs and cardiovascular disease. N Engl J Med 351: 1709-1711.
24. Funk CD, FitzGerald GA (2007) COX-2 inhibitors and cardiovascular risk. J Cardiovasc Pharmacol 50: 470-479.
25. Larsson K, Jakobsson PJ (2015) Inhibition of microsomal prostaglandin E synthase-1 as targeted therapy in cancer treatment. Prostaglandins Other Lipid Mediat 120: 161-165.
26. Schmidt M, Christiansen CF, Horvath-Puho E, Glynn RJ, Rothman KJ, et al. (2011) Non-steroidal anti-inflammatory drug use and risk of venous thromboembolism. J Thromb Haemost 9: 1326-1333.
27. Bulut D, Liaghat S, Hanefeld C, Koll R, Miebach T, et al. (2003) Selective cyclo-oxygenase-2 inhibition with parecoxib acutely impairs endothelium-dependent vasodilatation in patients with essential hypertension. J Hypertens 21: 1663-1667.
28. Moncada S, Higgs EA, Vane JR (1977) Human arterial and venous tissues generate prostacyclin (prostaglandin x), a potent inhibitor of platelet aggregation. Lancet 1: 18-20.
29. Tanioka T, Nakatani Y, Semmyo N, Murakami M, Kudo I (2000) Molecular identification of cytosolic prostaglandin E2 synthase that is functionally coupled with cyclooxygenase-1 in immediate prostaglandin E2 biosynthesis. J Biol Chem 275: 32775-32782.
30. Tanikawa N, Ohmiya Y, Ohkubo H, Hashimoto K, Kangawa K, et al. (2002) Identification and characterization of a novel type of membrane-associated prostaglandin E synthase. Biochem Biophys Res Commun 291: 884-889.
31. Smith DF, Faber LE, Toft DO (1990) Purification of unactivated progesterone receptor and identification of novel receptor-associated proteins. J Biol Chem 265: 3996-4003.
32. Murakami M, Nakashima K, Kamei D, Masuda S, Ishikawa Y, et al. (2003) Cellular prostaglandin E2 production by membrane-bound prostaglandin E synthase-2 via both cyclooxygenases-1 and -2. J Biol Chem 278: 37937-37947.
33. Kamei D, Murakami M, Sasaki Y, Nakatani Y, Majima M, et al. (2010) Microsomal prostaglandin E synthase-1 in both cancer cells and hosts contributes to tumour growth, invasion and metastasis. Biochem J 425: 361-371.
34. Kamei D, Murakami M, Nakatani Y, Ishikawa Y, Ishii T, et al. (2003) Potential role of microsomal prostaglandin E synthase-1 in tumorigenesis. J Biol Chem 278: 19396-19405.
35. Saha S, Engstrom L, Mackerlova L, Jakobsson PJ, Blomqvist A (2005) Impaired febrile responses to immune challenge in mice deficient in microsomal prostaglandin E synthase-1. Am J Physiol Regul Integr Comp Physiol 288: R1100-1107.
36. Trebino CE, Stock JL, Gibbons CP, Naiman BM, Wachtmann TS, et al. (2003) Impaired inflammatory and pain responses in mice lacking an inducible prostaglandin E synthase. Proc Natl Acad Sci U S A 100: 9044-9049.
37. Nakanishi M, Gokhale V, Meuillet EJ, Rosenberg DW (2010) mPGES-1 as a target for cancer suppression: A comprehensive invited review "Phospholipase A2 and lipid mediators". Biochimie 92: 660-664.
38. Kojima F, Naraba H, Sasaki Y, Okamoto R, Koshino T, et al. (2002) Coexpression of microsomal prostaglandin E synthase with cyclooxygenase-2 in human rheumatoid synovial cells. J Rheumatol 29: 1836-1842.
39. Stichtenoth DO, Thoren S, Bian H, Peters-Golden M, Jakobsson PJ, et al. (2001) Microsomal prostaglandin E synthase is regulated by proinflammatory cytokines and glucocorticoids in primary rheumatoid synovial cells. J Immunol 167: 469-474.

8 References

40. Jakobsson PJ, Morgenstern R, Mancini J, Ford-Hutchinson A, Persson B (1999) Common structural features of MAPEG -- a widespread superfamily of membrane associated proteins with highly divergent functions in eicosanoid and glutathione metabolism. Protein Sci 8: 689-692.
41. Filion F, Bouchard N, Goff AK, Lussier JG, Sirois J (2001) Molecular cloning and induction of bovine prostaglandin E synthase by gonadotropins in ovarian follicles prior to ovulation in vivo. J Biol Chem 276: 34323-34330.
42. Hamza A, Tong M, AbdulHameed MD, Liu J, Goren AC, et al. (2010) Understanding microscopic binding of human microsomal prostaglandin E synthase-1 (mPGES-1) trimer with substrate PGH2 and cofactor GSH: insights from computational alanine scanning and site-directed mutagenesis. J Phys Chem B 114: 5605-5616.
43. Jegerschold C, Pawelzik SC, Purhonen P, Bhakat P, Gheorghe KR, et al. (2008) Structural basis for induced formation of the inflammatory mediator prostaglandin E2. Proc Natl Acad Sci U S A 105: 11110-11115.
44. Naraba H, Yokoyama C, Tago N, Murakami M, Kudo I, et al. (2002) Transcriptional regulation of the membrane-associated prostaglandin E2 synthase gene. Essential role of the transcription factor Egr-1. J Biol Chem 277: 28601-28608.
45. Thoren S, Weinander R, Saha S, Jegerschold C, Pettersson PL, et al. (2003) Human microsomal prostaglandin E synthase-1: purification, functional characterization, and projection structure determination. J Biol Chem 278: 22199-22209.
46. Jakobsson PJ, Thoren S, Morgenstern R, Samuelsson B (2002) Characterization of microsomal, glutathione dependent prostaglandin E synthase. Adv Exp Med Biol 507: 287-291.
47. Radmark O, Werz O, Steinhilber D, Samuelsson B (2007) 5-Lipoxygenase: regulation of expression and enzyme activity. Trends Biochem Sci 32: 332-341.
48. Thoren S, Jakobsson PJ (2000) Coordinate up- and down-regulation of glutathione-dependent prostaglandin E synthase and cyclooxygenase-2 in A549 cells. Inhibition by NS-398 and leukotriene C4. Eur J Biochem 267: 6428-6434.
49. Sampey AV, Monrad S, Crofford LJ (2005) Microsomal prostaglandin E synthase-1: the inducible synthase for prostaglandin E2. Arthritis Res Ther 7: 114-117.
50. Samuelsson B, Morgenstern R, Jakobsson PJ (2007) Membrane prostaglandin E synthase-1: a novel therapeutic target. Pharmacol Rev 59: 207-224.
51. Wang J, Limburg D, Carter J, Mbalaviele G, Gierse J, et al. (2010) Selective inducible microsomal prostaglandin E(2) synthase-1 (mPGES-1) inhibitors derived from an oxicam template. Bioorg Med Chem Lett 20: 1604-1609.
52. Bruno A, Di Francesco L, Coletta I, Mangano G, Alisi MA, et al. (2010) Effects of AF3442 [N-(9-ethyl-9H-carbazol-3-yl)-2-(trifluoromethyl)benzamide], a novel inhibitor of human microsomal prostaglandin E synthase-1, on prostanoid biosynthesis in human monocytes in vitro. Biochem Pharmacol 79: 974-981.
53. Leclerc P, Idborg H, Spahiu L, Larsson C, Nekhotiaeva N, et al. (2013) Characterization of a human and murine mPGES-1 inhibitor and comparison to mPGES-1 genetic deletion in mouse models of inflammation. Prostaglandins Other Lipid Mediat 107: 26-34.
54. Xu D, Rowland SE, Clark P, Giroux A, Cote B, et al. (2008) MF63 [2-(6-chloro-1H-phenanthro[9,10-d]imidazol-2-yl)-isophthalonitrile], a selective microsomal prostaglandin E synthase-1 inhibitor, relieves pyresis and pain in preclinical models of inflammation. J Pharmacol Exp Ther 326: 754-763.
55. Riendeau D, Aspiotis R, Ethier D, Gareau Y, Grimm EL, et al. (2005) Inhibitors of the inducible microsomal prostaglandin E2 synthase (mPGES-1) derived from MK-886. Bioorg Med Chem Lett 15: 3352-3355.

8 References

56. Bannenberg G, Dahlen SE, Luijerink M, Lundqvist G, Morgenstern R (1999) Leukotriene C4 is a tight-binding inhibitor of microsomal glutathione transferase-1. Effects of leukotriene pathway modifiers. J Biol Chem 274: 1994-1999.
57. Leclerc P, Pawelzik SC, Idborg H, Spahiu L, Larsson C, et al. (2013) Characterization of a new mPGES-1 inhibitor in rat models of inflammation. Prostaglandins Other Lipid Mediat 102-103: 1-12.
58. Finetti F, Terzuoli E, Bocci E, Coletta I, Polenzani L, et al. (2012) Pharmacological inhibition of microsomal prostaglandin E synthase-1 suppresses epidermal growth factor receptor-mediated tumor growth and angiogenesis. PLoS One 7: e40576.
59. Pawelzik SC, Uda NR, Spahiu L, Jegerschold C, Stenberg P, et al. (2010) Identification of key residues determining species differences in inhibitor binding of microsomal prostaglandin E synthase-1. J Biol Chem 285: 29254-29261.
60. Sjogren T, Nord J, Ek M, Johansson P, Liu G, et al. (2013) Crystal structure of microsomal prostaglandin E2 synthase provides insight into diversity in the MAPEG superfamily. Proc Natl Acad Sci U S A 110: 3806-3811.
61. Murakami M, Naraba H, Tanioka T, Semmyo N, Nakatani Y, et al. (2000) Regulation of prostaglandin E2 biosynthesis by inducible membrane-associated prostaglandin E2 synthase that acts in concert with cyclooxygenase-2. J Biol Chem 275: 32783-32792.
62. Kobayashi T, Narumiya S (2002) Function of prostanoid receptors: studies on knockout mice. Prostaglandins Other Lipid Mediat 68-69: 557-573.
63. Wang D, Dubois RN (2010) Eicosanoids and cancer. Nat Rev Cancer 10: 181-193.
64. Roberts HR, Smartt HJ, Greenhough A, Moore AE, Williams AC, et al. (2011) Colon tumour cells increase PGE(2) by regulating COX-2 and 15-PGDH to promote survival during the microenvironmental stress of glucose deprivation. Carcinogenesis 32: 1741-1747.
65. Greenhough A, Smartt HJ, Moore AE, Roberts HR, Williams AC, et al. (2009) The COX-2/PGE2 pathway: key roles in the hallmarks of cancer and adaptation to the tumour microenvironment. Carcinogenesis 30: 377-386.
66. Breyer RM, Bagdassarian CK, Myers SA, Breyer MD (2001) Prostanoid receptors: subtypes and signaling. Annu Rev Pharmacol Toxicol 41: 661-690.
67. Mantovani A, Allavena P, Sica A, Balkwill F (2008) Cancer-related inflammation. Nature 454: 436-444.
68. Karin M (2009) NF-kappaB as a critical link between inflammation and cancer. Cold Spring Harb Perspect Biol 1: a000141.
69. Harris RE, Alshafie GA, Abou-Issa H, Seibert K (2000) Chemoprevention of breast cancer in rats by celecoxib, a cyclooxygenase 2 inhibitor. Cancer Res 60: 2101-2103.
70. Hanaka H, Pawelzik SC, Johnsen JI, Rakonjac M, Terawaki K, et al. (2009) Microsomal prostaglandin E synthase 1 determines tumor growth in vivo of prostate and lung cancer cells. Proc Natl Acad Sci U S A 106: 18757-18762.
71. Nakanishi M, Montrose DC, Clark P, Nambiar PR, Belinsky GS, et al. (2008) Genetic deletion of mPGES-1 suppresses intestinal tumorigenesis. Cancer Res 68: 3251-3259.
72. Tennis MA, Van Scoyk M, Heasley LE, Vandervest K, Weiser-Evans M, et al. (2010) Prostacyclin inhibits non-small cell lung cancer growth by a frizzled 9-dependent pathway that is blocked by secreted frizzled-related protein 1. Neoplasia 12: 244-253.
73. Nemenoff R, Meyer AM, Hudish TM, Mozer AB, Snee A, et al. (2008) Prostacyclin prevents murine lung cancer independent of the membrane receptor by activation of peroxisomal proliferator--activated receptor gamma. Cancer Prev Res (Phila) 1: 349-356.

8 References

74. Monrad SU, Kojima F, Kapoor M, Kuan EL, Sarkar S, et al. (2011) Genetic deletion of mPGES-1 abolishes PGE2 production in murine dendritic cells and alters the cytokine profile, but does not affect maturation or migration. Prostaglandins Leukot Essent Fatty Acids 84: 113-121.
75. Kapoor M, Kojima F, Qian M, Yang L, Crofford LJ (2006) Shunting of prostanoid biosynthesis in microsomal prostaglandin E synthase-1 null embryo fibroblasts: regulatory effects on inducible nitric oxide synthase expression and nitrite synthesis. FASEB J 20: 2387-2389.
76. Idborg H, Olsson P, Leclerc P, Raouf J, Jakobsson PJ, et al. (2013) Effects of mPGES-1 deletion on eicosanoid and fatty acid profiles in mice. Prostaglandins Other Lipid Mediat 107: 18-25.
77. Wilson JW, Potten CS (2000) The effect of exogenous prostaglandin administration on tumor size and yield in Min/+ mice. Cancer Res 60: 4645-4653.
78. Nakanishi M, Rosenberg DW (2013) Multifaceted roles of PGE2 in inflammation and cancer. Semin Immunopathol 35: 123-137.
79. Venkatesh S, Workman JL (2015) Histone exchange, chromatin structure and the regulation of transcription. Nat Rev Mol Cell Biol 16: 178-189.
80. Gorlach M, Burd CG, Dreyfuss G (1994) The mRNA poly(A)-binding protein: localization, abundance, and RNA-binding specificity. Exp Cell Res 211: 400-407.
81. Jackson RJ, Hellen CU, Pestova TV (2010) The mechanism of eukaryotic translation initiation and principles of its regulation. Nat Rev Mol Cell Biol 11: 113-127.
82. Gallie DR (1998) A tale of two termini: a functional interaction between the termini of an mRNA is a prerequisite for efficient translation initiation. Gene 216: 1-11.
83. Halees AS, Hitti E, Al-Saif M, Mahmoud L, Vlasova-St Louis IA, et al. (2011) Global assessment of GU-rich regulatory content and function in the human transcriptome. RNA Biol 8: 681-691.
84. Cenik C, Derti A, Mellor JC, Berriz GF, Roth FP (2010) Genome-wide functional analysis of human 5' untranslated region introns. Genome Biol 11: R29.
85. Majewski J, Ott J (2002) Distribution and characterization of regulatory elements in the human genome. Genome Res 12: 1827-1836.
86. Houseley J, Tollervey D (2009) The many pathways of RNA degradation. Cell 136: 763-776.
87. Gilbert W (1978) Why genes in pieces? Nature 271: 501.
88. Kinniburgh AJ, Mertz JE, Ross J (1978) The precursor of mouse beta-globin messenger RNA contains two intervening RNA sequences. Cell 14: 681-693.
89. Wahl MC, Will CL, Luhrmann R (2009) The spliceosome: design principles of a dynamic RNP machine. Cell 136: 701-718.
90. Burset M, Seledtsov IA, Solovyev VV (2001) SpliceDB: database of canonical and non-canonical mammalian splice sites. Nucleic Acids Res 29: 255-259.
91. Gao K, Masuda A, Matsuura T, Ohno K (2008) Human branch point consensus sequence is yUnAy. Nucleic Acids Res 36: 2257-2267.
92. Black DL (2003) Mechanisms of alternative pre-messenger RNA splicing. Annu Rev Biochem 72: 291-336.
93. Will CL, Luhrmann R (2011) Spliceosome structure and function. Cold Spring Harb Perspect Biol 3.
94. Deutsch M, Long M (1999) Intron-exon structures of eukaryotic model organisms. Nucleic Acids Res 27: 3219-3228.
95. Ast G (2004) How did alternative splicing evolve? Nat Rev Genet 5: 773-782.
96. Berget SM (1995) Exon recognition in vertebrate splicing. J Biol Chem 270: 2411-2414.

8 References

97. Fox-Walsh KL, Dou Y, Lam BJ, Hung SP, Baldi PF, et al. (2005) The architecture of pre-mRNAs affects mechanisms of splice-site pairing. Proc Natl Acad Sci U S A 102: 16176-16181.
98. Graveley BR (2000) Sorting out the complexity of SR protein functions. RNA 6: 1197-1211.
99. Blencowe BJ, Bowman JA, McCracken S, Rosonina E (1999) SR-related proteins and the processing of messenger RNA precursors. Biochem Cell Biol 77: 277-291.
100. Merkhofer EC, Hu P, Johnson TL (2014) Introduction to cotranscriptional RNA splicing. Methods Mol Biol 1126: 83-96.
101. Listerman I, Sapra AK, Neugebauer KM (2006) Cotranscriptional coupling of splicing factor recruitment and precursor messenger RNA splicing in mammalian cells. Nat Struct Mol Biol 13: 815-822.
102. Han J, Xiong J, Wang D, Fu XD (2011) Pre-mRNA splicing: where and when in the nucleus. Trends Cell Biol 21: 336-343.
103. Pan Q, Shai O, Lee LJ, Frey J, Blencowe BJ (2008) Deep surveying of alternative splicing complexity in the human transcriptome by high-throughput sequencing. Nature Genetics 40: 1413-1415.
104. Wang ET, Sandberg R, Luo S, Khrebtukova I, Zhang L, et al. (2008) Alternative isoform regulation in human tissue transcriptomes. Nature 456: 470-476.
105. Sammeth M, Foissac S, Guigo R (2008) A general definition and nomenclature for alternative splicing events. PLoS Comput Biol 4: e1000147.
106. Keren H, Lev-Maor G, Ast G (2010) Alternative splicing and evolution: diversification, exon definition and function. Nat Rev Genet 11: 345-355.
107. Alekseyenko AV, Kim N, Lee CJ (2007) Global analysis of exon creation versus loss and the role of alternative splicing in 17 vertebrate genomes. RNA 13: 661-670.
108. Thanaraj TA, Clark F (2001) Human GC-AG alternative intron isoforms with weak donor sites show enhanced consensus at acceptor exon positions. Nucleic Acids Res 29: 2581-2593.
109. Timchenko LT, Miller JW, Timchenko NA, DeVore DR, Datar KV, et al. (1996) Identification of a (CUG)n triplet repeat RNA-binding protein and its expression in myotonic dystrophy. Nucleic Acids Res 24: 4407-4414.
110. Howard JM, Sanford JR (2015) The RNAissance family: SR proteins as multifaceted regulators of gene expression. Wiley Interdiscip Rev RNA 6: 93-110.
111. Krecic AM, Swanson MS (1999) hnRNP complexes: composition, structure, and function. Curr Opin Cell Biol 11: 363-371.
112. Erkelenz S, Mueller WF, Evans MS, Busch A, Schoneweis K, et al. (2013) Position-dependent splicing activation and repression by SR and hnRNP proteins rely on common mechanisms. RNA 19: 96-102.
113. Hamilton BJ, Burns CM, Nichols RC, Rigby WF (1997) Modulation of AUUUA response element binding by heterogeneous nuclear ribonucleoprotein A1 in human T lymphocytes. The roles of cytoplasmic location, transcription, and phosphorylation. J Biol Chem 272: 28732-28741.
114. Michael WM, Choi M, Dreyfuss G (1995) A nuclear export signal in hnRNP A1: a signal-mediated, temperature-dependent nuclear protein export pathway. Cell 83: 415-422.
115. Bonnal S, Pileur F, Orsini C, Parker F, Pujol F, et al. (2005) Heterogeneous nuclear ribonucleoprotein A1 is a novel internal ribosome entry site trans-acting factor that modulates alternative initiation of translation of the fibroblast growth factor 2 mRNA. J Biol Chem 280: 4144-4153.
116. Tazi J, Bakkour N, Stamm S (2009) Alternative splicing and disease. Biochim Biophys Acta 1792: 14-26.

8 References

117. Krawczak M, Reiss J, Cooper DN (1992) The mutational spectrum of single base-pair substitutions in mRNA splice junctions of human genes: causes and consequences. Hum Genet 90: 41-54.
118. Zhang Z, Lotti F, Dittmar K, Younis I, Wan L, et al. (2008) SMN deficiency causes tissue-specific perturbations in the repertoire of snRNAs and widespread defects in splicing. Cell 133: 585-600.
119. Charames GS, Cheng H, Gilpin CA, Hunter AG, Berk T, et al. (2002) A novel aberrant splice site mutation in the APC gene. J Med Genet 39: 754-757.
120. Liu HX, Cartegni L, Zhang MQ, Krainer AR (2001) A mechanism for exon skipping caused by nonsense or missense mutations in BRCA1 and other genes. Nat Genet 27: 55-58.
121. Nagy E, Maquat LE (1998) A rule for termination-codon position within intron-containing genes: when nonsense affects RNA abundance. Trends Biochem Sci 23: 198-199.
122. Weischenfeldt J, Lykke-Andersen J, Porse B (2005) Messenger RNA surveillance: neutralizing natural nonsense. Curr Biol 15: R559-562.
123. Chang YF, Imam JS, Wilkinson MF (2007) The nonsense-mediated decay RNA surveillance pathway. Annu Rev Biochem 76: 51-74.
124. Silva AL, Romao L (2009) The mammalian nonsense-mediated mRNA decay pathway: to decay or not to decay! Which players make the decision? FEBS Lett 583: 499-505.
125. Jaillon O, Bouhouche K, Gout JF, Aury JM, Noel B, et al. (2008) Translational control of intron splicing in eukaryotes. Nature 451: 359-362.
126. Frischmeyer PA, Dietz HC (1999) Nonsense-mediated mRNA decay in health and disease. Hum Mol Genet 8: 1893-1900.
127. Linde L, Kerem B (2008) Introducing sense into nonsense in treatments of human genetic diseases. Trends Genet 24: 552-563.
128. Hentze MW, Kulozik AE (1999) A perfect message: RNA surveillance and nonsense-mediated decay. Cell 96: 307-310.
129. Nicholson P, Yepiskoposyan H, Metze S, Zamudio Orozco R, Kleinschmidt N, et al. (2010) Nonsense-mediated mRNA decay in human cells: mechanistic insights, functions beyond quality control and the double-life of NMD factors. Cell Mol Life Sci 67: 677-700.
130. Saltzman AL, Kim YK, Pan Q, Fagnani MM, Maquat LE, et al. (2008) Regulation of multiple core spliceosomal proteins by alternative splicing-coupled nonsense-mediated mRNA decay. Mol Cell Biol 28: 4320-4330.
131. Green RE, Lewis BP, Hillman RT, Blanchette M, Lareau LF, et al. (2003) Widespread predicted nonsense-mediated mRNA decay of alternatively-spliced transcripts of human normal and disease genes. Bioinformatics 19 Suppl 1: i118-121.
132. Ni JZ, Grate L, Donohue JP, Preston C, Nobida N, et al. (2007) Ultraconserved elements are associated with homeostatic control of splicing regulators by alternative splicing and nonsense-mediated decay. Genes Dev 21: 708-718.
133. Sun S, Zhang Z, Sinha R, Karni R, Krainer AR (2010) SF2/ASF autoregulation involves multiple layers of post-transcriptional and translational control. Nat Struct Mol Biol 17: 306-312.
134. Sureau A, Gattoni R, Dooghe Y, Stevenin J, Soret J (2001) SC35 autoregulates its expression by promoting splicing events that destabilize its mRNAs. EMBO J 20: 1785-1796.
135. Valacca C, Bonomi S, Buratti E, Pedrotti S, Baralle FE, et al. (2010) Sam68 regulates EMT through alternative splicing-activated nonsense-mediated mRNA decay of the SF2/ASF proto-oncogene. J Cell Biol 191: 87-99.

8 References

136. Lewis BP, Green RE, Brenner SE (2003) Evidence for the widespread coupling of alternative splicing and nonsense-mediated mRNA decay in humans. Proc Natl Acad Sci U S A 100: 189-192.
137. Lareau LF, Brooks AN, Soergel DA, Meng Q, Brenner SE (2007) The coupling of alternative splicing and nonsense-mediated mRNA decay. Adv Exp Med Biol 623: 190-211.
138. McGlincy NJ, Smith CW (2008) Alternative splicing resulting in nonsense-mediated mRNA decay: what is the meaning of nonsense? Trends Biochem Sci 33: 385-393.
139. Wittmann J, Hol EM, Jack HM (2006) hUPF2 silencing identifies physiologic substrates of mammalian nonsense-mediated mRNA decay. Mol Cell Biol 26: 1272-1287.
140. Weischenfeldt J, Damgaard I, Bryder D, Theilgaard-Monch K, Thoren LA, et al. (2008) NMD is essential for hematopoietic stem and progenitor cells and for eliminating by-products of programmed DNA rearrangements. Genes Dev 22: 1381-1396.
141. Linde L, Boelz S, Neu-Yilik G, Kulozik AE, Kerem B (2007) The efficiency of nonsense-mediated mRNA decay is an inherent character and varies among different cells. Eur J Hum Genet 15: 1156-1162.
142. Mazzoni C, Falcone C (2011) mRNA stability and control of cell proliferation. Biochem Soc Trans 39: 1461-1465.
143. Hoshino S (2012) Mechanism of the initiation of mRNA decay: role of eRF3 family G proteins. Wiley Interdiscip Rev RNA 3: 743-757.
144. Harigaya Y, Parker R (2010) No-go decay: a quality control mechanism for RNA in translation. Wiley Interdiscip Rev RNA 1: 132-141.
145. Gong C, Kim YK, Woeller CF, Tang Y, Maquat LE (2009) SMD and NMD are competitive pathways that contribute to myogenesis: effects on PAX3 and myogenin mRNAs. Genes Dev 23: 54-66.
146. Gong C, Maquat LE (2011) lncRNAs transactivate STAU1-mediated mRNA decay by duplexing with 3' UTRs via Alu elements. Nature 470: 284-288.
147. Anantharaman V, Koonin EV, Aravind L (2002) Comparative genomics and evolution of proteins involved in RNA metabolism. Nucleic Acids Res 30: 1427-1464.
148. Millevoi S, Loulergue C, Dettwiler S, Karaa SZ, Keller W, et al. (2006) An interaction between U2AF 65 and CF I(m) links the splicing and 3' end processing machineries. EMBO J 25: 4854-4864.
149. Rigo F, Martinson HG (2008) Functional coupling of last-intron splicing and 3'-end processing to transcription in vitro: the poly(A) signal couples to splicing before committing to cleavage. Mol Cell Biol 28: 849-862.
150. Hilleren P, McCarthy T, Rosbash M, Parker R, Jensen TH (2001) Quality control of mRNA 3'-end processing is linked to the nuclear exosome. Nature 413: 538-542.
151. Yu TX, Rao JN, Zou T, Liu L, Xiao L, et al. (2013) Competitive binding of CUGBP1 and HuR to occludin mRNA controls its translation and modulates epithelial barrier function. Mol Biol Cell 24: 85-99.
152. Marchand V, Gaspar I, Ephrussi A (2012) An intracellular transmission control protocol: assembly and transport of ribonucleoprotein complexes. Curr Opin Cell Biol 24: 202-210.
153. Holt CE, Bullock SL (2009) Subcellular mRNA localization in animal cells and why it matters. Science 326: 1212-1216.
154. Curtis D, Lehmann R, Zamore PD (1995) Translational regulation in development. Cell 81: 171-178.
155. Musunuru K (2003) Cell-specific RNA-binding proteins in human disease. Trends Cardiovasc Med 13: 188-195.

8 References

156. Ostrowski J, Sims JE, Sibley CH, Valentine MA, Dower SK, et al. (1991) A serine/threonine kinase activity is closely associated with a 65-kDa phosphoprotein specifically recognized by the kappa B enhancer element. J Biol Chem 266: 12722-12733.
157. Shen EC, Henry MF, Weiss VH, Valentini SR, Silver PA, et al. (1998) Arginine methylation facilitates the nuclear export of hnRNP proteins. Genes Dev 12: 679-691.
158. Vassileva MT, Matunis MJ (2004) SUMO modification of heterogeneous nuclear ribonucleoproteins. Mol Cell Biol 24: 3623-3632.
159. Maris C, Dominguez C, Allain FH (2005) The RNA recognition motif, a plastic RNA-binding platform to regulate post-transcriptional gene expression. FEBS J 272: 2118-2131.
160. Wurth L (2012) Versatility of RNA-Binding Proteins in Cancer. Comp Funct Genomics 2012: 178525.
161. David CJ, Manley JL (2010) Alternative pre-mRNA splicing regulation in cancer: pathways and programs unhinged. Genes Dev 24: 2343-2364.
162. Fredericks AM, Cygan KJ, Brown BA, Fairbrother WG (2015) RNA-Binding Proteins: Splicing Factors and Disease. Biomolecules 5: 893-909.
163. Wang J, Guo Y, Chu H, Guan Y, Bi J, et al. (2013) Multiple functions of the RNA-binding protein HuR in cancer progression, treatment responses and prognosis. Int J Mol Sci 14: 10015-10041.
164. Jin X, Zhai B, Fang T, Guo X, Xu L (2016) FXR1 is elevated in colorectal cancer and acts as an oncogene. Tumour Biol 37: 2683-2690.
165. Fu K, Sun X, Wier EM, Hodgson A, Liu Y, et al. (2016) Sam68/KHDRBS1 is critical for colon tumorigenesis by regulating genotoxic stress-induced NF-kappaB activation. Elife 5.
166. Sebestyen E, Singh B, Minana B, Pages A, Mateo F, et al. (2016) Large-scale analysis of genome and transcriptome alterations in multiple tumors unveils novel cancer-relevant splicing networks. Genome Res 26: 732-744.
167. Boultwood J, Dolatshad H, Varanasi SS, Yip BH, Pellagatti A (2014) The role of splicing factor mutations in the pathogenesis of the myelodysplastic syndromes. Adv Biol Regul 54: 153-161.
168. Dolatshad H, Pellagatti A, Fernandez-Mercado M, Yip BH, Malcovati L, et al. (2015) Disruption of SF3B1 results in deregulated expression and splicing of key genes and pathways in myelodysplastic syndrome hematopoietic stem and progenitor cells. Leukemia 29: 1798.
169. Yoshida K, Sanada M, Shiraishi Y, Nowak D, Nagata Y, et al. (2011) Frequent pathway mutations of splicing machinery in myelodysplasia. Nature 478: 64-69.
170. Haferlach T, Nagata Y, Grossmann V, Okuno Y, Bacher U, et al. (2014) Landscape of genetic lesions in 944 patients with myelodysplastic syndromes. Leukemia 28: 241-247.
171. Papaemmanuil E, Gerstung M, Malcovati L, Tauro S, Gundem G, et al. (2013) Clinical and biological implications of driver mutations in myelodysplastic syndromes. Blood 122: 3616-3627; quiz 3699.
172. Glisovic T, Bachorik JL, Yong J, Dreyfuss G (2008) RNA-binding proteins and post-transcriptional gene regulation. FEBS Lett 582: 1977-1986.
173. Clement SL, Scheckel C, Stoecklin G, Lykke-Andersen J (2011) Phosphorylation of tristetraprolin by MK2 impairs AU-rich element mRNA decay by preventing deadenylase recruitment. Mol Cell Biol 31: 256-266.
174. Liao B, Hu Y, Brewer G (2007) Competitive binding of AUF1 and TIAR to MYC mRNA controls its translation. Nat Struct Mol Biol 14: 511-518.

8 References

175. Abdelmohsen K, Pullmann R, Jr., Lal A, Kim HH, Galban S, et al. (2007) Phosphorylation of HuR by Chk2 regulates SIRT1 expression. Mol Cell 25: 543-557.
176. Vlasova IA, Bohjanen PR (2008) Posttranscriptional regulation of gene networks by GU-rich elements and CELF proteins. RNA Biol 5: 201-207.
177. Vlasova IA, Tahoe NM, Fan D, Larsson O, Rattenbacher B, et al. (2008) Conserved GU-rich elements mediate mRNA decay by binding to CUG-binding protein 1. Mol Cell 29: 263-270.
178. Timchenko LT, Salisbury E, Wang GL, Nguyen H, Albrecht JH, et al. (2006) Age-specific CUGBP1-eIF2 complex increases translation of CCAAT/enhancer-binding protein beta in old liver. J Biol Chem 281: 32806-32819.
179. Hwang DM, Hwang WS, Liew CC (1994) Single pass sequencing of a unidirectional human fetal heart cDNA library to discover novel genes of the cardiovascular system. J Mol Cell Cardiol 26: 1329-1333.
180. Barreau C, Paillard L, Mereau A, Osborne HB (2006) Mammalian CELF/Bruno-like RNA-binding proteins: molecular characteristics and biological functions. Biochimie 88: 515-525.
181. Jones K, Timchenko L, Timchenko NA (2012) The role of CUGBP1 in age-dependent changes of liver functions. Ageing Res Rev 11: 442-449.
182. Pullmann R, Jr., Kim HH, Abdelmohsen K, Lal A, Martindale JL, et al. (2007) Analysis of turnover and translation regulatory RNA-binding protein expression through binding to cognate mRNAs. Mol Cell Biol 27: 6265-6278.
183. Ladd AN, Charlet N, Cooper TA (2001) The CELF family of RNA binding proteins is implicated in cell-specific and developmentally regulated alternative splicing. Mol Cell Biol 21: 1285-1296.
184. Good PJ, Chen Q, Warner SJ, Herring DC (2000) A family of human RNA-binding proteins related to the Drosophila Bruno translational regulator. J Biol Chem 275: 28583-28592.
185. Choi DK, Ito T, Tsukahara F, Hirai M, Sakaki Y (1999) Developmentally-regulated expression of mNapor encoding an apoptosis-induced ELAV-type RNA binding protein. Gene 237: 135-142.
186. Roberts R, Timchenko NA, Miller JW, Reddy S, Caskey CT, et al. (1997) Altered phosphorylation and intracellular distribution of a (CUG)n triplet repeat RNA-binding protein in patients with myotonic dystrophy and in myotonin protein kinase knockout mice. Proc Natl Acad Sci U S A 94: 13221-13226.
187. Ladd AN, Cooper TA (2004) Multiple domains control the subcellular localization and activity of ETR-3, a regulator of nuclear and cytoplasmic RNA processing events. J Cell Sci 117: 3519-3529.
188. Mankodi A, Takahashi MP, Jiang H, Beck CL, Bowers WJ, et al. (2002) Expanded CUG repeats trigger aberrant splicing of ClC-1 chloride channel pre-mRNA and hyperexcitability of skeletal muscle in myotonic dystrophy. Mol Cell 10: 35-44.
189. Charlet BN, Savkur RS, Singh G, Philips AV, Grice EA, et al. (2002) Loss of the muscle-specific chloride channel in type 1 myotonic dystrophy due to misregulated alternative splicing. Mol Cell 10: 45-53.
190. Zhang W, Liu H, Han K, Grabowski PJ (2002) Region-specific alternative splicing in the nervous system: implications for regulation by the RNA-binding protein NAPOR. RNA 8: 671-685.
191. Timchenko LT, Iakova P, Welm AL, Cai ZJ, Timchenko NA (2002) Calreticulin interacts with C/EBPalpha and C/EBPbeta mRNAs and represses translation of C/EBP proteins. Mol Cell Biol 22: 7242-7257.

8 References

192. Young SG (1990) Recent progress in understanding apolipoprotein B. Circulation 82: 1574-1594.
193. Mukhopadhyay D, Houchen CW, Kennedy S, Dieckgraefe BK, Anant S (2003) Coupled mRNA stabilization and translational silencing of cyclooxygenase-2 by a novel RNA binding protein, CUGBP2. Mol Cell 11: 113-126.
194. Vlasova-St Louis I, Bohjanen PR (2011) Coordinate regulation of mRNA decay networks by GU-rich elements and CELF1. Curr Opin Genet Dev 21: 444-451.
195. Rattenbacher B, Beisang D, Wiesner DL, Jeschke JC, von Hohenberg M, et al. (**2010**) Analysis of CUGBP1 targets identifies GU-repeat sequences that mediate rapid mRNA decay. Mol Cell Biol 30: 3970-3980.
196. Masuda A, Andersen HS, Doktor TK, Okamoto T, Ito M, et al. (2012) CUGBP1 and MBNL1 preferentially bind to 3' UTRs and facilitate mRNA decay. Sci Rep 2: 209.
197. Timchenko NA, Welm AL, Lu X, Timchenko LT (1999) CUG repeat binding protein (CUGBP1) interacts with the 5' region of C/EBPbeta mRNA and regulates translation of C/EBPbeta isoforms. Nucleic Acids Res 27: 4517-4525.
198. Stein GH, Drullinger LF, Soulard A, Dulic V (1999) Differential roles for cyclin-dependent kinase inhibitors p21 and p16 in the mechanisms of senescence and differentiation in human fibroblasts. Mol Cell Biol 19: 2109-2117.
199. Timchenko NA, Iakova P, Cai ZJ, Smith JR, Timchenko LT (2001) Molecular basis for impaired muscle differentiation in myotonic dystrophy. Mol Cell Biol 21: 6927-6938.
200. Iakova P, Wang GL, Timchenko L, Michalak M, Pereira-Smith OM, et al. (2004) Competition of CUGBP1 and calreticulin for the regulation of p21 translation determines cell fate. EMBO J 23: 406-417.
201. Kuyumcu-Martinez NM, Wang GS, Cooper TA (2007) Increased steady-state levels of CUGBP1 in myotonic dystrophy 1 are due to PKC-mediated hyperphosphorylation. Mol Cell 28: 68-78.
202. Detivaud L, Pascreau G, Karaiskou A, Osborne HB, Kubiak JZ (2003) Regulation of EDEN-dependent deadenylation of Aurora A/Eg2-derived mRNA via phosphorylation and dephosphorylation in Xenopus laevis egg extracts. J Cell Sci 116: 2697-2705.
203. Beisang D, Rattenbacher B, Vlasova-St Louis IA, Bohjanen PR (2012) Regulation of CUG-binding protein 1 (CUGBP1) binding to target transcripts upon T cell activation. J Biol Chem 287: 950-960.
204. Timchenko NA, Patel R, Iakova P, Cai ZJ, Quan L, et al. (2004) Overexpression of CUG triplet repeat-binding protein, CUGBP1, in mice inhibits myogenesis. J Biol Chem 279: 13129-13139.
205. Jiao W, Zhao J, Wang M, Wang Y, Luo Y, et al. (2013) CUG-binding protein 1 (CUGBP1) expression and prognosis of non-small cell lung cancer. Clin Transl Oncol 15: 789-795.
206. Zhao J, Zhao Y, Xuan Y, Jiao W, Qiu T, et al. (2015) Prognostic impact of CUG-binding protein 1 expression and vascular invasion after radical surgery for stage IB nonsmall cell lung cancer. Indian J Cancer 52 Suppl 2: e125-129.
207. Wang X, Jiao W, Zhao Y, Zhang L, Yao R, et al. (2016) CUG-binding protein 1 (CUGBP1) expression and prognosis of brain metastases from non-small cell lung cancer. Thorac Cancer 7: 32-38.
208. Lu H, Yu Z, Liu S, Cui L, Chen X, et al. (2015) CUGBP1 promotes cell proliferation and suppresses apoptosis via down-regulating C/EBPalpha in human non-small cell lung cancers. Med Oncol 32: 82.
209. Gao C, Yu Z, Liu S, Xin H, Li X (2015) Overexpression of CUGBP1 is associated with the progression of non-small cell lung cancer. Tumour Biol 36: 4583-4589.
210. Ambros V (2004) The functions of animal microRNAs. Nature 431: 350-355.

8 References

211. Zhao Y, Samal E, Srivastava D (2005) Serum response factor regulates a muscle-specific microRNA that targets Hand2 during cardiogenesis. Nature 436: 214-220.
212. Cheng AM, Byrom MW, Shelton J, Ford LP (2005) Antisense inhibition of human miRNAs and indications for an involvement of miRNA in cell growth and apoptosis. Nucleic Acids Res 33: 1290-1297.
213. Bartel DP (2004) MicroRNAs: genomics, biogenesis, mechanism, and function. Cell 116: 281-297.
214. Lee RC, Feinbaum RL, Ambros V (1993) The C. elegans heterochronic gene lin-4 encodes small RNAs with antisense complementarity to lin-14. Cell 75: 843-854.
215. Lee Y, Jeon K, Lee JT, Kim S, Kim VN (2002) MicroRNA maturation: stepwise processing and subcellular localization. EMBO J 21: 4663-4670.
216. Yeom KH, Lee Y, Han J, Suh MR, Kim VN (2006) Characterization of DGCR8/Pasha, the essential cofactor for Drosha in primary miRNA processing. Nucleic Acids Res 34: 4622-4629.
217. Lee Y, Ahn C, Han J, Choi H, Kim J, et al. (2003) The nuclear RNase III Drosha initiates microRNA processing. Nature 425: 415-419.
218. Denli AM, Tops BB, Plasterk RH, Ketting RF, Hannon GJ (2004) Processing of primary microRNAs by the Microprocessor complex. Nature 432: 231-235.
219. Yi R, Qin Y, Macara IG, Cullen BR (2003) Exportin-5 mediates the nuclear export of pre-microRNAs and short hairpin RNAs. Genes Dev 17: 3011-3016.
220. Chendrimada TP, Gregory RI, Kumaraswamy E, Norman J, Cooch N, et al. (2005) TRBP recruits the Dicer complex to Ago2 for microRNA processing and gene silencing. Nature 436: 740-744.
221. Gregory RI, Yan KP, Amuthan G, Chendrimada T, Doratotaj B, et al. (2004) The Microprocessor complex mediates the genesis of microRNAs. Nature 432: 235-240.
222. Li Z, Rana TM (2014) Therapeutic targeting of microRNAs: current status and future challenges. Nat Rev Drug Discov 13: 622-638.
223. Schwarz DS, Hutvagner G, Du T, Xu Z, Aronin N, et al. (2003) Asymmetry in the assembly of the RNAi enzyme complex. Cell 115: 199-208.
224. Ruby JG, Jan CH, Bartel DP (2007) Intronic microRNA precursors that bypass Drosha processing. Nature 448: 83-86.
225. Okamura K, Hagen JW, Duan H, Tyler DM, Lai EC (2007) The mirtron pathway generates microRNA-class regulatory RNAs in Drosophila. Cell 130: 89-100.
226. Schamberger A, Sarkadi B, Orban TI (2012) Human mirtrons can express functional microRNAs simultaneously from both arms in a flanking exon-independent manner. RNA Biol 9: 1177-1185.
227. Cifuentes D, Xue H, Taylor DW, Patnode H, Mishima Y, et al. (2010) A novel miRNA processing pathway independent of Dicer requires Argonaute2 catalytic activity. Science 328: 1694-1698.
228. Hansen TB, Veno MT, Jensen TI, Schaefer A, Damgaard CK, et al. (2016) Argonaute-associated short introns are a novel class of gene regulators. Nat Commun 7: 11538.
229. Lytle JR, Yario TA, Steitz JA (2007) Target mRNAs are repressed as efficiently by microRNA-binding sites in the 5' UTR as in the 3' UTR. Proc Natl Acad Sci U S A 104: 9667-9672.
230. Forman JJ, Legesse-Miller A, Coller HA (2008) A search for conserved sequences in coding regions reveals that the let-7 microRNA targets Dicer within its coding sequence. Proc Natl Acad Sci U S A 105: 14879-14884.
231. Bartel DP (2009) MicroRNAs: target recognition and regulatory functions. Cell 136: 215-233.

8 References

232. Bagga S, Bracht J, Hunter S, Massirer K, Holtz J, et al. (2005) Regulation by let-7 and lin-4 miRNAs results in target mRNA degradation. Cell 122: 553-563.
233. Lim LP, Lau NC, Garrett-Engele P, Grimson A, Schelter JM, et al. (2005) Microarray analysis shows that some microRNAs downregulate large numbers of target mRNAs. Nature 433: 769-773.
234. Vimalraj S, Partridge NC, Selvamurugan N (2014) A positive role of microRNA-15b on regulation of osteoblast differentiation. J Cell Physiol 229: 1236-1244.
235. Eiring AM, Harb JG, Neviani P, Garton C, Oaks JJ, et al. (2010) miR-328 functions as an RNA decoy to modulate hnRNP E2 regulation of mRNA translation in leukemic blasts. Cell 140: 652-665.
236. Saul MJ, Stein S, Grez M, Jakobsson PJ, Steinhilber D, et al. (2016) UPF1 regulates myeloid cell functions and S100A9 expression by the hnRNP E2/miRNA-328 balance. Sci Rep 6: 31995.
237. Tavazoie SF, Alarcon C, Oskarsson T, Padua D, Wang Q, et al. (2008) Endogenous human microRNAs that suppress breast cancer metastasis. Nature 451: 147-152.
238. Ma L, Teruya-Feldstein J, Weinberg RA (2007) Tumour invasion and metastasis initiated by microRNA-10b in breast cancer. Nature 449: 682-688.
239. Foss KM, Sima C, Ugolini D, Neri M, Allen KE, et al. (2011) miR-1254 and miR-574-5p: serum-based microRNA biomarkers for early-stage non-small cell lung cancer. J Thorac Oncol 6: 482-488.
240. Calin GA, Sevignani C, Dumitru CD, Hyslop T, Noch E, et al. (2004) Human microRNA genes are frequently located at fragile sites and genomic regions involved in cancers. Proc Natl Acad Sci U S A 101: 2999-3004.
241. Karube Y, Tanaka H, Osada H, Tomida S, Tatematsu Y, et al. (2005) Reduced expression of Dicer associated with poor prognosis in lung cancer patients. Cancer Sci 96: 111-115.
242. Melo SA, Ropero S, Moutinho C, Aaltonen LA, Yamamoto H, et al. (2009) A TARBP2 mutation in human cancer impairs microRNA processing and DICER1 function. Nature Genetics 41: 365-370.
243. Dohner H, Stilgenbauer S, Benner A, Leupolt E, Krober A, et al. (2000) Genomic aberrations and survival in chronic lymphocytic leukemia. N Engl J Med 343: 1910-1916.
244. Calin GA, Dumitru CD, Shimizu M, Bichi R, Zupo S, et al. (2002) Frequent deletions and down-regulation of micro- RNA genes miR15 and miR16 at 13q14 in chronic lymphocytic leukemia. Proc Natl Acad Sci U S A 99: 15524-15529.
245. Cimmino A, Calin GA, Fabbri M, Iorio MV, Ferracin M, et al. (2005) miR-15 and miR-16 induce apoptosis by targeting BCL2. Proc Natl Acad Sci U S A 102: 13944-13949.
246. Takamizawa J, Konishi H, Yanagisawa K, Tomida S, Osada H, et al. (2004) Reduced expression of the let-7 microRNAs in human lung cancers in association with shortened postoperative survival. Cancer Res 64: 3753-3756.
247. Johnson SM, Grosshans H, Shingara J, Byrom M, Jarvis R, et al. (2005) RAS is regulated by the let-7 microRNA family. Cell 120: 635-647.
248. Hayashita Y, Osada H, Tatematsu Y, Yamada H, Yanagisawa K, et al. (2005) A polycistronic microRNA cluster, miR-17-92, is overexpressed in human lung cancers and enhances cell proliferation. Cancer Res 65: 9628-9632.
249. Olive V, Bennett MJ, Walker JC, Ma C, Jiang I, et al. (2009) miR-19 is a key oncogenic component of mir-17-92. Genes Dev 23: 2839-2849.
250. Friedman JM, Jones PA, Liang G (2009) The tumor suppressor microRNA-101 becomes an epigenetic player by targeting the polycomb group protein EZH2 in cancer. Cell Cycle 8: 2313-2314.

8 References

251. Friedman JM, Liang G, Liu CC, Wolff EM, Tsai YC, et al. (2009) The putative tumor suppressor microRNA-101 modulates the cancer epigenome by repressing the polycomb group protein EZH2. Cancer Res 69: 2623-2629.
252. Varambally S, Cao Q, Mani RS, Shankar S, Wang X, et al. (2008) Genomic loss of microRNA-101 leads to overexpression of histone methyltransferase EZH2 in cancer. Science 322: 1695-1699.
253. Michael MZ, SM OC, van Holst Pellekaan NG, Young GP, James RJ (2003) Reduced accumulation of specific microRNAs in colorectal neoplasia. Mol Cancer Res 1: 882-891.
254. Cherukuri DP, Deignan JL, Das K, Grody WW, Herschman H (2015) Instability of a dinucleotide repeat in the 3'-untranslated region (UTR) of the microsomal prostaglandin E synthase-1 (mPGES-1) gene in microsatellite instability-high (MSI-H) colorectal carcinoma. Mol Oncol 9: 1252-1258.
255. Li Q, Li X, Guo Z, Xu F, Xia J, et al. (2012) MicroRNA-574-5p was pivotal for TLR9 signaling enhanced tumor progression via down-regulating checkpoint suppressor 1 in human lung cancer. PLoS One 7: e48278.
256. Sambrook JR, D. (2001) Molecular Cloning: a Laboratory Manual. 3rd ed. Cold Spring Harbor, NY: Cold Spring Harbor Laboratory.
257. Kemmerer K, Weigand JE (2014) Hypoxia reduces MAX expression in endothelial cells by unproductive splicing. FEBS Lett 588: 4784-4790.
258. Walker SC, Avis JM, Conn GL (2003) General plasmids for producing RNA in vitro transcripts with homogeneous ends. Nucleic Acids Res 31: e82.
259. Vockenhuber MP, Heueis N, Suess B (2015) Identification of metE as a Second Target of the sRNA scr5239 in Streptomyces coelicolor. PLoS One 10.
260. Westman M, Korotkova M, af Klint E, Stark A, Audoly LP, et al. (2004) Expression of microsomal prostaglandin E synthase 1 in rheumatoid arthritis synovium. Arthritis Rheum 50: 1774-1780.
261. Lee JE, Lee JY, Wilusz J, Tian B, Wilusz CJ (2010) Systematic analysis of cis-elements in unstable mRNAs demonstrates that CUGBP1 is a key regulator of mRNA decay in muscle cells. PLoS One 5: e11201.
262. Kalsotra A, Xiao X, Ward AJ, Castle JC, Johnson JM, et al. (2008) A postnatal switch of CELF and MBNL proteins reprograms alternative splicing in the developing heart. Proc Natl Acad Sci U S A 105: 20333-20338.
263. He F, Jacobson A (2015) Nonsense-Mediated mRNA Decay: Degradation of Defective Transcripts Is Only Part of the Story. Annu Rev Genet 49: 339-366.
264. Moraes KC, Wilusz CJ, Wilusz J (2006) CUG-BP binds to RNA substrates and recruits PARN deadenylase. RNA 12: 1084-1091.
265. Stoddart MJ (2011) Cell viability assays: introduction. Methods Mol Biol 740: 1-6.
266. Cougot N, Babajko S, Seraphin B (2004) Cytoplasmic foci are sites of mRNA decay in human cells. J Cell Biol 165: 31-40.
267. Balagopal V, Parker R (2009) Polysomes, P bodies and stress granules: states and fates of eukaryotic mRNAs. Curr Opin Cell Biol 21: 403-408.
268. Decker CJ, Parker R (2012) P-bodies and stress granules: possible roles in the control of translation and mRNA degradation. Cold Spring Harb Perspect Biol 4: a012286.
269. Kedersha N, Stoecklin G, Ayodele M, Yacono P, Lykke-Andersen J, et al. (2005) Stress granules and processing bodies are dynamically linked sites of mRNP remodeling. J Cell Biol 169: 871-884.
270. Yang Z, Jakymiw A, Wood MR, Eystathioy T, Rubin RL, et al. (2004) GW182 is critical for the stability of GW bodies expressed during the cell cycle and cell proliferation. J Cell Sci 117: 5567-5578.

8 References

271. Yu TX, Gu BL, Yan JK, Zhu J, Yan WH, et al. (2016) CUGBP1 and HuR regulate E-cadherin translation by altering recruitment of E-cadherin mRNA to processing bodies and modulate epithelial barrier function. Am J Physiol Cell Physiol 310: C54-65.
272. Mazzola JL, Sirover MA (2003) Subcellular localization of human glyceraldehyde-3-phosphate dehydrogenase is independent of its glycolytic function. Biochim Biophys Acta 1622: 50-56.
273. Han J, Cooper TA (2005) Identification of CELF splicing activation and repression domains in vivo. Nucleic Acids Res 33: 2769-2780.
274. Zhou R, Zhou X, Yin Z, Guo J, Hu T, et al. (2015) Tumor invasion and metastasis regulated by microRNA-184 and microRNA-574-5p in small-cell lung cancer. Oncotarget 6: 44609-44622.
275. Zhou R, Zhou X, Yin Z, Guo J, Hu T, et al. (2016) MicroRNA-574-5p promotes metastasis of non-small cell lung cancer by targeting PTPRU. Sci Rep 6: 35714.
276. Keller A, Leidinger P, Borries A, Wendschlag A, Wucherpfennig F, et al. (2009) miRNAs in lung cancer - studying complex fingerprints in patient's blood cells by microarray experiments. BMC Cancer 9: 353.
277. Del Vescovo V, Grasso M, Barbareschi M, Denti MA (2014) MicroRNAs as lung cancer biomarkers. World J Clin Oncol 5: 604-620.
278. Das MK, Andreassen R, Haugen TB, Furu K (2016) Identification of Endogenous Controls for Use in miRNA Quantification in Human Cancer Cell Lines. Cancer Genomics Proteomics 13: 63-68.
279. Masuko-Hongo K, Berenbaum F, Humbert L, Salvat C, Goldring MB, et al. (2004) Up-regulation of microsomal prostaglandin E synthase 1 in osteoarthritic human cartilage: critical roles of the ERK-1/2 and p38 signaling pathways. Arthritis Rheum 50: 2829-2838.
280. Diaz-Munoz MD, Osma-Garcia IC, Cacheiro-Llaguno C, Fresno M, Iniguez MA (2010) Coordinated up-regulation of cyclooxygenase-2 and microsomal prostaglandin E synthase 1 transcription by nuclear factor kappa B and early growth response-1 in macrophages. Cell Signal 22: 1427-1436.
281. Savkur RS, Philips AV, Cooper TA (2001) Aberrant regulation of insulin receptor alternative splicing is associated with insulin resistance in myotonic dystrophy. Nat Genet 29: 40-47.
282. Kino Y, Mori D, Oma Y, Takeshita Y, Sasagawa N, et al. (2004) Muscleblind protein, MBNL1/EXP, binds specifically to CHHG repeats. Hum Mol Genet 13: 495-507.
283. Miller JW, Urbinati CR, Teng-Umnuay P, Stenberg MG, Byrne BJ, et al. (2000) Recruitment of human muscleblind proteins to (CUG)(n) expansions associated with myotonic dystrophy. EMBO J 19: 4439-4448.
284. Liu L, Ouyang M, Rao JN, Zou T, Xiao L, et al. (2015) Competition between RNA-binding proteins CELF1 and HuR modulates MYC translation and intestinal epithelium renewal. Mol Biol Cell 26: 1797-1810.
285. Ohsawa N, Koebis M, Mitsuhashi H, Nishino I, Ishiura S (2015) ABLIM1 splicing is abnormal in skeletal muscle of patients with DM1 and regulated by MBNL, CELF and PTBP1. Genes Cells 20: 121-134.
286. Dansithong W, Wolf CM, Sarkar P, Paul S, Chiang A, et al. (2008) Cytoplasmic CUG RNA foci are insufficient to elicit key DM1 features. PLoS One 3: e3968.
287. Berger DS, Ladd AN (2012) Repression of nuclear CELF activity can rescue CELF-regulated alternative splicing defects in skeletal muscle models of myotonic dystrophy. PLoS Curr 4: RRN1305.
288. Katoh T, Hojo H, Suzuki T (2015) Destabilization of microRNAs in human cells by 3' deadenylation mediated by PARN and CUGBP1. Nucleic Acids Res 43: 7521-7534.

8 References

289. Xiao L, Rao JN, Zou T, Liu L, Marasa BS, et al. (2007) Induced JunD in intestinal epithelial cells represses CDK4 transcription through its proximal promoter region following polyamine depletion. Biochem J 403: 573-581.
290. Chu CY, Rana TM (2006) Translation repression in human cells by microRNA-induced gene silencing requires RCK/p54. PLoS Biol 4: e210.
291. Kulkarni M, Ozgur S, Stoecklin G (2010) On track with P-bodies. Biochem Soc Trans 38: 242-251.
292. Saito K, Kondo E, Matsushita M (2011) MicroRNA 130 family regulates the hypoxia response signal through the P-body protein DDX6. Nucleic Acids Res 39: 6086-6099.
293. Gay S, Gay RE, Koopman WJ (1993) Molecular and cellular mechanisms of joint destruction in rheumatoid arthritis: two cellular mechanisms explain joint destruction? Ann Rheum Dis 52 Suppl 1: S39-47.
294. Szekanecz Z, Koch AE (2001) Update on synovitis. Curr Rheumatol Rep 3: 53-63.
295. Zwerina J, Redlich K, Schett G, Smolen JS (2005) Pathogenesis of rheumatoid arthritis: targeting cytokines. Ann N Y Acad Sci 1051: 716-729.
296. Kojima F, Naraba H, Sasaki Y, Beppu M, Aoki H, et al. (2003) Prostaglandin E2 is an enhancer of interleukin-1beta-induced expression of membrane-associated prostaglandin E synthase in rheumatoid synovial fibroblasts. Arthritis Rheum 48: 2819-2828.
297. Crofford LJ, Lipsky PE, Brooks P, Abramson SB, Simon LS, et al. (2000) Basic biology and clinical application of specific cyclooxygenase-2 inhibitors. Arthritis Rheum 43: 4-13.
298. Kojima F, Matnani RG, Kawai S, Ushikubi F, Crofford LJ (2011) Potential roles of microsomal prostaglandin E synthase-1 in rheumatoid arthritis. Inflamm Regen 31: 157-166.
299. Timchenko NA, Wang GL, Timchenko LT (2005) RNA CUG-binding protein 1 increases translation of 20-kDa isoform of CCAAT/enhancer-binding protein beta by interacting with the alpha and beta subunits of eukaryotic initiation translation factor 2. J Biol Chem 280: 20549-20557.
300. Yoshimatsu K, Altorki NK, Golijanin D, Zhang F, Jakobsson PJ, et al. (2001) Inducible prostaglandin E synthase is overexpressed in non-small cell lung cancer. Clin Cancer Res 7: 2669-2674.
301. MacDonald NJ, Steeg PS (1993) Molecular basis of tumour metastasis. Cancer Surv 16: 175-199.
302. Chiang AC, Massague J (2008) Molecular basis of metastasis. N Engl J Med 359: 2814-2823.
303. Slater TF, Sawyer B, Straeuli U (1963) Studies on Succinate-Tetrazolium Reductase Systems. Iii. Points of Coupling of Four Different Tetrazolium Salts. Biochim Biophys Acta 77: 383-393.
304. Mosmann T (1983) Rapid colorimetric assay for cellular growth and survival: application to proliferation and cytotoxicity assays. J Immunol Methods 65: 55-63.
305. Goldring MB, Goldring SR (1991) Cytokines and cell growth control. Crit Rev Eukaryot Gene Expr 1: 301-326.
306. Peng Y, Croce CM (2016) The role of MicroRNAs in human cancer. Signal Transduction And Targeted Therapy 1: 15004.
307. Yanaihara N, Caplen N, Bowman E, Seike M, Kumamoto K, et al. (2006) Unique microRNA molecular profiles in lung cancer diagnosis and prognosis. Cancer Cell 9: 189-198.
308. Lu J, Getz G, Miska EA, Alvarez-Saavedra E, Lamb J, et al. (2005) MicroRNA expression profiles classify human cancers. Nature 435: 834-838.

8 References

309. Cui R, Meng W, Sun HL, Kim T, Ye Z, et al. (2015) MicroRNA-224 promotes tumor progression in nonsmall cell lung cancer. Proc Natl Acad Sci U S A 112: E4288-4297.
310. Garofalo M, Quintavalle C, Di Leva G, Zanca C, Romano G, et al. (2008) MicroRNA signatures of TRAIL resistance in human non-small cell lung cancer. Oncogene 27: 3845-3855.
311. Garofalo M, Di Leva G, Romano G, Nuovo G, Suh SS, et al. (2009) miR-221&222 regulate TRAIL resistance and enhance tumorigenicity through PTEN and TIMP3 downregulation. Cancer Cell 16: 498-509.
312. Kawamori T, Rao CV, Seibert K, Reddy BS (1998) Chemopreventive activity of celecoxib, a specific cyclooxygenase-2 inhibitor, against colon carcinogenesis. Cancer Res 58: 409-412.

IV Curriculum vitae

Persönliche Daten

Name: Isabell Baumann, geboren am 12.09.1985 in Offenbach

Akademische Karriere

07/2013 – 12/2016	Promotion bei Prof. Dr. Beatrix Suess von der Technischen Universität Darmstadt in Kooperation mit Prof. Dr. Dieter Steinhilber am Institut für Pharmazeutische Chemie der Goethe-Universität Frankfurt und Prof. Dr. P.-J. Jakobsson vom Karolinska Institut in Stockholm; Mitglied der Graduiertenschule FIRST, sowie Stipendiatin der Else-Kröner-Fresenius Stiftung
10/2011 – 07/2013	Masterstudiengang „Molekulare Biowissenschaften“ an der Goethe-Universität Frankfurt, Abschluss: Master of Science (1.5)
09/2008 – 09/2011	Bachelorstudiengang „Biotechnologie“ an der Hochschule Darmstadt, Abschluss: Bachelor of Science (2.1)
08/2005 – 03/2008	Ausbildung zur Pharmazeutisch-technischen Assistentin an der Martin-Behaim-Schule in Darmstadt, Abschluss: PTA (1.3)
08/2002 – 06/2005	Claus-von-Stauffenberg Schule, Abschluss: Abitur (2.3)

Projekte:

07/2013 – 12/2016	Promotionsprojekt im Bereich Biologie bei Prof. Beatrix Süß und Prof. Dr. Dieter Steinhilber an der TU Darmstadt und der Goethe-Universität Frankfurt Thema: Post-transcriptional regulation of mPGES-1 by the balance of CUGBP1 and miR-574-5p
10/2015 – 12/2015	Forschungsprojekt in Kooperation mit Prof. Dr. P.-J. Jakobsson am Karolinska Institut in Stockholm Thema: „Globale Proteomics Studie zur Identifizierung von miR-574-5p und CUGBP1 targets, sowie miR-328 targets in MM6 Zellen“
01/2012 – 07/2013	Masterarbeit im Bereich der Lantibiotika bei Prof. Dr. K.-D. Entian an der Goethe-Universität Frankfurt Thema: „Untersuchungen der Lokalisation und Expression der LanI Proteine in *L. lactis“*
03/2011 – 08/2011	Bachelorarbeit im Bereich der Molekularbiologie und Biotechnologie bei Sanofi in Frankfurt am Main (Upstream Processing Dr. Hauptmann) in Koop. mit Prof. Dr. Koepp-Bank, Hochschule Darmstadt Thema: „Evaluation of a novel micro bioreactor for recombinant protein expression in *Kluyveromyces lactis”*

Berufliche Tätigkeiten:

07/2012 – 10/2012	Werkstudent bei Sanofi als QA-Assistenz im Bereich der Qualitätskontrolle, Analytik und Mikrobiologie der Insuline; bei Dr. K. Runge und Dr. C. Havenith Industriepark Frankfurt Höchst
05/2009 – 04/2011	PTA in der Sonnen Apotheke in Rodgau
02/2008 – 04/2009	PTA in der Schwanen Apotheke am Markt in Offenbach

Lehrtätigkeit:

2013	Betreuung der Wahlpflichtpraktikant/innen des Studiengangs Pharmazie an der Goethe-Universität Frankfurt
2014 – 2016	Betreuung von Praktikanten, Bachelor und Masterstudenten der TU-Darmstadt
07/2016	Tutorin des Genetik Praktikums an der TU-Darmstadt

Tagungen:

2013	EKFS Symposium, Bad Homburg vor der Höhe, Hessen
2015	Keystone meeting „miRNAs and noncoding RNAs“, Colorado, USA
2015	EKFS Symposium, Bad Homburg vor der Höhe, Hessen

Vorträge:

2013-2016	Summer- und Winterschool in Löwenstein und Obergurgl (2 x im Jahr)
2014	EKFS Retreat (Poster und Präsentation), Frankfurt
2014	EU PhD School Bioactive Lipids in Pescara, Italien
2015	Doktorandensymposium der TU Darmstadt, Darmstadt

Publikationen:

Fertiges Manuskript: miR-574-5p acts as miRNA decoy to CUGBP1 functions and regulates lung tumour growth via microsomal prostaglandin E synthase-1

Ehrenwörtliche Erklärung:

Ich erkläre hiermit ehrenwörtlich, dass ich die vorliegende Arbeit entsprechend den Regeln guter wissenschaftlicher Praxis selbstständig und ohne unzulässige Hilfe Dritter angefertigt habe.

Sämtliche aus fremden Quellen direkt oder indirekt übernommenen Gedanken sowie sämtliche von Anderen direkt oder indirekt übernommenen Daten, Techniken und Materialien sind als solche kenntlich gemacht. Die Arbeit wurde bisher bei keiner anderen Hochschule zu Prüfungszwecken eingereicht.

Darmstadt, den 24.11.2016

……..

Isabell Baumann

V Acknowledgements

Mein besonderer Dank gilt Prof. Dr. Dieter Steinhilber und Prof. Dr. Beatrix Süß für die hervorragende Betreuung während meiner Doktorarbeit und die Möglichkeit an diesem interessanten Projekt zu arbeiten. Ich hatte eine tolle Zeit in euren Arbeitskreisen.

I would like to thank Prof. Per-Johan Jakobsson for giving me the opportunity to visit his lab in Stockholm for a research project during beautiful winter time in Sweden. Also I would like to thank his staff, especially Helena, Elena, Joan, Johan, Fari, Marina, Karin, Catia, Filip and Julia for great discussions, nice coffee breaks and the wonderful time in Sweden. Thank you Per Nordlund, Johan and Sara for introducing me in new cellular assays. Thank you Helena and Joan for doing LC-MS/MS analysis.

I would like to thank our cooperation partner Prof. Paola Patrignani and her lab members from Chieti University in Italy for having a great and fruitful cooperation. Thank you all for performing and analyzing the mice experiments.

Vielen Dank an Dr. Meike Saul, für Projektinitierung, die hervorragende Betreuung und die fachliche Unterstützung während der ganzen Promotionszeit.

Ein riesen großes Dankeschön an alle ehemaligen und derzeitigen Mitglieder meiner zwei Arbeitskreise Steinhilber und Süß für eure Hilfsbereitschaft, Kollegialität, die nette Arbeitsatmosphäre und den Spaß während der Arbeits- und Pausenzeit. Danke, dass ihr mich so schnell in euren Kreis aufgenommen habt. Ich hatte wirklich eine sehr schöne Zeit mit euch!

Danke auch an Astrid Brüggerhoff für das Bestellen so mancher Sachen und die netten Kaffeepausen mit dem Blick über die Frankfurter Skyline.

Ganz besonders bedanken möchte ich mich bei Britta Kluge und Anett Hegewald mit denen das Laborleben, die Kaffepausen und eigentlich jeder Tag immer ein Grund zur Freude waren.

Mein besonderer Dank gilt meiner ganzen Familie und meinen Freunden, besonders meinen Eltern und Matthias, die mich bei jedem Schritt in den letzten Jahren unterstützt haben.